

1-1-1990

The effect of coagulants on the microstructure and mechanical properties of lyotropic fiber-forming polymers/

Margaret A. Rakas
University of Massachusetts Amherst

Follow this and additional works at: https://scholarworks.umass.edu/dissertations_1

Recommended Citation

Rakas, Margaret A., "The effect of coagulants on the microstructure and mechanical properties of lyotropic fiber-forming polymers/" (1990). *Doctoral Dissertations 1896 - February 2014*. 764.
<https://doi.org/10.7275/ga72-ae36> https://scholarworks.umass.edu/dissertations_1/764

This Open Access Dissertation is brought to you for free and open access by ScholarWorks@UMass Amherst. It has been accepted for inclusion in Doctoral Dissertations 1896 - February 2014 by an authorized administrator of ScholarWorks@UMass Amherst. For more information, please contact scholarworks@library.umass.edu.

UMASS/AMHERST



312066007491911

THE EFFECT OF COAGULANTS ON THE
MICROSTRUCTURE AND MECHANICAL PROPERTIES OF
LYOTROPIC FIBER-FORMING POLYMERS

A Dissertation Presented

by

MARGARET A. RAKAS

Submitted to the Graduate School of the
University of Massachusetts in partial fulfillment
of the requirements for the degree of

DOCTOR OF PHILOSOPHY

February 1990

Polymer Science and Engineering

© Copyright by Margaret Ann Rakas 1990

All Rights Reserved

THE EFFECT OF COAGULANTS ON THE MICROSTRUCTURE AND
MECHANICAL PROPERTIES OF LYOTROPIC FIBER-FORMING
POLYMERS

A Dissertation Presented

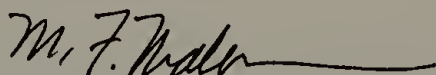
by

MARGARET A. RAKAS

Approved as to style and content by:



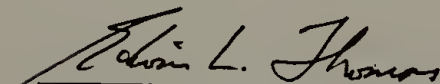
Richard J. Farris, Committee Chairman



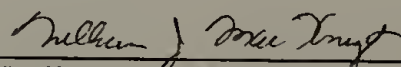
Michael F. Malone, Member



Thomas J. McCarthy, Member



Edwin L. Thomas, Member



William J. MacKnight, Department Head
Department of Polymer Science and Engineering

ACKNOWLEDGEMENTS

I'd like to thank my advisor, Professor Farris, first for his faith in me, and then for helping me to do the kind of thesis research I really wanted to do. I was slightly mechanically disinclined (think of the Gary Larson cartoon) when I joined the group; now, I look back on the time I was putting together the spinning equipment and high pressure lines as one of the most fulfilling parts of my life. Otherwise, I would never have known the feeling of amazement when you stand back and look at a piece of equipment that works, and know you were (at least partially) responsible.

I think I have had one of the best thesis committees ever--at least from a student's point of view. My committee members were exceptionally helpful and active. Dr. Thomas's help and criticism in the WAXS studies was instrumental in obtaining instrument time and evaluation of the effect of coagulant on crystal structure.

Richard Zink provided a lot of inspiration, as well as good machining; Norm Page and John Domian were responsible for all the wiring and for other tasks which absolutely had to be done right the first time. I would also like to thank the PSE secretaries, because all of them helped me many times. Special thanks to Carol and Chris for MAC help and rushing PO's.

This work was supported in large part by the Kevlar Division of E.I. du Pont de Nemours & Company, both in terms of financial and material support. I would like to thank Dr. Warren F. Knoff for facilitating this cooperative effort, and for providing the PPTA spinning

dopes. I would also like to thank Dr. Steven Allen, of Du Pont Pioneering Research Division, for many helpful, if not downright crucial, tips on PPTA fiber spinning.

Now, the difficult part--thanking my friends and colleagues. I'd like to thank the members of Dr. Farris's research group, for putting up with weird smells and both my good and bad moods. The camaraderie was what kept me coming back to lab when the results were bad. Thanks to Mike Satkowski, Yachin Cohen and John Reffner for their advice on WAXS experiments and analysis. Chuck Bauer and Cady Coleman provided heavy moral support, especially during those first few PPTA spinning experiments (strongly acidic yellow goo oozing everywhere...). Nancy Goldberg was always the voice of optimism and reason--and good humor.

Lastly, the real mush. To the women I lived with on McCormick Fifth West from September 1979 until June 1983--and to the man I've lived with since 1986--you have given me the strength, and the humor, to be who I am and to complete something I was not sure I could even begin. Thank you.

ABSTRACT

THE EFFECT OF COAGULANTS ON THE MICROSTRUCTURE AND MECHANICAL PROPERTIES OF LYOTROPIC FIBER-FORMING POLYMERS

FEBRUARY 1990

MARGARET A. RAKAS, S.B., MASSACHUSETTS INSTITUTE OF
TECHNOLOGY

Ph.D, UNIVERSITY OF MASSACHUSETTS

Directed by: Professor Richard J. Farris

The effect of coagulant on the mechanical properties and microstructure of three lyotropic fiber-forming polymers, poly(p-phenylene benzobisthiazole) [PBZT], poly(p-phenylene terephthalamide) [PPTA] and poly(p-phenylene benzobisoxazole) [PBO] was studied. Previous research found that the imbalance between tensile and compressive/shear properties in these high-modulus fibers is due to a low degree of lateral interaction between microfibrillar elements. In this work, coagulants were chosen which could have strong specific molecular interactions with some portion of the polymer chain; the goal of this research was to increase compressive and shear properties by creating lateral physical crosslinks among the polymer chains.

Results from these coagulation studies show that macroscopic properties such as compressive strength and torsion modulus are dependent on the coagulant; these interactions are strong enough to significantly affect mechanical and structural properties of the fiber. For

oxygen-containing lyotropic polymers, the cations present in the coagulant may be important in determining the occurrence of specific interactions.

As-spun PBZT fiber coagulated in iodine/ethanol solution with a spin/draw of 3 had a shear modulus of 1.14 GPa and tensile strength of 2.2 GPa; fiber coagulated in ethanol had respective values of 0.63 GPa and 1.8 GPa. Wide-angle X-ray scattering (WAXS) studies showed that I_3^- and I_5^- anions were present within the fiber, and that there was some disruption of the standard PBZT unit cell. PPTA fiber was coagulated into water, ethanol, iodine/ethanol and aqueous solutions of alkali salts. Coagulation in water produced PPTA fiber with the highest tensile, shear and compressive properties. The shear and/or compressive properties of PPTA fibers could be decreased without a corresponding change in crystal structure; these properties seem to be based on an element of microstructure above that of the unit cell. PBO fibers were coagulated in many of the same coagulants; mechanical properties were unaffected. Coagulation in aqueous potassium iodide produced fiber containing oriented potassium iodide crystals within the fiber.

TABLE OF CONTENTS

ACKNOWLEDGEMENTS	iv
ABSTRACT	vi
LIST OF TABLES	x
LIST OF FIGURES	xii
Chapter	
1 INTRODUCTION	1
1.1 The Role of Chemistry and Processing in Obtaining High-Performance Fibers	1
1.2 Processing, Structure and Properties of Lyotropic Fibers.....	4
1.3 Dissertation Overview	12
2 POLY(P-PHENYLENE BENZOBISTHIAZOLE) [PBZT] ...	15
2.1 Introduction.....	15
2.2 Production and Mechanical Characterization of PBZT Fibers	16
2.3 Fiber Impregnation	17
2.3.1 Experimental	17
2.3.2 Mechanical Properties	20
2.4 The Effect of Coagulant on the Structure and Mechanical Properties of PBZT Fibers	26
2.4.1 Introduction.....	26
2.4.2 Experimental	27
2.4.3 Fiber Microstructure	30
2.4.4 Mechanical Properties	52
2.4.5 Effect of Heat Treatment on Iodine/Iodide Content.....	57
2.5 Conclusions.....	58

3	POLY(P-PHENYLENE TEREPHTHALAMIDE) [PPTA]	70
3.1	Introduction.....	70
3.2	Fiber Production and Testing	73
3.3	The Effect of Coagulant on Structure and Mechanical Properties.....	80
3.3.1	Fiber Microstructure	80
3.3.2	Mechanical Properties	114
3.4	PPTA Fiber Blends and PPTA Fiber Impregnation	126
3.4.1	Experimental	126
3.4.2	Mechanical Properties	129
3.5	Conclusions.....	135
4	POLY(P-PHENYLENE BENZOBISOXAZOLE) [PBO]	139
4.1	Introduction.....	139
4.2	The Effect of Coagulant on the Structure and Mechanical Properties.....	140
4.2.1	Experimental	140
4.2.2	Fiber Microstructure.....	141
4.2.3	Mechanical Properties	165
4.3	Fiber Impregnation	177
4.3.1	Experimental	177
4.3.2	Mechanical Properties	178
4.4	Conclusions.....	180
5	SUMMARY AND FUTURE WORK	183
5.1	Summary.....	183
5.2	Future Work	191
	REFERENCES	194

LIST OF TABLES

2.1	Mechanical properties of AS-PBZT(8) and PBZT/SG	24
2.2	Mechanical properties of AS-PBZT and PBZT/SS.....	24
2.3	d-spacings of reflections of PBZT coagulated in water [PH9]	39
2.4	Assignment of wide-angle X-ray scattering reflections for PI9.....	40
2.5	Mechanical properties of PBZT fibers coagulated into water, ethanol, and iodine/ethanol.....	53
2.6	Mechanical properties for as-spun and iodine-impregnated PBZT fibers.....	54
2.7	Mechanical properties of as-spun PBZT [AS-PBZT] and PBZT coagulated and soaked in aqueous potassium iodide [PBZT/KI/KI]	54
3.1	Mechanical properties of as-spun PPTA fibers coagulated in water, ethanol and hexane.....	115
3.2	Mechanical properties of as-spun PPTA fibers coagulated in 8% aqueous LiCl solution and 0.5 M (8.3%) aqueous KI solution.....	117
3.3	Mechanical properties of as-spun PPTA fiber coagulated and soaked in iodine solution [PPTA/IET/IET] and coagulated in iodine solution but soaked in water [PPTA/IET/H ₂ O].....	121
3.4	Mechanical properties of as-spun PPTA fiber coagulated in strongly acidic and strongly basic aqueous solutions	125
4.1	d-spacings of PBO fiber coagulated in water [PBO/H ₂ O].....	155
4.2	d-spacings of PBO fiber coagulated and soaked in aqueous potassium iodide (PBO/KI/KI)	156
4.3	d-spacings and assignment of reflections found in the PBO/KI/KI fiber	164

4.4	The effect of coagulant on the mechanical properties of PBO fibers	166
4.5	The effect of impregnation with Tyzor LA [®] on the mechanical properties of PBO fibers	179

LIST OF FIGURES

1.1	Molecular structures of the lyotropic polymers studied in this dissertation.....	6
1.2	Schematic of the fiber spinning apparatus used to produce most of the PBZT fibers studied in this dissertation.	7
2.1	A schematic of the solution-exchange process used for fiber impregnation.....	19
2.2	Typical stress-strain curves for as-spun PBZT [AS-PBZT] and sol-gel impregnated PBZT [PBZT/SOL-GEL].....	23
2.3	Wide-angle X-ray diffractometer equatorial scans of PBZT fibers coagulated in water, with a spin/draw of 9.7 [PH9].	32
2.4	Wide-angle X-ray diffractometer equatorial scans of PBZT fibers coagulated in iodine/ethanol, with a spin/draw of 9.7 [PI9].....	34
2.5	<i>Top:</i> Statton film emphasizing the meridional reflections of PI9. <i>Bottom:</i> Schematic of meridional reflections.....	36
2.6	<i>Top:</i> Statton film emphasizing the meridional reflections of PH9. <i>Bottom:</i> Schematic of reflections.....	38
2.7	Statton photograph of PBZT coagulated in ethanol, having a spin/draw of 3 [PE3].	42
2.8	Statton film of iodine-impregnated PBZT fiber.	45
2.9	Statton film of as-spun PBZT fiber.....	47
2.10	Statton film of PBZT fiber coagulated in 0.5M (8.3%) aqueous potassium iodide solution, having a spin/draw of 20.	49
2.11	Statton film of PBZT fiber coagulated in water, spin/draw of 20.	51
2.12	Typical stress-strain curves for PBZT fibers coagulated in water, ethanol and iodine/ethanol.....	56
2.13	The amount of iodine species present in the PI9 fiber in March 1989 as a function of heating time.....	60

2.14	Proposed model, which shows iodide anions in between the microfibrillar network.....	65
2.15	Another aspect of the proposed model shown in figure 2.14. Iodide anions are complexed with PBZT chains within a microfibril.....	67
2.16	Another proposed model for the PBZT/iodide anions "alloy", which supposes a change in crystal structure of the PBZT chain.....	68
3.1	Schematic of the system used to spin PPTA fibers.	75
3.2	<i>Top:</i> Wide-angle X-ray scattering (WAXS) Statton film of PPTA fiber coagulated in water [PPTA/H ₂ O], S/D=12.2. <i>Bottom:</i> Schematic of reflections.	82
3.3	WAXS Statton films of PPTA fiber coagulated in ethanol [PPTA/ETH], S/D=3.	84
3.4	Scanning electron micrograph of PPTA/ETH fiber fractured in tension.....	87
3.5	A scanning electron micrograph of a PPTA/ETH fiber which has failed in compression during the recoil test.....	89
3.6	Scanning electron micrograph of a PPTA/H ₂ O fiber fractured in tension.....	91
3.7	<i>Top:</i> WAXS Statton film of PPTA fiber coagulated in aqueous potassium iodide [PPTA/KI], S/D=4.4. <i>Bottom:</i> Schematic of reflections.	93
3.8	The WAXS pattern of heat-treated/tension-dried PPTA/ETH fibers.....	95
3.9	The WAXS pattern of heat-treated/tension dried (230-250°C, 65-80 MPa tension) PPTA/KI fibers.....	97
3.10	Scanning electron micrograph of a PPTA/KI fiber which has failed in tension.....	100
3.11	Scanning electron micrograph of a PPTA/KI fiber which has failed in compression.....	102
3.12	The WAXS pattern for PPTA fiber which was coagulated and soaked in fresh iodine/ethanol solution [PPTA/IET/IET], S/D=3.....	104

3.13	<i>Top:</i> WAXS pattern of free fall PPTA/H ₂ O fiber [FF/H ₂ O]. <i>Bottom:</i> Schematic of reflections.	107
3.14	<i>Top:</i> WAXS pattern of as-spun PPTA fiber coagulated in 20% NaOH solution (aq), no draw [FF/BAS]. <i>Bottom:</i> Schematic of reflections.	109
3.15	Scanning electron micrograph of a PPTA/SS fiber which has failed in tension.	111
3.16	Scanning electron micrograph of a PPTA/SS fiber which has failed in compression.	113
3.17	Typical stress-strain curves for Kevlar 49 and as-spun PPTA fibers coagulated in water, ethanol and aqueous alkali salt solutions.	119
3.18	Typical stress-strain curves for as-spun PPTA fibers coagulated in water, 20% sulfuric acid, 20% sodium hydroxide and sodium silicate.	124
3.19	Tensile moduli of as-spun and impregnated PPTA fibers.	130
3.20	Torsion moduli of as-spun and impregnated PPTA fibers.	131
3.21	Typical stress-strain curves for as-spun PPTA [AS-PPTA] and PPTA impregnated with Tyzor LA [PPTA/TY].	133
3.22	Torsion modulus distribution for PPTA fibers impregnated with Tyzor LA [®]	134
4.1	<i>Top:</i> The WAXS pattern of as-spun PBO fiber which was coagulated and soaked in water [PBO/H ₂ O/H ₂ O]. <i>Bottom:</i> Schematic of reflections.	143
4.2	The WAXS pattern of as-spun PBO fiber which was coagulated and soaked in ethanol [PBO/ETH/ETH].	145
4.3	The WAXS pattern of as-spun PBO fiber which was coagulated and soaked in iodine/ethanol solution [PBO/IET/IET].	147
4.4	<i>Top:</i> The WAXS pattern of as-spun PBO fiber which was coagulated and soaked in 0.5 M potassium iodide solution [PBO/KI/KI]. <i>Bottom:</i> Schematic of reflections.	149

4.5	The WAXS pattern of as-spun PBO fiber which was coagulated in potassium iodide but then soaked in water [PBO/KI/H ₂ O].	151
4.6	The WAXS pattern of as-spun PBO fiber coagulated and soaked in water, then impregnated for 96 hours with a 0.5 M (8.3%) potassium iodide solution (PBO/H ₂ O/KI).....	154
4.7	WAXS pattern of PBO/H ₂ O/H ₂ O at a sample-to-film distance of 18.1 mm.	161
4.8	WAXS pattern of PBO/KI/KI at a sample-to-film distance of 18.1 mm.	163
4.9	A reproduction of a typical chart recording of a tensile test for PBO/KI/KI fibers, showing the partial load reduction before catastrophic failure.	168
4.10	Scanning electron micrograph of a typical tensile specimen of PBO/KI/KI.....	170
4.11	Two scanning electron micrographs of higher magnification of selected areas of the same sample shown in figure 4.10.	172
4.12	Scanning electron micrograph of a typical tensile specimen of PBO/H ₂ O/H ₂ O.	174
4.13	Two micrographs of higher magnification of selected areas from the same sample shown in figure 4.12. Top: Part of the fracture surface (with probable sample charging). Bottom: Further away from the fiber end.....	176
5.1	A plot of the experimental values of compressive strength versus torsion modulus for the PPTA fibers spun during the course of this thesis work, as well as calculated values.	190

CHAPTER 1

INTRODUCTION

1.1 The Role of Chemistry and Processing in Obtaining High-Performance Fibers

The high level of interest in the development of organic polymer fibers which have high modulus/high strength tensile properties has been primarily a response to the needs of aerospace and other users of composite materials. These polymer fibers have a principal advantage over inorganic fibers, in that they are lighter in weight while having greater specific stiffness and tensile strength.

The factors which are of prime importance in producing high-performance fibers are the chemical structure of the polymer, its chain conformation, and the processing techniques used to spin it into a fiber. Molecular structures of polymers which have successfully produced fibers with high tensile properties fit into one of three categories: 1) the low energy chain conformation is coiled, but the chain is linear and can be "drawn" into and maintain an extended conformation; 2) the polymer structure allows the carbon atoms to cyclize as the polymer is heated above the degradation point of all other substituents; and 3) the molecular architecture of liquid crystal polymers, whose chains are kept rigid and extended by steric forces.

Carbon fiber is produced through the second method outlined above. Processing is highly important in terms of the fiber's final mechanical properties. Carbon fiber is manufactured either by spinning oriented solutions of pitch, or by starting with highly-oriented poly(acrylonitrile) fiber; both sets of fibers require a series of heat treatments at extreme temperatures to produce the graphitic structure. The result is an axially-oriented microfibrillar microstructure which has the strong, stiff graphite crystal basal plane oriented along the long axis of the microfibril [Diefendorf and Tokarsky, 1975]. Carbon fiber has significantly greater shear and compressive properties than any of the other organic fibers, with a compressive strength of 1-3 GPa. The conductivity of these fibers, however, is perceived by some to be a possible hazard during the processing or failure of composites. Further, composites having carbon fiber reinforcements exhibit poor damping and brittleness, which is avoided when another fiber, such as poly(phenylene terephthalamide) [PPTA] is used instead [Wilfong and Zimmerman, 1977].

PPTA was the first liquid crystal polymer fiber commercially produced. These fibers are made by spinning from an ordered nematic phase. Special synthetic techniques were required [Bair et al. 1977] in order to produce an extended chain conformation via steric and bonding forces. This class of polymers generally are composed of stiff-chain, axially-oriented aromatic rings, with perhaps a minor amount of aliphatic units. Spinning from an ordered phase can be achieved in one of two ways: if the polymer is a thermotropic liquid crystal, it can be heated to effect transition from the solid phase to the ordered liquid-crystalline phase, and melt spun; or, if the polymer is lyotropic, it is spun from a solution whose concentration renders it a single, anisotropic phase.

During the fiber spinning process, the ordered polymer is uniaxially oriented, and this orientation can be perfected in post-processing treatments such as tension-drying or annealing. Processing of lyotropic polymers is more costly because of the constraints that fibers must be spun from solutions which cannot be highly concentrated due to lack of processibility, and also because of the solvents required and the need to engage some type of solvent-recovery system. These fibers generally have higher tensile moduli than the thermotropic fibers and some, such as poly(p-phenylene benzobisthiazole) [PBZT], have much greater temperature resistance.

Interest in developing high modulus fibers from flexible-chain polymers was sparked by theoretical and experimental investigations of the crystal moduli of some flexible chain polymers which predicted that moduli of 100-300 GPa were possible in an extended-chain conformation [Ward, 1982 and Holliday, 1975]. The challenge was then to find a processing method which would result in highly extended, crystalline chains. Early experimental techniques, while successful [Zwijnenburg and Pennings, 1976 and Pennings, 1977], were not commercially feasible. An alternate process, by which a gel solution of the polyethylene is continuously spun into fiber, cooled, and hot-drawn [Smith and Lemstra, 1980] has formed the basis of the commercially-spun high-performance polyethylene [Kavesh and Prevorsek, 1988 a, 1984], sold by Allied-Signal under the name of Spectra 9000. Spectra 9000 fibers have tensile moduli of approximately 120 GPa and tensile strengths of 2.6 GPa [Tam et al. 1988]. Recent developments in melt-drawing polyethylene have resulted in fibers with a tensile modulus of 125 GPa and a tensile strength of 3.6 GPa [Bashir and

Keller, 1989]. Finally, workers who combined a solid-state extrusion process with further tensile drawing have reported a tensile modulus of 220 GPa for the polyethylene fiber produced [Kanomoto et al. 1983].

Unfortunately, at this date, neither lyotropic nor thermotropic fibers can match the shear and compressive properties of carbon fibers. The values of shear modulus and compressive properties for the ultra-high modulus polyethylene fibers are also in the same range as the liquid-crystal fibers [DeTeresa, 1985]. Although the shear modulus and compressive strengths of the lyotropic polymers are generally higher than those of other polymers, more composite applications could be realized if these properties were significantly increased. In order to realize the full investment put into the research and development of these fibers, it is necessary to understand the factors which control shear and compressive properties.

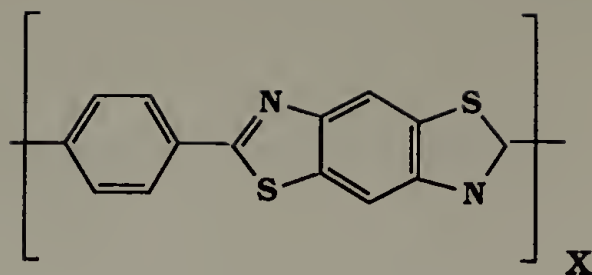
1.2 Processing, Structure and Properties of Lyotropic Fibers

Three major lyotropic polymers have been successfully developed as fibers. Poly(p-phenylene terephthalamide) [PPTA] is sold by the Du Pont de Nemours Company under the trade names of Kevlar 49[®] and Kevlar 29[®]. Poly(p-phenylene benzobisoxazole) [PBO] is presently being developed by the Dow Chemical Company. Both PBO and poly(p-phenylene benzobisthiazole) [PBZT] were synthesized by the Stanford Research Institute [Wolfe et al. 1981a, Wolfe and Arnold, 1981b] under the aegis of the Air Force Ordered Polymers Program. Initial

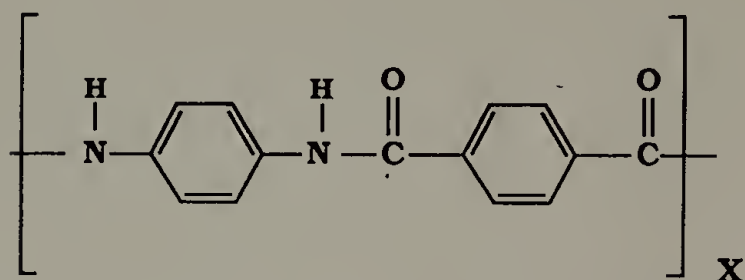
investigations of the mechanical properties of fibers and ribbons [Choe and Kim, 1981] indicated that these fibers could possibly serve as alternates to carbon and inorganic fibers.

These polymers all share a common structure: the polymer backbone is composed of 2 or more aromatic rings, with all substituents being located in the para positions (see figure 1.1). Thus, chain stiffness and rigidity are locked into place, and the molecule can be thought to have a rod-like conformation, rather than a coil. (Chain stiffness is the reason why these polymers will degrade before reaching their respective melting points). Due to strong intermolecular interactions [Bhaumik et al. 1981], these lyotropic polymers can only be dissolved in strongly protic solvents. High performance fibers of PBZT and PBO are spun from the polymerization solvent, poly(phosphoric acid), while PPTA fibers are commonly spun from concentrated sulfuric acid.

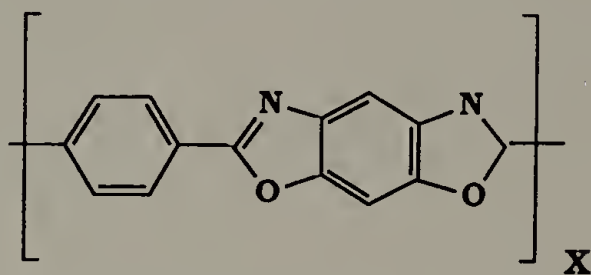
Fibers are spun from solutions in the nematic phase, generally from 14-20 weight percent polymer. Basically, in terms of viscosity, these solutions are as highly concentrated as possible while remaining processible. Figure 1.2 shows a typical dry-jet wet spinning apparatus used in fiber production. The technique of dry-jet wet spinning developed by Blades [Blades, 1973] takes advantage of the ordered solution and induces uniaxial orientation, so that polymer chains are aligned parallel to the fiber direction. This process is a result of the elongational flow which takes place in the air gap. The length of the air gap is highly important for PPTA fibers, with 0.5-1.5 centimeters being regarded as optimal [Morgan et al. 1983]. As the air gap length increases beyond 2 centimeters, spinning becomes increasingly more difficult and then impossible as surface forces cause the fiber line to break before the



Poly(p-phenylene benzobisthiazole) [PBZT]



Poly(p-phenylene terephthalamide) [PPTA]



Poly(p-phenylene benzobisoxazole) [PBO]

Figure 1.1 Molecular structures of the lyotropic polymers studied in this dissertation.

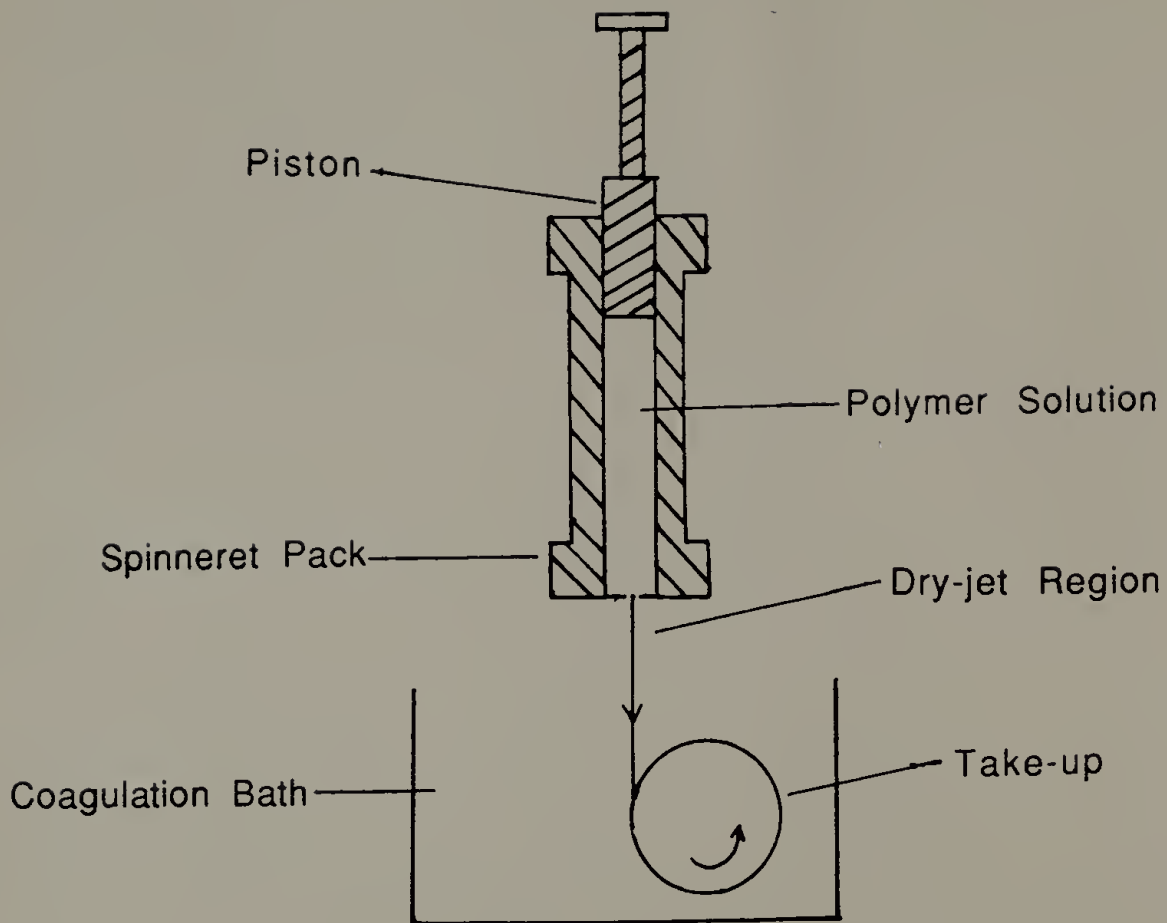


Figure 1.2 Schematic of the fiber spinning apparatus used to produce most of the PBZT fibers studied in this dissertation.

fiber can be coagulated. On the other hand, fibers spun from PBZT or PBO are not nearly as sensitive to the length of the air gap; poly(phosphoric acid) is a much more viscous solvent, permitting an air gap of up to 8 inches without breakdown of the fiber line.

After extrusion from the spinneret, the nematic to solid phase transition is effected by the coagulation process. Coagulation occurs when the fiber comes into contact with a liquid (generally water) which is a non-solvent for the polymer and a solvent for the acid. In this way, the highly-oriented structure produced in the air gap is effectively frozen in place as the fiber solidifies. This process should be thought of as a ternary system, because coagulant diffuses into the polymer fiber as the solvent (acid) diffuses out and is carried off by the coagulant. While the interactions of the coagulant with the polymer fiber are important and are the main focus of the thesis, the relationship between the acid and the coagulant is also important. Mutual solubilities and other molecular interactions may affect the rate of diffusion, and thus the time scale of coagulation. In turn, this has been shown to affect fiber morphology [Cohen, 1987].

In small-scale spinning of PBZT or PBO, immersion of the fiber in a large bath filled with the coagulant is the usual method of coagulation. Due to the very small air gap required for PPTA fiber, a falling stream of coagulant comes into contact with the fiber; this method can also be used to coagulate PBZT or PBO fibers. Regardless, fiber is kept wet and washed with fresh coagulant while it is being wrapped around the take-up wheel. The speed of the take-up can be varied, and is measured, so that it is possible to produce fibers of varying spin/draw. Spin/draw is defined as the ratio of the linear velocity of the take-up to the outlet

velocity at the spinneret, and is a measure of how much the fiber has been stretched in the air gap, before solidification of the fiber has taken place.

Spin/draw has been identified as instrumental in the development of high tensile modulus and strength in as-spun lyotropic polymers [Jaffee and Jones, 1985]. ("As-spun" refers to fibers which have been allowed to air dry while wrapped around the take-up wheel, with no additional tension added). For these rigid-rod fibers, however, a combination of heat treatment and tension drying significantly increase tensile moduli and for the most part, levels out any differences in tensile moduli between as-spun fibers of the same species which had different spin/draw ratios. The tensile strengths of PBZT and PBO can also be increased and the effect of spin/draw smoothed by such post-processing treatment [Allen, 1983, Pottick, 1985, and Adams et al. 1986]. For PPTA fibers, however, there is no increase in tensile strength with heat treatment, tension drying, or any combination of post-processing.

The microstructure of PBZT fiber was shown through morphological techniques to be essentially unchanged from coagulation through post-processing. Investigations utilizing small-angle X-ray scattering (SAXS) and transmission electron microscopy (TEM) showed that the as-coagulated PBZT fiber is composed of a microfibrillar network, each microfibril being on the order of 70-100 Å in diameter [Cohen, 1985]. ("As-coagulated" fiber is fiber that has been kept wet since its initial coagulation. This results in a fiber which is swollen with water and has a more open, porous structure than as-spun fiber). Microfibrils are aligned in the fiber direction, and are connected only sparingly via Y-shaped junctions. The concept that post-processing

helps perfect crystallite size and order, but does not change the fiber microstructure was further supported by investigations comparing the difference in tensile properties between as-spun and as-coagulated PBZT fiber. In this work, it was shown that the force required to break an as-spun fiber was the same as that required to break an as-coagulated fiber [Pottick, 1985].

Extensive characterization of the morphology of Kevlar 49[®] using wide-angle electron diffraction (WAED) and dark-field imaging [Dobb et al. 1977a, b] established that the fiber's microstructure consists of a system of radially-arranged, hydrogen-bonded sheets, regularly pleated along their long axes.

Spin/draw and post-processing, while conclusively shown to increase the tensile modulus of PPTA fibers and both tensile strength and modulus of PBZT and PBO fibers, have no measurable effect on shear or compressive values [Pottick, 1985; DeTeresa and Rakas, 1986]. Because the compressive strength of these fibers is about an order of magnitude less than the tensile strength, use of these fibers in engineering designs such as plates or beams is limited due to the imbalance in properties.

Of course, due to the high degree of anisotropy of these fibers, it is expected that fiber properties which are not in the principal direction of orientation would be less than those which are in the principal direction of orientation. Unfortunately, the problem is more serious than merely a case of "over-orienting" the fiber, as investigations of PBZT fiber microstructure show. The lack of lateral interactions between microfibrils is postulated to be the main agent responsible for the significant difference in magnitude of compressive and shear properties, compared to tensile values. Lateral interactions in solids are largely

dependent on the type, strength, and orientation of secondary interactions between the covalently bonded chains [DeTeresa, 1985]. These interactions are approximately 100 times weaker than covalent forces, and are relatively short-range [Rodriguez, 1982; Huheey, 1978; Andrews, 1975]. PPTA chains are covalently bonded along the fiber axis, but rely on secondary interactions and hydrogen bonds present throughout the microstructure to hold the fiber together as a three-dimensional solid.

Approaching this problem from a continuum mechanics aspect, the axial compressive failure of uniaxially-oriented fibers has been shown to be due to the onset of a microbuckling instability [DeTeresa, 1985]. This is physically evidenced by the presence of microscopic kink bands and macroscopic hinges. There are two ways in which the critical buckling stresses can cause the chains to buckle: either an extensional mode (uncooperative buckling of chains) or a shear mode (cooperative) buckling. Because the critical compressive stresses for shear mode buckling are calculated to be the lower of the two, it was expected that shear mode buckling would be the mechanism by which compressive failure occurs. From this model it was predicted that buckling would occur when the magnitude of the compressive strength (σ_c) equalled the torsion modulus (G). From experimental measurements of the longitudinal shear (torsion) modulus and the axial compressive strength, it was found that torsion modulus and compressive strength do correlate according to the relation

$$- \sigma_c = 0.3G$$

This model accurately related the values of torsion modulus and compressive strength for a number of uniaxially-oriented fibers, including Kevlar 49[®], PBO, and PBZT.

1.3 Dissertation Overview

Applications of these lyotropic high-performance polymers are limited by their compressive and shear properties which are an order of magnitude less than their tensile strengths. The need to address this problem is not merely a matter of economics, as there is a real engineering demand for fibers with their good damping and tensile properties and temperature resistance. Since compressive and shear properties are not influenced by post-processing treatments, intuition would indicate that a closer look at the coagulation process and the role of coagulant would be a starting point for gaining a deeper understanding of the development of fiber microstructure and thus perhaps influencing shear and compressive properties.

The effect of coagulation variables, including the effect of the coagulation bath, on acrylic fibers had been studied in the early 1960's [Knudsen, 1963]. In fact, the coagulation process and role of coagulant in the properties of two of the lyotropic polymers, PPTA and PBZT, had been studied by two others at the time this work was begun. By inducing slow coagulation of a PBZT/methanesulfonic acid (MSA) solution through introduction of atmospheric water only, a solid phase crystal solvate of PBZT and MSA was formed [Cohen et al. 1987].

Further, when an oriented, uncoagulated film of PBZT in PPA was coagulated in a solution of 85% PPA/15% water, the resulting solid was found to be a crystal solvate of PBZT and PPA, with a totally unique crystal structure [Cohen, 1987]. Again, the formation of the crystal solvate was partially linked to the slow coagulation. Earlier work with PPTA films [Haraguchi et al. 1979 a,b] showed that coagulation of these films into water produced one crystal structure; coagulation into organic solvents produced another. Also, the mechanical behavior of the films were different, with the PPTA/water film exhibiting ductile tensile failure and PPTA/organic solvent films showing brittle tensile failure.

Based on these previous results, a detailed study of the effect of coagulant on the structure and mechanical properties of monofilament fibers produced from PBZT, PPTA, and PBO was initiated. Instrumental to the relevance of this work was to implement these studies while using standard fiber-spinning technology, in order to produce large quantities of fiber and show the possibility of extending this concept to "real world" fiber spinning. Coagulants were chosen for their ability to interact strongly with a polymer, either through molecular or physical interactions. This work was strongly slanted towards fiber mechanics, particularly tensile, shear and compressive properties, but wide-angle X-ray studies were conducted in order to determine if a significant change in torsion modulus or compressive strength correlated with any change in crystal structure.

Finally, another approach to increasing lateral interactions between microfibrils by impregnation of the fiber with a material which would act as a fibrillar glue [DeTeresa, Cohen and Farris, 1988] was

explored as an alternative to coagulation studies. This technique was applied to PBZT, PPTA and PBO fibers, using a number of different impregnation materials.

Chapter II details investigation of the effect of coagulant and impregnation on PBZT fiber; Chapter III concerns coagulation and impregnation studies of PPTA fiber; and in Chapter IV, the results of impregnation and coagulation studies on PBO fiber are discussed. Chapter V presents the major findings of this work and proposes future studies in this area.

CHAPTER 2

POLY(P-PHENYLENE BENZOBISTHIAZOLE) [PBZT]

2.1 Introduction

Poly(p-phenylene benzobisthiazole) [PBZT] was the first fiber studied during the course of this work, and the results obtained from these coagulation and impregnation studies led to the study of their effects on the other two fibers, PPTA and PBO. Both fiber impregnation and coagulation into other non-solvents were viewed as ways in which the lateral interactions between microfibrils might be increased. Impregnation would physically connect microfibrils to their neighbors; coagulation of the fiber into a solution containing molecules which could form a strong association with the PBZT molecule would provide a chemical approach to achieving the same goal. Materials which would form a hard glass after moderate heat treatment were chosen for impregnation studies. Since iodine and iodide ion species were known to form complexes with both large and small molecules [Hassell and Romming, 1962], it was decided to adapt processing conditions by replacing the conventional water bath with an iodine/ethanol solution. The nature of the solvent for the iodide species and its effect on the PBZT fibers was also studied by coagulation of PBZT into an aqueous solution of potassium iodide. Tensile properties and torsion moduli were

obtained for all fibers, and wide-angle X-ray scattering was used to monitor changes in PBZT crystal structure during the coagulation studies.

2.2 Production and Mechanical Characterization of PBZT Fibers

All fibers were spun into monofilaments from a 15.5 weight percent solution of polymer in poly(phosphoric acid). Fibers used in impregnation studies and in the iodine/ethanol coagulation studies were spun from a spinning dope obtained from Stanford Research Institute (SRI) which had an intrinsic viscosity of 25 dl/g (25 IV, $M_w=36,000$). Spinning dopes were loaded, under dry nitrogen, into a spinning cell of the type shown in figure 1.1. The cell was then placed in a vacuum oven at 80°C for 36-48 hours, in order to remove large air bubbles which may have been introduced while loading the dope. Upon removal from the oven, the cell was wrapped with heating tape and the entire assembly was heated to 80°C in 10 minutes or less. Spinning began approximately one hour later; all fibers spun with this system used a 330 μm (13 mil) stainless steel wire-drawing die as a spinneret. Fiber for impregnation studies was coagulated into a large bath filled with chilled water (4-6°C), and the air gap was approximately 2-3 inches. Coagulation studies with iodine/ethanol solutions and ethanol used a smaller bath which necessitated a larger air gap, of approximately 6-8 inches. Coagulant solutions were used at room temperature.

Fiber coagulated in aqueous potassium iodide was produced from a spinning dope provided by the Du Pont Company which had a slightly higher intrinsic viscosity (27 IV). These fibers were spun into a falling stream of coagulant, using a 200 μm (8 mil) stainless steel wire-drawing die (Fort Wayne Wire and Die Company, Fort Wayne, Indiana); this spinning system is fully detailed in Chapter 3.

Fiber tensile properties were measured on 30-mm gage length samples in an Instron Universal Tester equipped with a 2-kg load cell. Tensile moduli are corrected for machine compliance. Torsional moduli were measured on 20-mm gage length samples using a torsion pendulum device that has been described elsewhere [DeTeresa, 1985]. Fiber diameters greater than 70 μm were measured by using a Vickers optical microscope with a calibrated eyepiece; smaller fibers were measured by a laser diffraction method [Perry et al. 1974].

2.3 Fiber Impregnation

2.3.1 Experimental

Previous studies [Cohen, 1985; DeTeresa, 1984] had shown that conventionally spun PBZT fiber which is kept wet after coagulation (and thus retains a more expanded, swollen structure) is readily impregnated by a variety of materials. A solution exchange procedure was developed that takes advantage of the swollen structure and

water- or alcohol-soluble glasses, and works with the concentration gradient in the fiber's environment [Farris, Cohen and DeTeresa, 1987]. This procedure is detailed in figure 2.1, and shows fiber impregnation with either a water-soluble glass (a sodium silicate solution) or an alcohol-soluble glass (a silicate-based sol-gel).

The sodium silicate solution was used as received (Fisher, 40° Baume). The silicate-based sol-gel was based on a formulation from the literature [Brinker et al. 1982]; the formulation as given was

Tetraethylorthosilicate (TEOS)	53.5 mls (0.2400 moles)
H ₂ O (distilled)	86.4 mls (4.80 moles)
Ethanol (100%)	11.0 mls (0.48 moles)
HCl	0.1 ml

All chemicals were used as received. The four ingredients were stirred together at room temperature, and the result was a two-phase immiscible system that would not mix even when stirred overnight. Heating the solution might have resulted in miscibility, but it was highly desirable, in terms of uniformity and safety, to be able to perform these solution exchanges at room temperature. Instead, since a number of articles on this subject had included phase diagrams of the TEOS/H₂O/EtOH system, it seemed apparent that ethanol acted as a compatibilizer [Sakka and Kamiya, 1982; Wallace and Hench, 1984]. For this reason, enough ethanol was added with stirring to result in a clear, one-phase solution. Fifty-five more milliliters of ethanol was required for this to occur.

DIFFUSION-CONTROLLED SOLUTION EXCHANGE PROCESS

WET PBZT IN WATER

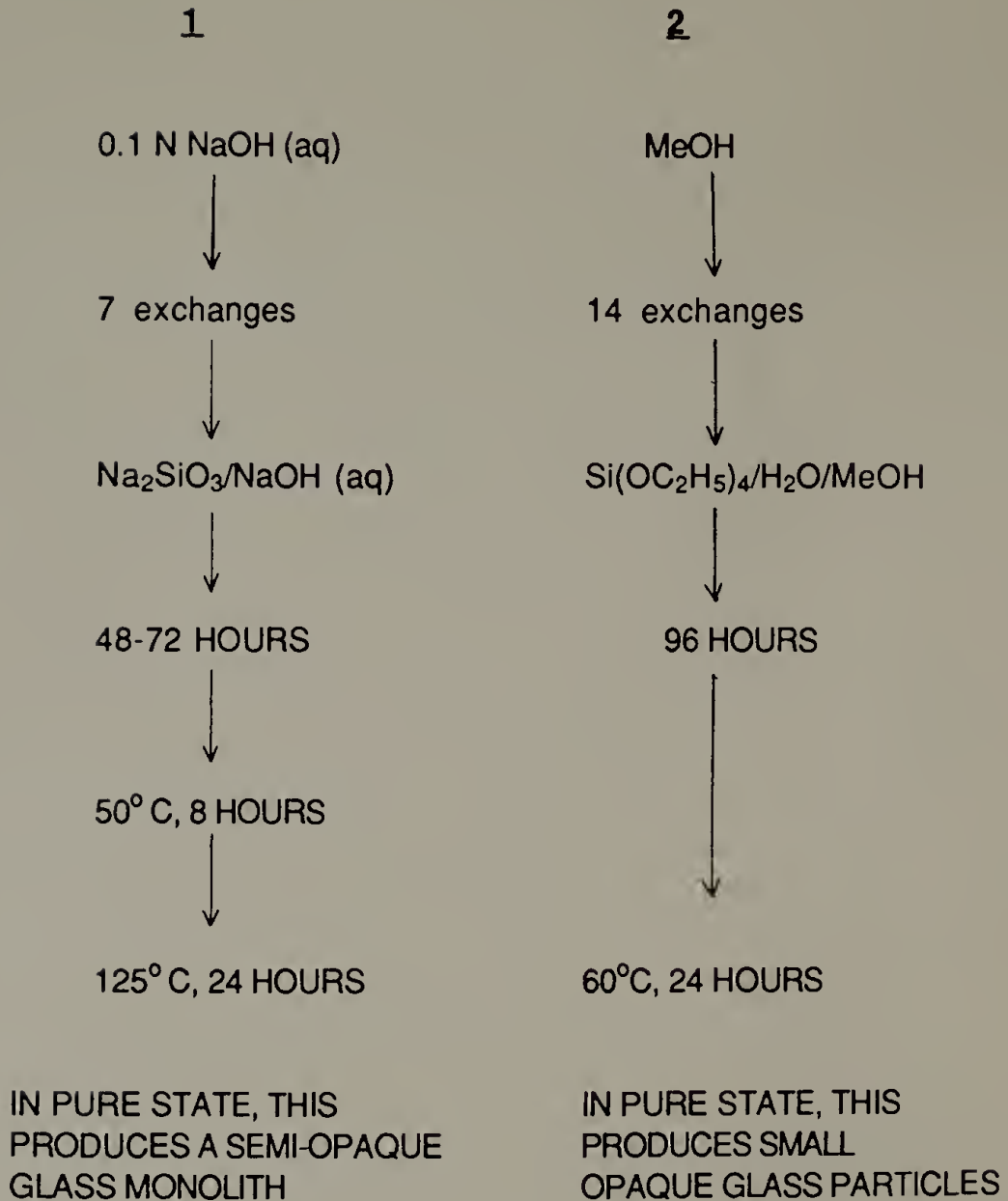


Figure 2.1 A schematic of the solution-exchange process used for fiber impregnation.

Before this solution was used to impregnate PBZT fiber, part was placed in a 60°C forced-air oven and the rest placed in a covered beaker at room temperature. The next morning, the container in the oven was removed and it was found that the solution had dried into small, clear, hard grains, approximately 500 microns in diameter. The sample at room temperature was observed for ten days; in that time, it did not gel. This solution, then, was found to have the two desired properties: it solidified to a hard glass at moderate temperature, and it would be quite feasible to immerse a fiber in it and allow the fiber to stay at room temperature in the solution for several days without gelling. This is the sol-gel system that is referred to in figure 2.1.

Fibers were heat treated according to the temperature needed to harden the impregnator material. To facilitate handling and prevent damage, fiber was loosely wrapped lengthwise around a glass holder that was 8 inches long and 0.5 inches wide. After the impregnation period was over, fibers remained on the holders and were quickly rinsed with water to remove any material which might have adhered to the glass or fiber surface, to prevent sticking. During drying/heat treatment, fibers remained wrapped around these holders; tension was not increased. There was no outward change of appearance after impregnation.

2.3.2 Mechanical Properties

Impregnation of PBZT fibers with the sol-gel ceramic and sodium silicate resulted in fibers with enhanced tensile moduli, as well as

increases in torsion moduli. Figure 2.2 shows a typical stress-strain curve for as-spun PBZT [AS-PBZT(8)] and PBZT impregnated with the sol-gel [PBZT/SG], with both fibers having a spin/draw of 8. The values of tensile properties and torsion moduli for these fibers are given in table 2.1. Impregnation with the sol-gel solution increases the tensile modulus (E) from 150 GPa to 200 GPa, an increase of 33% over the as-spun modulus. Breaking strength (σ_b) is slightly increased without significant loss of elongation to break (ϵ_b). Most important, the torsion modulus (G) of sol-gel impregnated fiber is increased by more than 50%, from 575 MPa to 900 MPa. PBZT fiber used in the sodium silicate impregnation studies had a spin/draw of 3. Tensile properties and torsion moduli for as-spun PBZT [AS-PBZT(3)] and PBZT impregnated with sodium silicate [PBZT/SS] are shown in table 2.2. While this material also raised the torsion modulus by over 50%, the breaking strain for a sodium silicate-impregnated fiber was only 64% of the breaking strain of an as-spun fiber. The accompanying loss in breaking strength, however, was quite small.

Unfortunately, no direct measurements of compressive strength could be made on these fibers. PBZT suffers from severe drying stresses, and fiber allowed to dry under only a small amount of tension is found to contain numerous kink bands throughout the fiber.

Drying stresses cause the microfibrillar elements to buckle upon each other, and no meaningful information about the critical compressive strength or critical compressive strain can be obtained from fibers in this condition. If as-coagulated PBZT fibers are dried under strong tension, drying stresses are minimized and there is no formation of kink bands. When sodium silicate-impregnated fiber was kept wet

Figure 2.2 Typical stress-strain curves for as-spun PBZT [AS-PBZT] and sol-gel impregnated PBZT [PBZT/SOL-GEL].

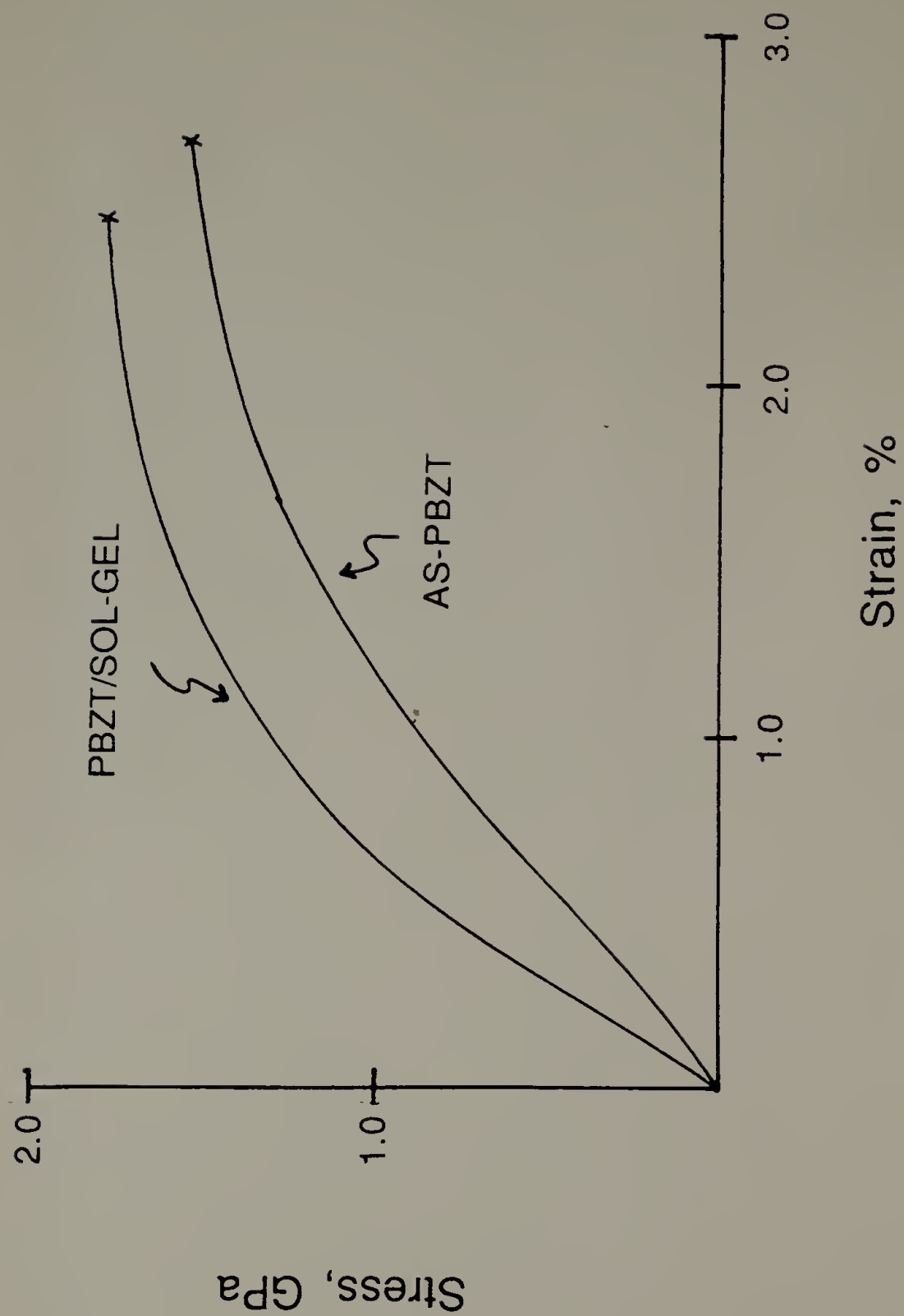


Table 2.1 Mechanical properties of AS-PBZT(8) and PBZT/SG

	<u>AS-PBZT(8)</u>	<u>PBZT/SG</u>
E, GPa	150 ± 10	200 ± 10
σ_b , GPa	1.57 ± 0.1	1.77 ± 0.1
ε_b , %	2.71 ± 0.2	2.51 ± 0.3
G, MPa	575 ± 40	900 ± 22

Table 2.2 Mechanical properties of AS-PBZT and PBZT/SS

	<u>AS-PBZT(3)</u>	<u>PBZT/SS</u>
E, GPa	90 ± 2	150 ± 7
σ_b , GPa	1.53 ± 0.03	1.37 ± 0.05
ε_b , %	2.52 ± 0.1	1.61 ± 0.1
G, GPa	0.82 ± 0.10	1.40 ± 0.07

and dried at 125°C under heavy tension (100-150 MPa), the fiber emerged from the drying oven in ragged shreds. Attempts to obtain mechanical properties on this fiber were ultimately fruitless, due to extreme variations in diameter and irreproducibility of results. Similar heat treatment of as-coagulated fiber produced a smooth fiber with few kink bands, and having tensile properties higher than the as-spun fiber. And as mentioned before, sodium-silicate impregnated fiber which was dried at that temperature under little tension had microscopic kink bands throughout, but visually appeared no different than the as-spun fiber, while having superior properties. The weight percent of either impregnator material within the fiber was unknown; chemical microanalysis facilities at the University cannot detect the presence of silicates or silicon residue and TGA results were not helpful.

One possible explanation for the destruction of the impregnated fiber upon heating is that the sodium silicate began to contract as vitrification set in. The fiber, already constrained under a significant applied tensile load, was then "ripped apart" by this combination of forces.

2.4 The Effect of Coagulant on the Structure and Mechanical Properties of PBZT Fibers

2.4.1 Introduction

Recently, a number of investigators have been interested in the molecular and macroscopic changes which occur when such different polymers as nylon 6, polyacetylene or poly(vinyl alcohol) are exposed to molecular iodine (via solution or vapor) or iodide anions (in solution). When a nylon 6 film having the α crystal structure is exposed to aqueous iodine/potassium iodide solution, its interchain hydrogen bonding is destroyed and a nylon 6-iodide complex is formed. This new material can be easily drawn in order to increase the tensile modulus; when the iodide anions are removed, the crystal structure transforms to the γ form [Arimoto, 1962; Chuah, 1985; Murthy et al. 1985]. The mechanisms responsible for the changes in crystal structure and iodine sorption in iodine-doped polyacetylene is believed to be a "hybrid" polyacetylene/iodine unit cell [Baughman et al. 1983; Danno et al. 1983]. The formation of a chromophore as a result of poly(vinyl acetate)/iodine/iodide complexation, while not yet definitively explained, is the basis for an analytical technique to determine the degree of hydrolysis of poly(vinyl acetate) [Ahmed et al. 1984].

These complexations occur because iodine, along with the other halogens (except fluorine), is able to form a charge-transfer complex with a wide variety of electron donors. There are two types of suitable donors:

σ donors, a wide variety of molecules which include nitrogen and oxygen bases; and π -donors, which include aromatic systems and molecules with localized π bonding, such as alkenes [Downs and Adams, 1973]. The ability of halogens to greatly increase the conductivity in low-dimensional materials is linked to their tendency to form stable, linear polyhalide ions; their sizes and shapes are highly compatible with stacked and planar organic materials [Marks and Kalina, 1982]. With regard to the ability of iodine to form charge-transfer complexes, Mulliken and others have shown that iodine and its compounds form an association with nitrogen-containing molecules which is intermediate in strength between Van der Waals forces and covalent bonding [Mulliken and Person, 1967]. Examples of such systems are iodine in solution with pyridine, triethylamine, or benzene/benzamide [Hassel and Romming, 1962].

2.4.2 Experimental

PBZT (Stanford Research Institute, IV=25dl/g, M_w =36,000, 15.5% polymer in poly-phosphoric acid (PPA)) was heated to 80°C and coagulated in distilled water, 95% ethanol or an 18% iodine/ethanol solution (w/w). Fibers were allowed to soak in fresh aliquots of coagulant overnight, to leach out any remaining acid. All fibers were allowed to air dry while on the take-up wheel; those coagulated in iodine/ethanol were first rinsed with ethanol to remove surface iodine.

The solution exchange technique described in section 2.3.1 was employed in order to determine differences, if any, between fibers coagulated in an iodine/ethanol solution and those produced by the impregnation technique. PBZT fibers were spun from the same solution, coagulated in a water bath and washed to remove excess acid. The water in the fiber was slowly replaced with ethanol, until the fiber's environment consisted of 100% ethanol. At this point, enough iodine was added to the ethanol to make a 20% solution (w/w). The fiber remained in this environment for one week; it was then removed, quickly rinsed in ethanol to remove surface iodine, and allowed to air dry.

27 IV PBZT spinning dope was used in the aqueous potassium iodide coagulation study, since no more 25 IV spinning dope was available. The concentration of potassium iodide in water was 8.3 weight percent, which corresponds to 0.5M. Fibers with identical spin draw, but on different bobbins, were soaked either in water or a fresh aliquot of aqueous potassium iodide to remove remaining acid.

A Statton camera and a Siemens D-500 X-ray diffractometer, both utilizing Cu K α radiation, were used in wide-angle X-ray scattering (WAXS) studies. Fibers were wrapped in bundles around cardboard mounts; when using the diffractometer, a lead shield was placed over the cardboard to prevent extraneous scattering. Equatorial scans were taken on the diffractometer using line focus collimation, with incident beam slits of 0.3 $^{\circ}$ (2 θ) with a final slit of 0.15 $^{\circ}$ (2 θ). In Statton studies, sample-to-film distances were 74.1 mm, unless otherwise stated. Schematics are included when needed to show fine details which do not transfer to photographic media as well. Fiber densities were obtained by measuring exactly one meter of fiber, then weighing on a Mettler

balance that was accurate to 10^{-6} grams. The sample was weighed three times and an average was taken. An average diameter was determined by measuring the fiber in 100 places along its length using the laser diffraction technique mentioned earlier; this average diameter was used in calculating the density. Unless stated otherwise, all mechanical and physical data was obtained from as-spun fibers.

Heat treatment of selected fibers which had been coagulated into iodine/ethanol was done in a tube furnace, under no tension. The design of the quartz tube which fit into the oven prevented the fiber from being taken up or tensioned; fiber was positioned along the middle two-thirds of the tube. Keeping in mind that iodine sublimates slightly above room temperature, and that PBZT is stable under nitrogen up to 600°C , fibers were quickly heated (in 15 minutes or less) to 395°C under nitrogen. They were held at this temperature for 5 minutes, then allowed to cool to room temperature by leaving the nitrogen flow on while turning off the heating element; this process took 1-1/2 to 2 hours before a temperatures of $40\text{-}60^{\circ}\text{C}$ were obtained. Before and after heat treatment 100 diameters were measured along the fiber length, again using the laser diffraction technique. No mechanical properties were obtained for this fiber.

Two years after these fibers were spun, this experiment was repeated using these same fibers, with heating times at 395°C being 5, 30 or 60 minutes.

Dr. Chih Chang performed resonance Raman spectroscopy on all fibers coagulated in iodine/ethanol, and on a control fiber of PBZT.

2.4.3 Fiber Microstructure

Figures 2.3 and 2.4 show wide-angle X-ray equatorial diffractometer scans of PBZT fibers with a spin/draw ratio of 9.7 coagulated in water or in the iodine/ethanol solution (designated as PH9 and PI9, respectively). Meridional reflections of PI9 are shown in the Statton film and schematic (figure 2.5); figure 2.6 is the Statton film of PH9, with meridional reflections emphasized. The standard equatorial (E) and meridional (M) reflections for PBZT coagulated in water are found in the PH9 fiber and are listed in table 2.3. Table 2.4 lists the meridional and equatorial reflections for the PI9 fiber, the associated d-spacings and, where possible, assigns the reflections seen in the PI9 fiber.

The PI9 fiber does not contain all reflections present in the (standard) PH9 fiber. Also, several new reflections are present. The equatorial spacings of 9.76 Å and 4.87 Å are unique to the PBZT/iodide fiber, and are also present in the wide-angle flat film of PBZT coagulated into iodine/ethanol with a spin/draw of 3. While the standard PBZT E₃ reflection at 3.40 Å is present in PI9 and PI3, the E₂ reflection at 5.60 Å is missing. Furthermore, two meridional reflections which correspond to d-spacings of 15.4 Å and 10.6 Å are found in the Statton photograph of PI9, but are not found in the Statton photographs of either PH9 or in PBZT fibers coagulated into 95% ethanol with a spin/draw ratio of 3 (PE3, shown in figure 2.7).

The equatorial spacing of 9.76 Å and the meridional spacing of 15.4 Å have been observed in a number of other molecular complexes

Figure 2.3 Wide-angle X-ray diffractometer equatorial scans of PBZT fibers coagulated in water, with a spin/draw of 9.7 [PH9].

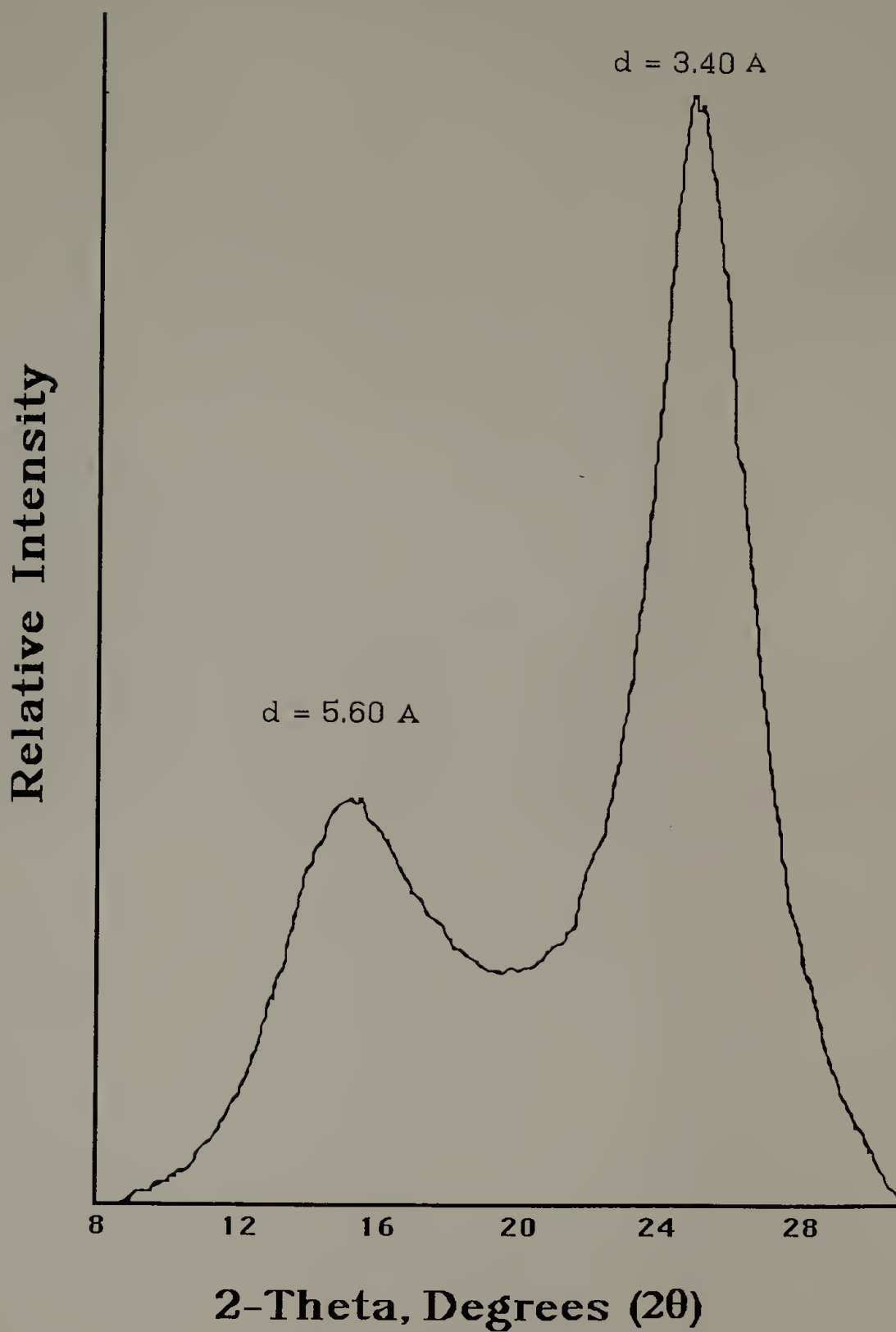


Figure 2.4 Wide-angle X-ray diffractometer equatorial scans of PBZT fibers coagulated in iodine/ethanol, with a spin/draw of 9.7 [PI9].

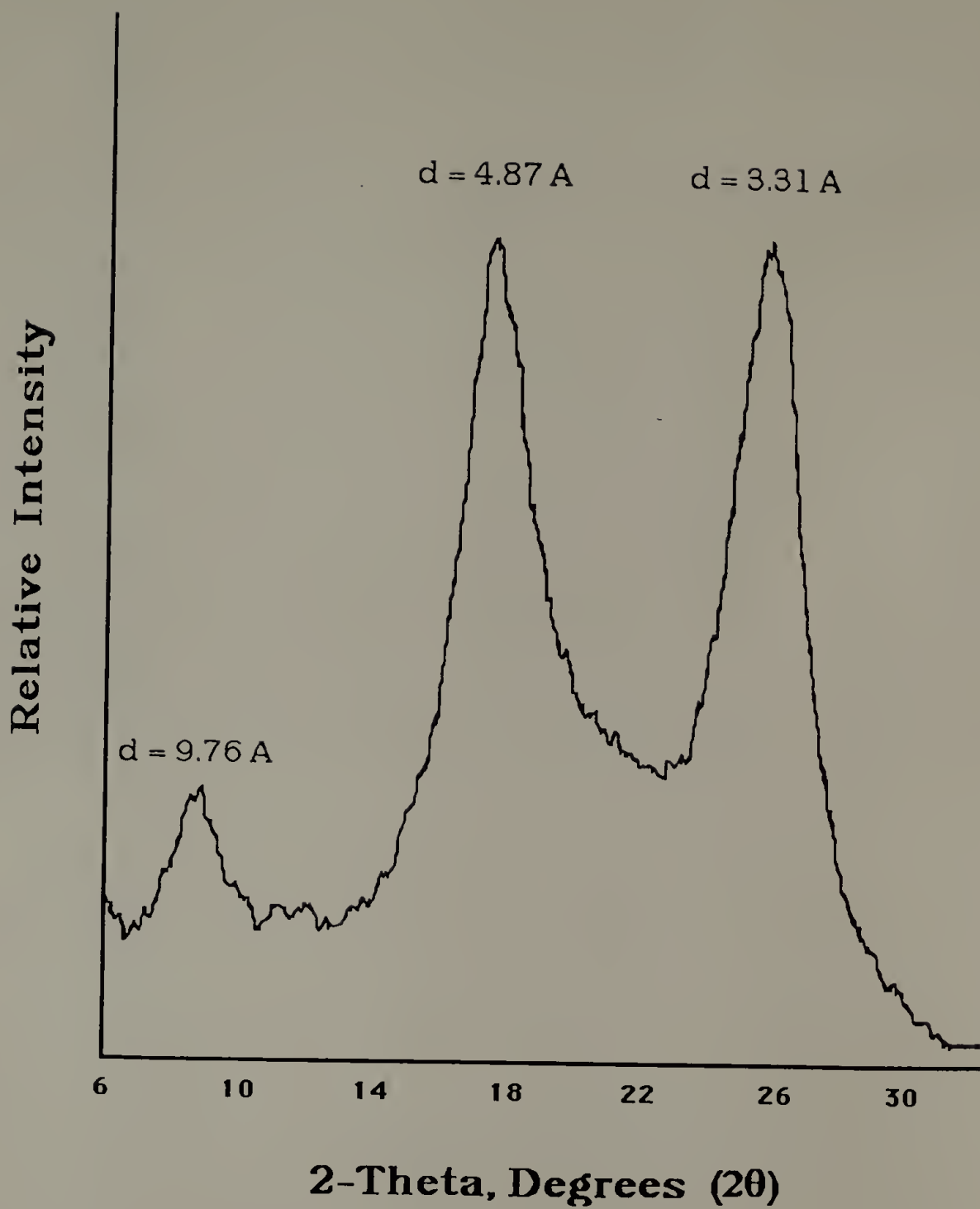


Figure 2.5 *Top:* Statton film emphasizing the meridional reflections of PI9. *Bottom:* Schematic of meridional reflections.

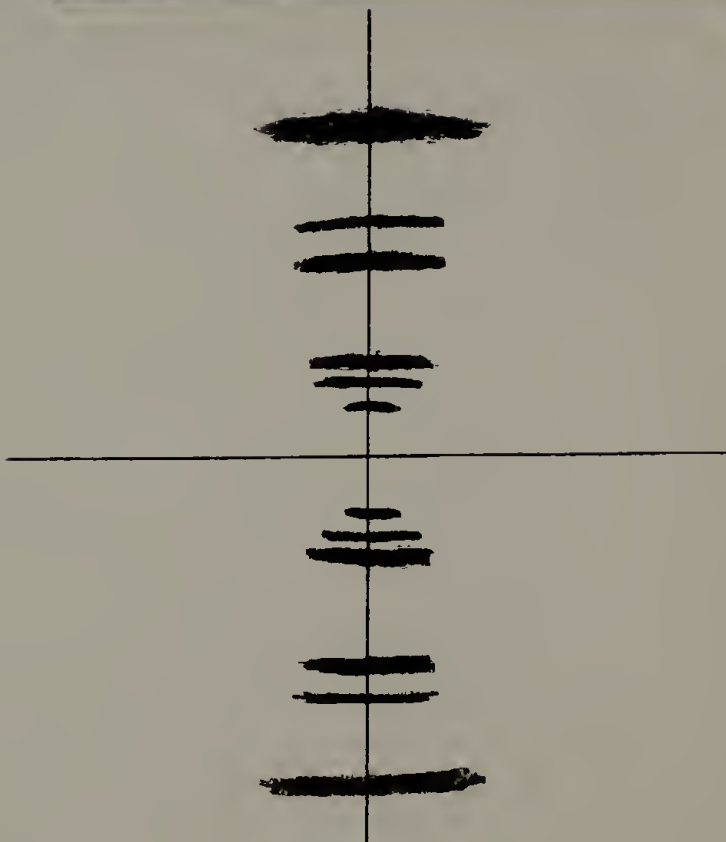


Figure 2.6 *Top:* Statton film emphasizing the meridional reflections of PH9. *Bottom:* Schematic of reflections.



4.4

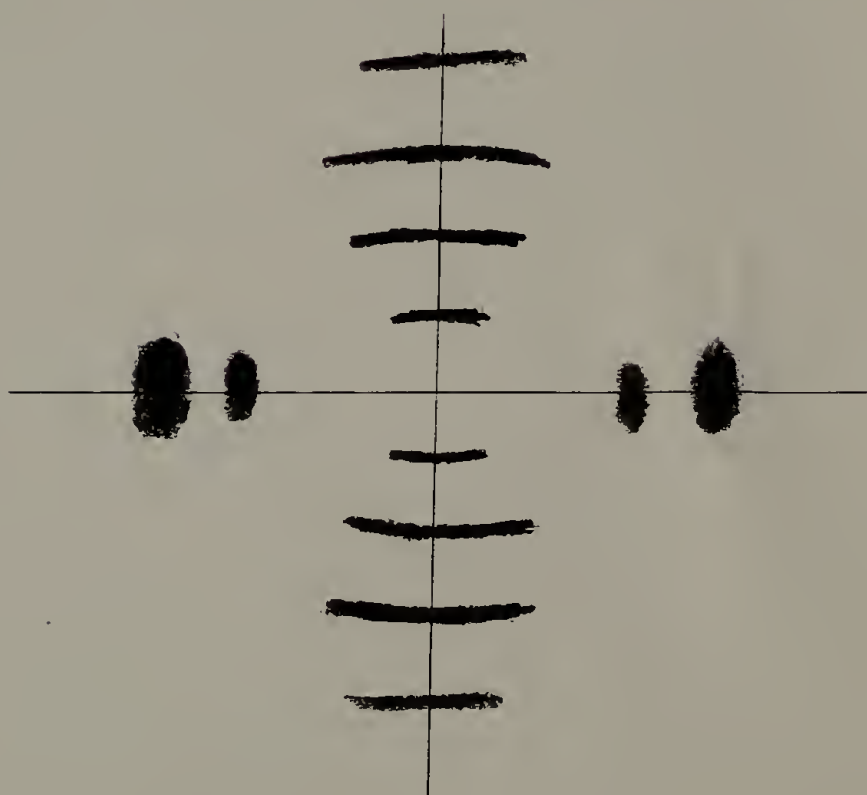


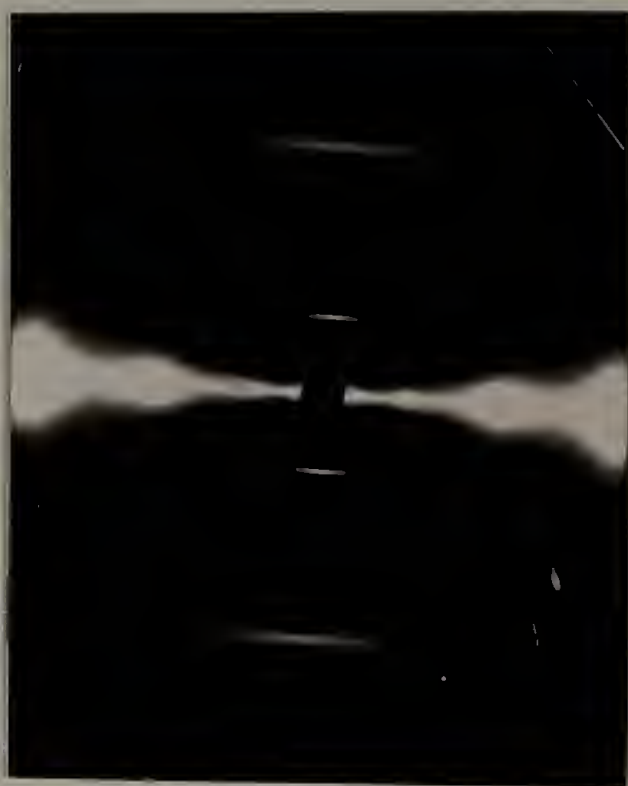
Table 2.3 d-spacings of reflections of PBZT coagulated in water [PH9]

<u>Reflection</u>	<u>d(Å)</u>
E ₁	5.60
E ₂	3.40
M ₁	12.5
M ₂	6.13
M ₃	4.10

Table 2.4 Assignment of wide-angle X-ray scattering reflections for PI9

<u>Reflection</u>	<u>d (Å)</u>	<u>Assignment</u>
E ₁	9.76	I ₃ ⁻
E ₂	4.87	Unknown
E ₃	3.31	PBZT
M ₁	15.4	I ₅ ⁻
M ₂	12.5	Unknown
M ₃	10.6	Unknown
M ₄	4.70	Unknown
M ₅	4.10	PBZT

Figure 2.7 Statton photograph of PBZT coagulated in ethanol, having a spin/draw of 3 [PE3].



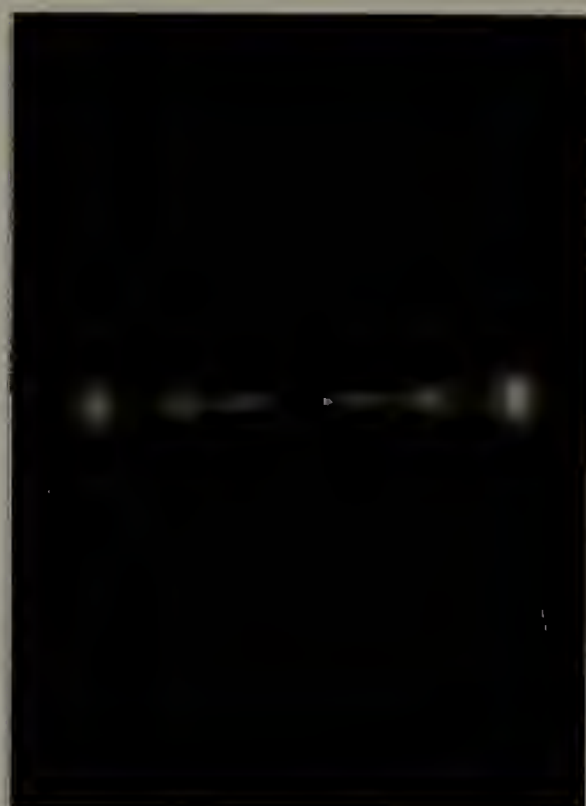
involving iodine and an electron donor molecule. These reflections are "fingerprints" for the I_3^- and the I_5^- anions, respectively [Coppens, 1982].

Resonance Raman spectroscopy was performed in order to independently confirm the presence of the I_3^- and the I_5^- anions. Both these species appear at characteristic wavenumbers that have been well-documented in the literature [Keifer, 1974; Teitelbaum et al. 1978]. The I_3^- anion generally appears at $109\text{-}113\text{ cm}^{-1}$ and the I_5^- anion at 160 cm^{-1} . A control sample of PH9 fiber was run to "tune" the laser to the region to be investigated. Spectra of all fibers which were coagulated in iodine/ethanol contained absorbance bands at both locations, showing that these fibers contained both the I_3^- and I_5^- anions; the spectrum of the PH9 fiber did not exhibit these absorbance bands

PBZT fiber which was impregnated with iodine in a 20% (by weight) iodine/ethanol solution, according to the procedure given in section 2.3.1, exhibited the same deep purple color as the iodine-coagulated fiber (PBZT is normally bright red). The Statton WAXS pattern of the iodine-impregnated fiber (figure 2.8) appears no different than the pattern for the as-spun PBZT fiber of the same spin/draw, shown in figure 2.9.

The wide-angle X-ray scattering pattern of PBZT fiber which was coagulated into an aqueous solution of potassium iodide is shown in figure 2.10; there are no changes in d-spacings from the control fiber which was coagulated into distilled water (figure 2.11). Further, there was no difference in Statton diffraction patterns between fiber coagulated into the aqueous KI solution and soaked in a fresh aliquot of that solution, versus that soaked in water.

Figure 2.8 Statton film of iodine-impregnated PBZT fiber.



110

Figure 2.9 Statton film of as-spun PBZT fiber.






Figure 2.10 Statton film of PBZT fiber coagulated in 0.5M (8.3%) aqueous potassium iodide solution, having a spin/draw of 20.



Figure 2.11 Statton film of PBZT fiber coagulated in water, spin/draw of 20.



2.4.4 Mechanical Properties

Iodine complexation can also affect the mechanical properties of these as-spun fibers; the amount of iodine present in the fiber may be an important factor. Table 2.5 lists mechanical properties, average diameter, weight percent iodine (as obtained through standard chemical microanalysis techniques [Ma and Rittner, 1979]) and the densities for PBZT fibers coagulated into water, 95% ethanol, and iodine/ethanol. The most striking results are those for tensile strength and shear modulus for PBZT coagulated in iodine/ethanol, having a spin/draw of 3 (PI3). When compared to the control fiber, PE3, there seems to be an improvement in the strength of the microfibrils in the direction of the chain axis as well as perpendicular to it. The shear modulus can be used as a measure of lateral cohesiveness between chains or microfibrillar regions, and has been shown to be related to the compressive strength of rigid-rod fibers [DeTeresa, 1988]. Table 2.6 lists the mechanical properties for the iodine-impregnated and control fibers; there is no apparent difference in the tensile or shear modulus of the two groups of fiber. The stress-strain behavior of these fibers is summarized in figure 2.12.

The tensile properties and shear moduli of fibers of coagulated in water and in aqueous potassium iodide are shown in table 2.7. The fibers coagulated in potassium iodide were then further soaked in potassium iodide solution immediately after spinning. Within the standard deviation, there is really no difference in the mechanical properties of these two fibers.

Table 2.5 Mechanical properties of PBZT fibers coagulated into water, ethanol and iodine/ethanol

Coagulant	PI3	PE3	PI9	PH9
	Iodine/ Ethanol	Ethanol	Iodine/ Ethanol	Water
Spin/Draw	3	3	9.7	9.7
Diameter, μm	77 ± 1	48 ± 2	68 ± 2	48 ± 2
Tensile Modulus (E), GPa	170 ± 7	230 ± 50	150 ± 50	140 ± 50
Tensile Strength (σ_b), GPa	$2.2 \pm .1$	$1.8 \pm .1$	$1.5 \pm .1$	$1.6 \pm .1$
Shear Modulus (G), GPa	1.14 ± 0.04	0.630 ± 0.02	0.610 ± 0.05	0.600 ± 0.06
Wt. % Iodine	19.5	0	40.0	0
Density, g/cm^3	1.84 ± 0.25	1.50 ± 0.25	-----	-----

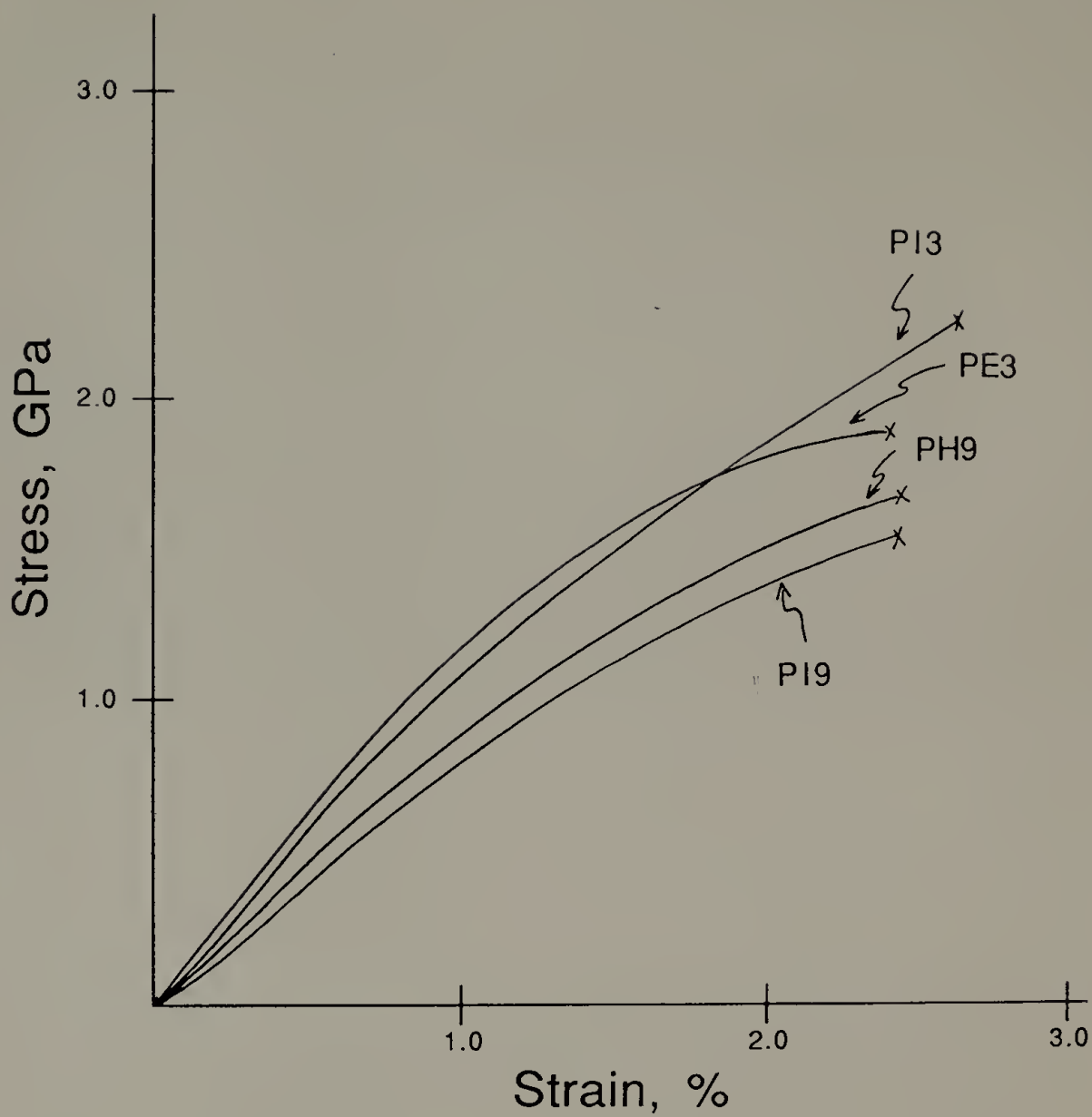
Table 2.6 Mechanical properties for as-spun and iodine-impregnated PBZT fibers

	AS-PBZT	PBZT*I
Spin/Draw	8.0	8.0
Average Diameter, μm	74.1 ± 12.7	65.0 ± 11
Tensile Modulus, E (GPa)	150 ± 9	102 ± 18
Tensile Strength, σ_b (GPa)	1.6 ± 0.1	1.6 ± 0.2
Shear Modulus, G (GPa)	0.58 ± 0.04	0.58 ± 0.02

Table 2.7 Mechanical properties of as-spun PBZT [AS-PBZT] and PBZT coagulated and soaked in aqueous potassium iodide [PBZT/KI/KI]

	<u>AS-PBZT</u>	<u>PBZT/KI/KI</u>
S/D	20	20
E, GPa	137 ± 10	138 ± 15
σ_b , GPa	1.70 ± 0.1	1.64 ± 0.2
ϵ , %	1.90	1.99
G, GPa	0.52 ± 0.06	0.56 ± 0.07

Figure 2.12 Typical stress-strain curves for PBZT fibers coagulated in water, ethanol and iodine/ethanol.



2.4.5 Effect of Heat Treatment on Iodine /Iodide Content

Heat treatment of PI9 and PH9 fibers was carried out in order to determine how strongly the iodine anions complexed with the PBZT molecules. As stated in section 2.4.2, fibers were quickly heated to 395°C, held at this temperature (under nitrogen) for five minutes, then allowed to slowly cool down to room temperature. For both PH9 and PI9 fibers, there was no change in average fiber diameter after heat treatment. Chemical microanalysis showed that as-spun PI9 contained 40% iodine species by weight while the heat-treated fiber contained 29% iodine species; the heat-treated fiber retained almost 75% of the original weight percent iodine species, even at temperatures far above the sublimation and boiling points of iodine.

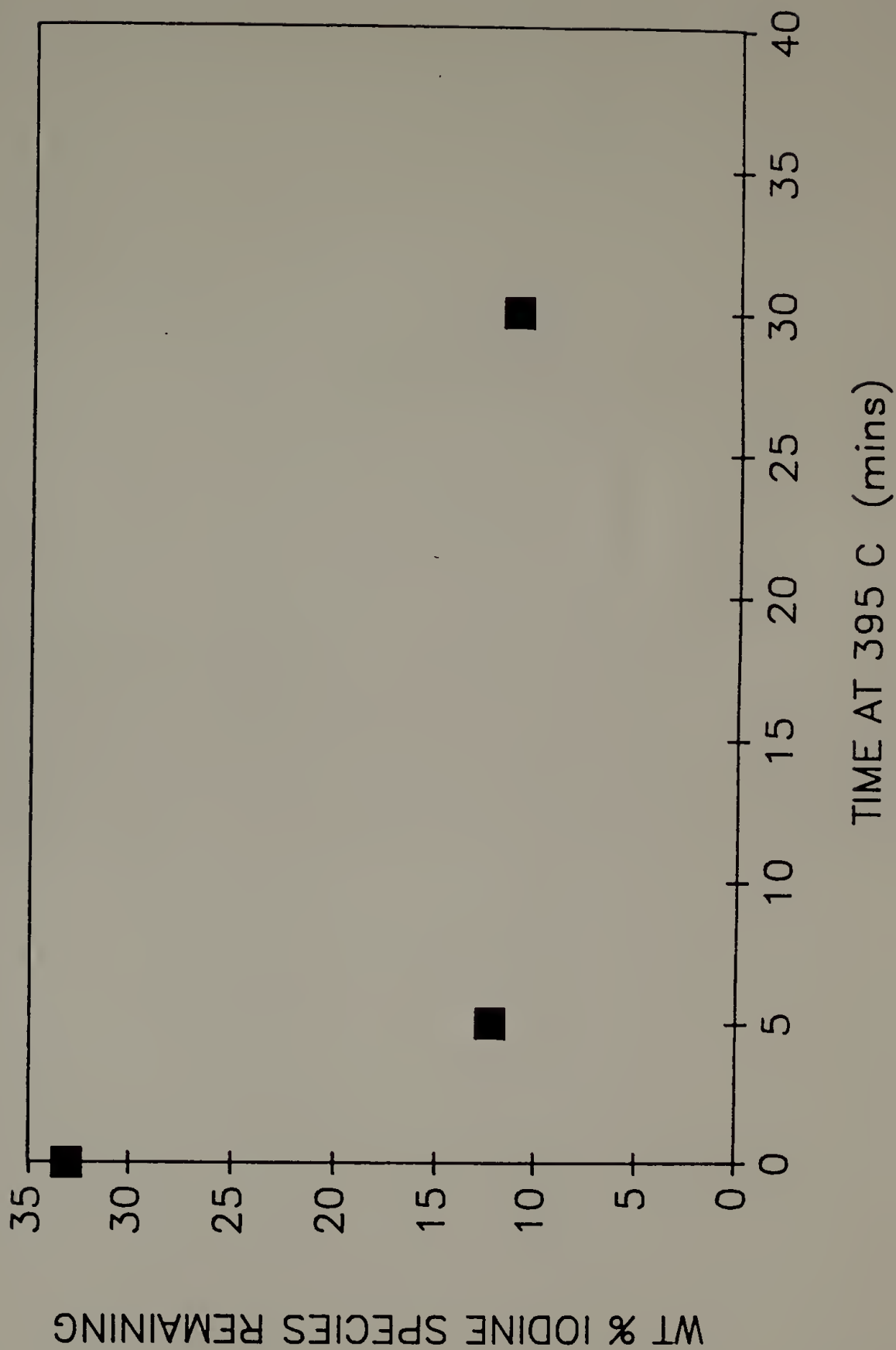
As a result of discussions with this thesis committee two years later after the original investigations, it was suggested that the fibers be heat-treated for varying lengths of time, in order to determine the equilibrium amount of iodine species in the fiber after extended heat treatment. The same procedure was followed, but fiber was held in the oven for 5, 30 or 60 minutes. Although fiber diameters were measured along the length prior to heat treatment, measuring them after heat treatment was impossible because the fibers had become extremely brittle. This happened even when the sample had been heated for only five minutes, clearly showing a difference between this fiber in March 1989 and the same fiber in March 1987, when the first heat treatment studies had been run.

Due to extreme brittleness, fiber heat-treated for 60 minutes could not be recovered or analyzed. Figure 2.13 graphs the amount of iodine present in the fiber as a function of heating time. Chemical microanalysis of these treated fibers and the control fiber shows that the control fiber has less iodine species present in it than was found in the same fiber two years ago (33 weight percent versus 40 weight percent) and that most of the iodine species appears to be lost in the first five minutes of heating. No mechanical properties were obtained for these fibers, due to limited amount of sample and fiber brittleness.

2.5 Conclusions

These results have shown that the composition of the coagulation bath can measurably affect both the structural and mechanical properties of a fiber spun from an anisotropic solution of a lyotropic polymer, and raises the possibility of tailoring fiber properties through judicious choice of coagulants. Neither impregnation of a water-coagulated PBZT fiber with iodine/ethanol solution nor coagulation of PBZT into an aqueous potassium iodide solution had any apparent effect on structural or mechanical properties. On the other hand, coagulation into iodine/ethanol solution can greatly change both structural and mechanical properties of the PBZT fiber, most probably through the construction of a "host-guest" relationship between the polymer and iodide anion species.

Figure 2.13 The amount of iodine species present in the PI9 fiber in March 1989 as a function of heating time.



Among the best known host-guest relationships between molecules are the intercalation compounds formed by graphite and a variety of substances, such as sulfuric acid and alkali metals. These intercalated structures differ from pure graphite in that the distance between carbon layers is increased by the thickness of the intercalated layer. Intercalation in carbon is based on the occurrence of specific interactions between the host and guest; electrons are either transferred from the carbon layers to the guest, or from the guest into the carbon layers. Further, the guest layers can be separated by one or more carbon layers--this is known as the staging phenomenon [Boehm et al. 1986].

A type of host-guest relationship which does not depend on chemical interactions between the two species, but rather compatibility of shapes, is the one formed between poly(ethylene oxide) and p-dibromobenzene (p-C₆H₄Br₂). A proposed model of the compound is an alternating structure of polymer chains and p-C₆H₄Br₂ molecules, with the p-C₆H₄Br₂ molecules neatly filling the channels between the polymer chains [Point and Coutelier, 1985].

The "intercalation" or "host-guest" compounds formed between iodine and/or its anions and a variety of molecules often have a similar structure, although their formation is based on relatively strong molecular interactions. X-ray diffraction work with iodine-doped polyacetylene has found that a structure exists in which iodine-rich planes alternate with planes of polyacetylene chains. Packing calculations for this proposed model, which assumes that a column of iodide anions (I₃⁻ or I₅⁻) displaces either 1 or 2 chains, produce spacings which closely match those obtained experimentally [Baughman et al.

1983]. Another system, which was held to be a model of the starch-iodine complex, was composed of a host which consisted of dimerized benzamide molecules which were stacked to form long channels. Each channel was filled with the "guest", a double chain of tri-iodide (I_3^-) ions, which ran the entire length of the channel [Reddy et al. 1964].

The structure of the nylon-6/iodine complex is still not completely resolved, although different groups have proposed similar models which differ only in the anion species present. An alternating structure of nylon-6 chains and I_3^- ions was proposed by researchers who did not see a strong Raman absorption band in the region which corresponds to the I_5^- region [Chuah, 1985]. Other researchers obtained data from both wide-angle X-ray scattering and resonance Raman, and concluded both the I_5^- and the I_3^- ions were present. Their interpretation of the wide-angle X-ray scattering data resulted in a model where I_5^- anions are in columns and oriented parallel to the polymer chain; the I_3^- ions are aligned perpendicular to the nylon 6 chain direction [Murthy et al, 1985; Burzynski et al. 1986].

The PBZT fiber has been shown [Cohen and Thomas, 1985; Cohen, 1987] to be composed of a microfibrillar network; each microfibril is 70-100 Å in diameter. While these microfibrils are both physically entwined and connected via Y-shaped junctions, there is a significant void volume in the macroscopic fiber. Certainly, further investigation of the chemical and physical interactions of the iodide species with the microfibrillar network and the PBZT molecule are necessary--the actual ratio of I_3^- to I_5^- is unknown at this time, as is the degree of "staging". However, one possible model for the iodine/PBZT composite fiber is

shown in figures 2.14 and 2.15. The heat treatment results suggest that some of the iodide anions are located between microfibrils, while WAXS results verify that others are located within the microfibrils, strongly complexed to individual PBZT chains. In this figure, the I_3^- and I_5^- anions are purposely aligned perpendicular and parallel to the fiber/chain axis, because of their respective equatorial and meridional locations in the WAXS studies. This model assumes that there is no change in the crystal structure of the PBZT unit cell, even though some standard PBZT reflections are missing.

Another model is similar in terms of stacking the iodide ions but differs in that it proposes the crystal structure has changed [Martin, 1989]. This model, shown in figure 2.16, has iodide columns (composed of both I_3^- and I_5^- ions) stacked in between the PBZT chains. The b and c axes of the unit cell remain unchanged, at 3.6 Å and 12.5 Å, respectively. But the absence of the equatorial reflection at 5.60 Å, and the new equatorial reflections at 9.76 Å suggests that the new unit cell is larger, with an a axis of 9.76 Å. In either case, the bridging scheme has been postulated for other polymer/iodine systems, such as in poly(N-vinyl pyrrolidone). Here, pyrrolidone rings not complexed with iodine are in equilibrium with species consisting of two rings connected by an iodine bridge [Cheng et al. 1985]. Similar phenomena were noted with the increase in the tensile modulus of a film of poly(vinyl alcohol) soaked in KI (aq). This was postulated to be a consequence of the formation of extra junction points due to the iodide/PVA "complex" [Kojima et al. 1985], although admittedly much more study in this area is required.

Figure 2.14 Proposed model, which shows iodide anions in between the microfibrillar network. The diameter of the microfibrils has been found to be in the 70-100 Å range; their length, and the number of Y-shaped junctions, is unknown [Cohen and Thomas, 1985].

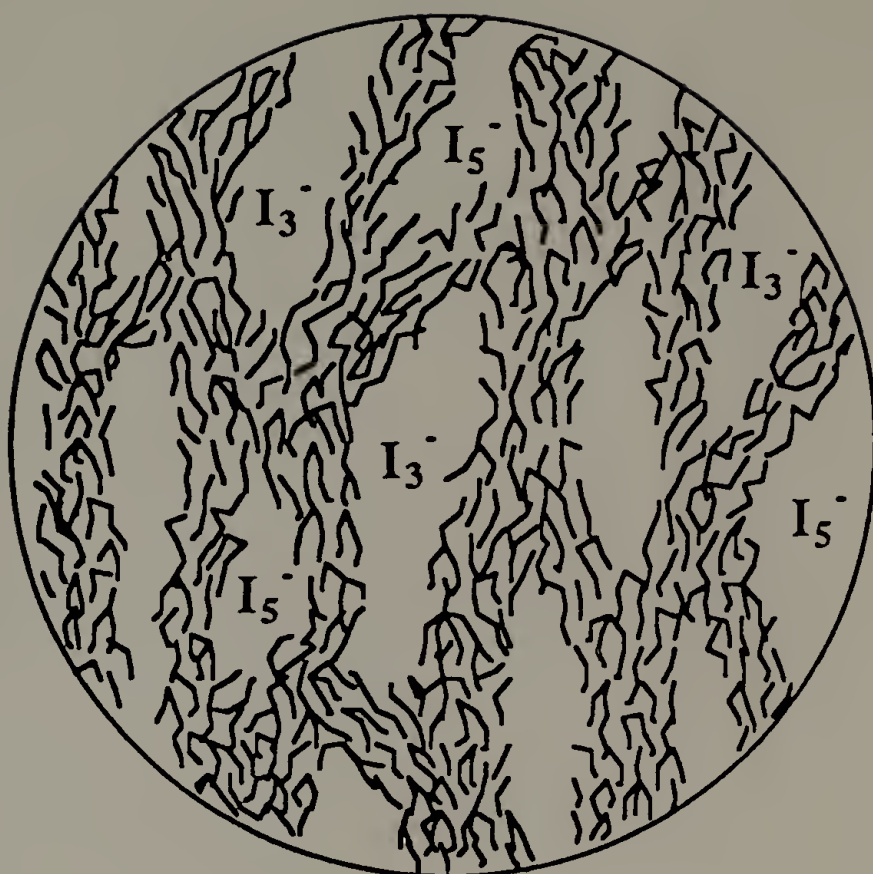
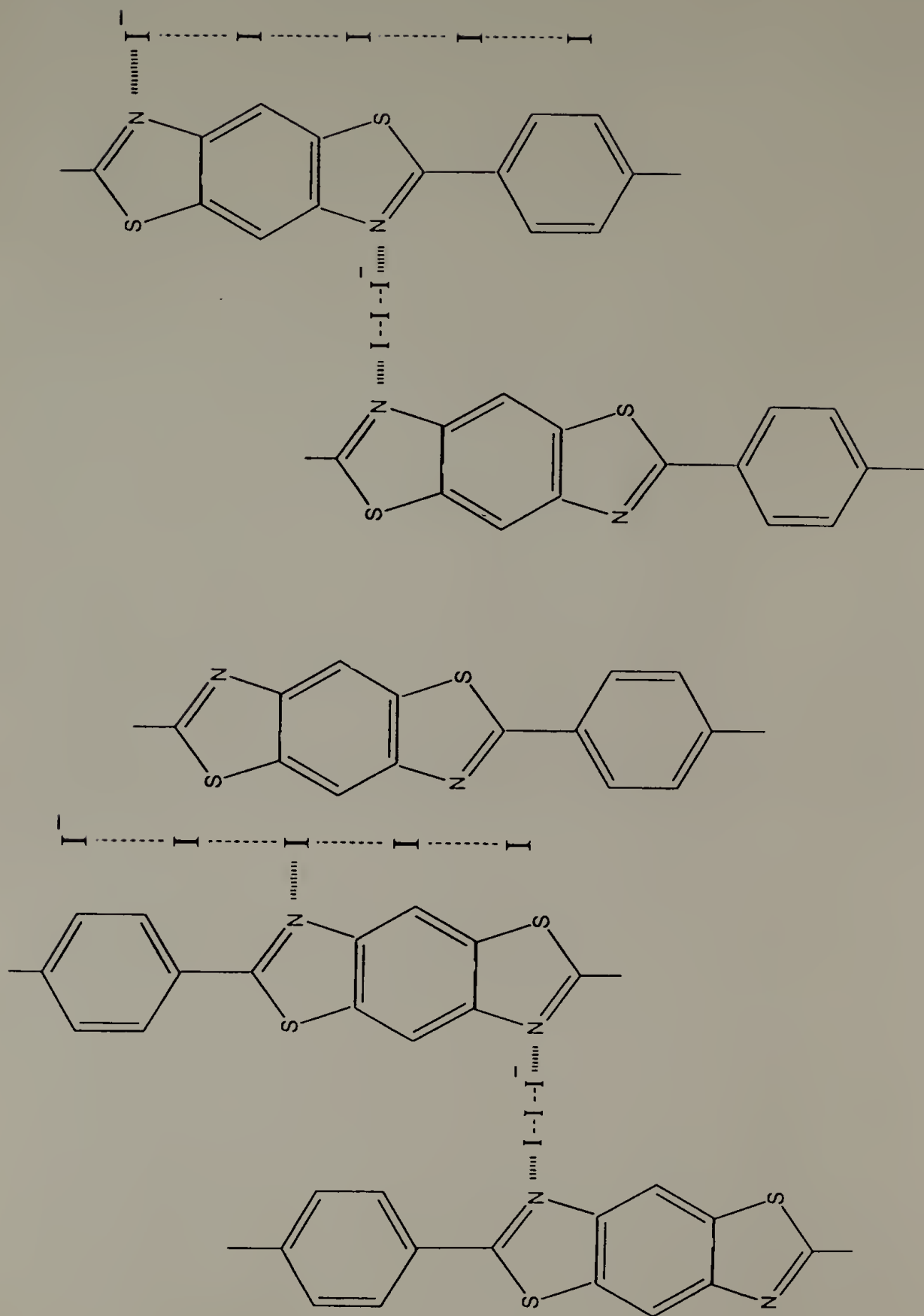


Figure 2.15 Another aspect of the proposed model shown in figure 2.14. Iodide anions are complexed with PBZT chains within a microfibril.



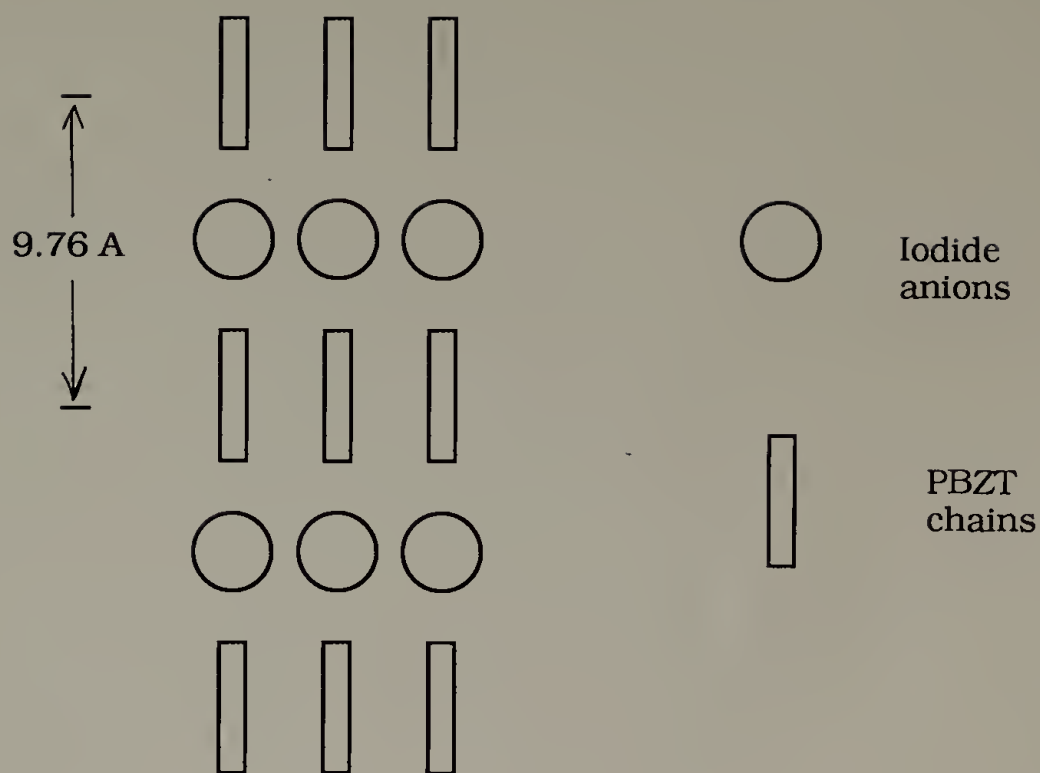


Figure 2.16 Another proposed model for the PBZT/iodide anions "alloy", which supposes a change in crystal structure of the PBZT chain.

Either of these models would also help to explain the increased tensile and shear properties found in the as-spun PI3 fiber; they have effectively increased the lateral interactions between the PBZT microstructure. The PBZT fiber had a shear modulus of 1.14 GPa (almost double that of PE3) and a breaking strength of 2.2 GPa; these values are the highest seen in this laboratory for as-spun fibers of either equivalent spin/draw or diameter. Finally, it is noted that the shear modulus appears to be sensitive to the amount of iodine present in the fiber, which in itself may be a function of the spin/draw ratio. These models also account for the stability of the fibers under vacuum and in air.

CHAPTER 3

POLY(P-PHENYLENE TEREPHTHALAMIDE) [PPTA]

3.1 Introduction

Poly(p-phenylene terephthalamide) [PPTA] was the first lyotropic liquid crystalline polymer to be spun into fibers having exceptionally high tensile properties [Bair and Morgan, 1975; Blades, 1974 a,b] and become commercially successful. Fibers of PPTA are commonly referred to as Kevlar[®], and are a product of the Du Pont Company; they are manufactured in Europe by the Dutch chemical company AKZO under the name of Twaron[®]. Typical tensile properties for these fibers after heat treatment are a Young's modulus of 120-125 GPa and tensile strengths in the range of 3.2-3.5 GPa [Jaffe and Jones, 1985].

An entirely new class of liquid crystal polymers whose liquid-crystal nature is derived solely from its extended-chain conformation, the synthesis and solution properties of PPTA were described in two seminal papers published in the mid-1970's [P.W. Morgan, 1977; Bair et al. 1977]. PPTA forms nematic liquid-crystal domains in fuming sulfuric acid at approximately 10 weight percent. A drop in solution viscosity accompanies the formation of the anisotropic state. At room temperature, solutions containing more than 12% PPTA in sulfuric acid are anisotropic solids

[Jaffee and Jones, 1985]; at concentrations greater than 15%, these anisotropic solids are composed of a crystal-solvate complex which forms between H_2SO_4 and PPTA molecules [Iovleva and Papkov, 1982].

Extensive characterization of the morphology of Kevlar 49[®], using wide-angle electron diffraction (WAED) and dark-field imaging [Dobb et al. 1977a,b] established that the fiber's microstructure consists of a system of radially-arranged, hydrogen-bonded sheets, regularly pleated along their long axes. Further, it was found that crystallographic register exists between adjacent ordered zones due to the extended-chain structure of PPTA molecules [Panar et al. 1983].

While these molecular characteristics result in a fiber whose tensile properties are very impressive, this anisotropy leads to weaker torsion modulus and compressive strength. The compressive strength for Kevlar[®] fibers was estimated to be 620 MPa by a technique which directly measured critical compressive strain [DeTeresa, 1985], and 370-420 MPa by the tensile recoil technique which directly measures compressive strength [Allen, 1987]; the values obtained by the recoil technique are closer to the value of compressive failure observed in composites. The tensile strength, with a value between 3.2-3.5 GPa, is approximately 8 times the compressive strength. The torsion modulus, at 1.50 GPa, is approximately 1% of the tensile modulus of Kevlar 49[®]. Post-processing heat treatment and tension-drying will increase the tensile modulus but has been found to have no effect on the torsion modulus or compressive strength of rigid-rod polymeric fibers, including PPTA [DeTeresa and Rakas, 1986]. Axial compressive failure in Kevlar fibers has been shown to be due to the onset of a microbuckling instability; it is physically evidenced by the presence of microscopic kink

bands and macroscopic hinges [Rose and Greenwood, 1974; Dobb et al. 1981]. At the time of this paper, this was a startling new discovery.

Due to the results from our earlier work with PBZT fibers, it was decided to explore the effect of coagulant on the structural and mechanical properties of PPTA fibers, with particular regard to the effect on shear modulus and compressive strength. Although work has been done on the rheology, phase transitions and spinning of dopes prepared from dissolved Kevlar[®] yarns [Hancock et al. 1977; Aoki et al. 1978], there apparently have been no published efforts to systematically observe the influence of coagulant on the shear and compressive properties of the PPTA fiber.

This chapter presents data on PPTA fibers which were coagulated in a variety of non-solvents; coagulants were chosen which were known or projected as being able to complex with or alter the fiber during coagulation. Coagulants included one of two organic liquids, ethanol (a solvent for sulfuric acid) or hexane (a non-solvent for sulfuric acid). "Coagulation" in hexane would then be due solely to humidity, and would be slower than direct coagulation in a stream of coagulant. Also, the effects of coagulating into aqueous solutions of two alkali salts, an 8% lithium chloride solution and an 8.3% (0.5 M) potassium iodide solution, are studied. Lithium chloride is listed as an additive to the spinning dope in the patent literature [Blades, 1977b]; its function is described as increasing the solubility of the polymer. Again, coagulation in this solution would hopefully result in a slower phase transition. Coagulation in potassium iodide was indicated by our earlier work with PBZT and iodide anions, and also through the numerous work that has been done involving various nylons and iodine. Coagulation into an

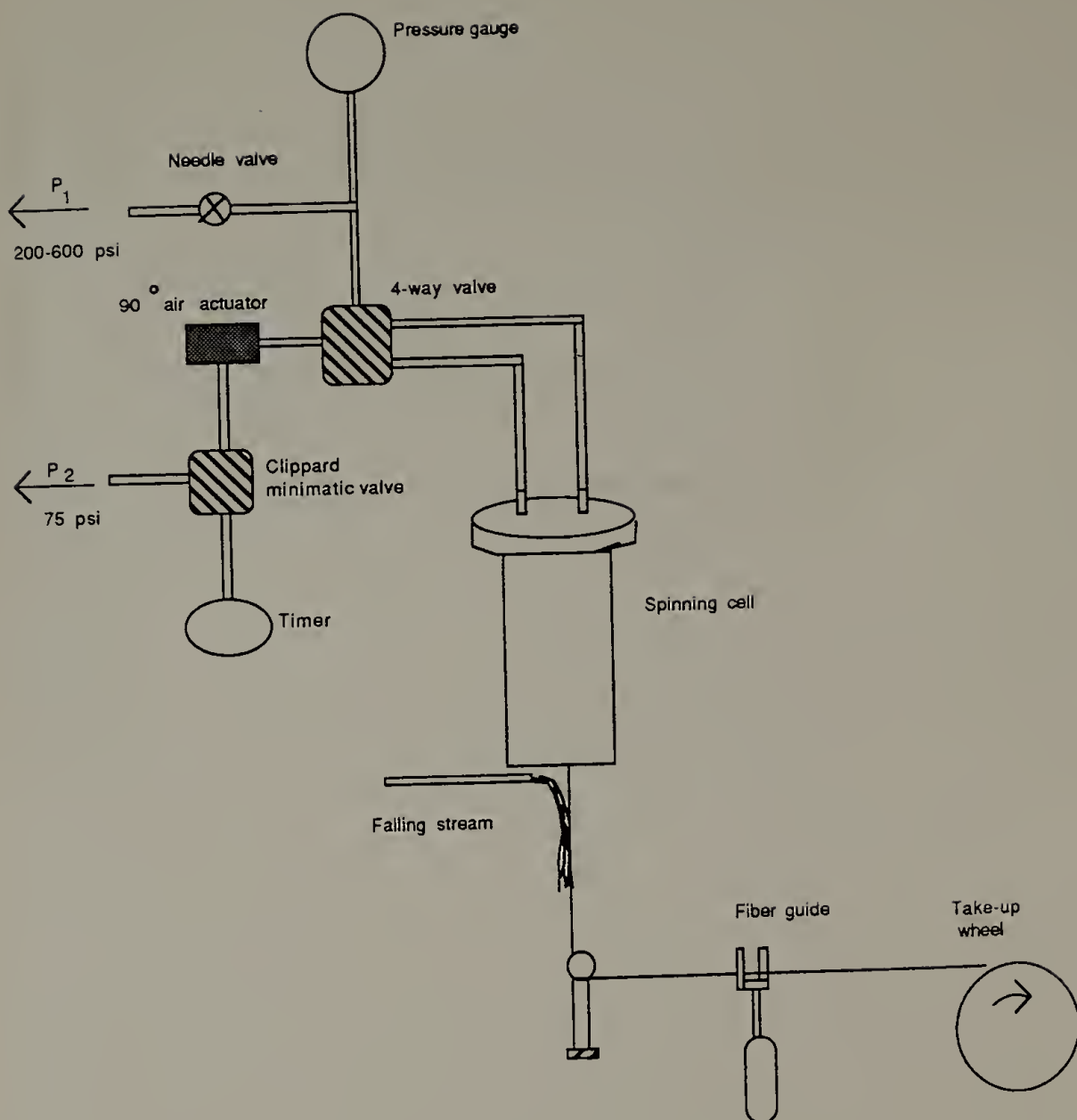
iodine/ethanol solution was done to determine if cation and solvent affected the complexing ability of the iodide ion. The effect of pH on fiber structure and properties was studied through coagulation by either 20% sulfuric acid or 20% sodium hydroxide (aqueous). Impregnation of the PPTA fiber was attempted both by the method detailed in figure 2.1 and by coagulation of PPTA fiber directly into a material which had been successfully used in PBZT impregnation, sodium silicate solution. The dope was also diluted with sulfuric acid to produce a less-concentrated solution which would result in a fiber having a more porous structure. Finally, PPTA dope was mixed with poly(amic acid) in order to attempt to produce "molecular composite" structures.

3.2 Fiber Production and Testing

Spinning dopes, consisting of a solution of approximately 18% solids in fuming sulfuric acid, were provided by the Kevlar[®] Division of the Du Pont Company. Dopes were kept refrigerated until use. A billet of the spinning dope which was nearly the same circumference as the spinning barrel and approximately 1-1/2 inches long was inserted into the spinning barrel under nitrogen. The spinning cell was assembled under nitrogen, and was then heated using a band heater. Heating times were 2-1/2 hours, at 85°C.

A schematic of the entire spinning system is shown in figure 3.1. The spinning cell used contained a piston which was pressure-driven and which could be vertically linked with a linear variable displacement

Figure 3.1 Schematic of the system used to spin PPTA fibers.



transducer (LVDT), in order to accurately measure piston speed. The LVDT, in turn, was linked to a Fisher chart recorder. The take-up system consisted of three elements: a variable-speed motor, a take-up wheel, and a traverse, which spread fiber evenly along the width of the take-up wheel. A glass "dog bone", basically a supported horizontal rod, was used to change the fiber direction from vertical to horizontal. Take-up speeds were measured using a Cole-Parmer hand-held tachometer. Stainless steel wire-drawing dies, 102- or 152 μm (4 or 6 mils) in diameter, were obtained from the Fort Wayne Wire and Die Company (Indiana) and used to spin all fibers.

Fiber exit velocities (v_f) ranged from 1020-3300 centimeters per minute (400-1300 in/min), with most fibers spun in the range of 1270-2030 cm/min (500-800 in/min). Because it was not possible to measure the exit velocity during actual fiber spinning, an attempt was made to spin under standardized conditions, fixing heating time and temperature, die size, and especially pressure. With these factors fixed, the fiber of the greatest possible spin-draw was spun by increasing the angular velocity of the take-up wheel until the fiber line began to break. The speed was slightly reduced, and spinning was continued.

All fibers were dry-jet wet spun through an air gap of approximately 1 centimeter into a falling stream of coagulant that was approximately 0.17 inches in diameter; the vertical distance the fiber traveled (from outer die face to the dogbone) was 15.2 cm. Fiber was then guided under the glass "dog bone", threaded through the traverse, and wrapped around the rotating bobbin. The take-up wheel was constantly bathed with fresh coagulant; once the bobbin was full, it was pulled off the frame, placed in a water bath and a new bobbin was

snapped in place. Coagulants were pumped using a Cole-Parmer peristaltic pump, which insured that these liquids would not become contaminated during pumping. Unless otherwise stated, all coagulant used was "fresh"; it had not been recycled during the course of the spinning experiment. Coagulant temperature was 4-6°C while spinning, except for the 18% iodine/ethanol solution, which was used at room temperature. All aqueous solutions contained distilled water; solution mixtures are defined on a per-weight basis. Fibers were allowed to soak for 48 hours after spinning and the pH of the bath was kept neutral by adding fresh water. Fibers were allowed to air dry on the bobbins.

Fibers which were spun from diluted or mixed solutions (three or more components) were mixed in an Atlantic mixer. The spinning dope was broken up in a glove bag and approximately 100 grams weighed out. The mixer, which consisted of a jacketed, removable bowl, mixing blades, and side ports, was flushed with nitrogen while being heated to 85°C using a recirculating oil bath. The dope was quickly added to the mixer through a large powder funnel placed in one of the side ports. The other components to be mixed into the dope were also added at this time. 100% sulfuric acid was used after first degassing with a nitrogen stream for 1 hour. Other additives were used as received, although they were dispensed and weighed in a glove bag. The spinning mixture was allowed to sit under nitrogen for one-half hour while being heated; the bowl was then evacuated and kept under vacuum while the mixture was stirred for 2 hours. During this time, the spinning cell and the first spinning plate were heated to 85°C. After 2 hours of mixing, the dope was allowed to flow through the bottom exit port of the mixer directly into the hot spinning cell. The cell was then quickly assembled, the

band heater added, and allowed to sit for one-half hour before fiber spinning began so that all the spinning plates could warm up to temperature. There were no differences in properties of fibers spun from as-received PPTA spinning dope that was handled this way, relative to fibers spun from the PPTA dope billet.

All data, both mechanical and structural, is from fibers having the highest spin/draw for fibers spun into that particular coagulant. While elongational flow of the nematic solution takes place only in the air gap, and cannot itself be affected by coagulant, as-coagulated solid fiber did show a lack of integrity or strength under some coagulation conditions. In these cases, the fiber line would repeatedly break above a certain take-up speed, and a lower speed would be required for take-up. For this reason, the "spinnability" of coagulants is qualitatively rated.

Fiber diameters and tensile and torsion properties were obtained using the same methods described in section 2.2, and only data for as-spun fibers will be presented in this thesis (most fibers spun were heat treated, generally giving the predicted results that only tensile modulus increased while all other properties remained unchanged).

Compressive strength measurements were made on 30 mm gage length samples using the "snap-back technique" developed by S.A. Allen [Allen, 1987]. In this technique, a known tensile force is applied to the sample, which is then instantaneously severed near the middle of the fiber using extremely sharp surgical scissors. This produces an unloading wave followed by a compressive shock wave equal to the magnitude of the applied tensile force when the wave reflects from the clamped end. Monitoring this process with an oscilloscope (rather than a chart recorder) showed that if the fiber was very slightly perturbed

during cutting, the applied tensile load could be greater or less than what was originally applied. To counteract this, a piece of Lycra rubber fiber was attached to the bottom end of the sample tab and the force was applied to this end. The oscilloscope showed that the Lycra acted as a dampening agent for small perturbations--the applied load remained constant. For larger perturbations, such as poor cutting or jolting the sample during cutting, the Lycra was ineffective but it seemed that these macroscopic effects could be seen by the chart recorder, and those samples discarded.

Both ends of the severed fiber were examined under an optical microscope to determine whether or not formation of kink bands (microscopic) or hinges (macroscopic) had occurred. These kink bands have been shown [Rose and Greenwood, 1974; Dobb et al. 1981] to signal that the fiber has failed in compression. If no kink bands or hinges are found, the next sample is subjected to a slightly higher tensile stress; if signs of compressive failure are found, the tensile stress is decreased until no signs of compressive failure are found.

Tensile values are the average of twelve to eighteen samples; the average shear modulus is determined from fourteen to twenty-one samples. Due to the criteria imposed by the snap-back test, the critical compressive strength has been determined from approximately eighteen to thirty-six samples, and is the value above which all fiber samples tested showed signs of compressive failure.

3.3 The Effect of Coagulant on Structure and Mechanical Properties

3.3.1 Fiber Microstructure

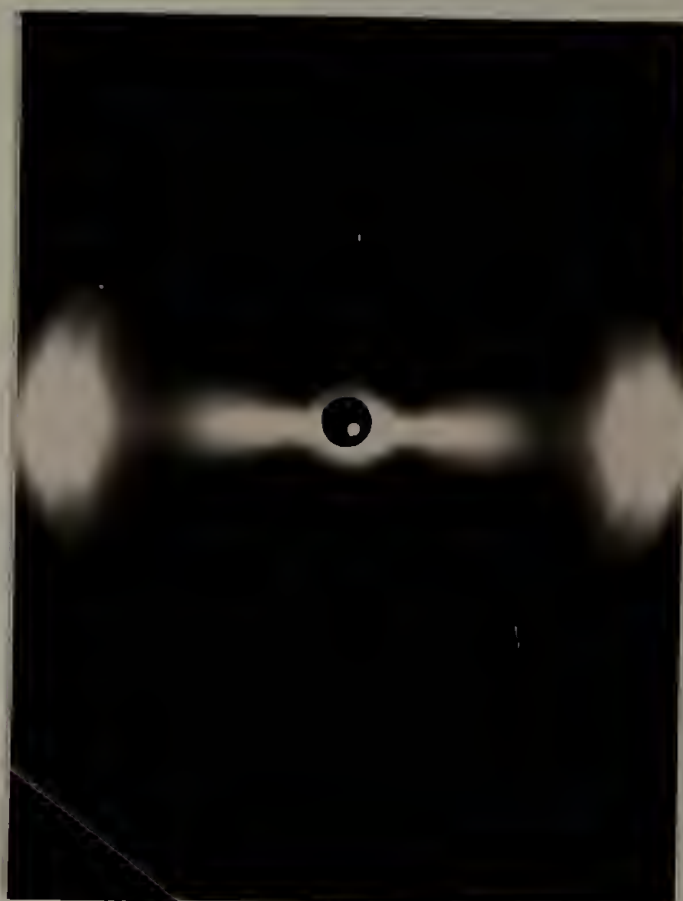
Wide-angle X-ray scattering studies were performed on all PPTA fibers produced for these coagulation studies, using the same techniques described in section 2.4.2. There were two main objectives here: to see if any of the coagulants were able to complex with or alter the crystal structure of the PPTA molecules, and to observe if there were any correlation between changes in shear modulus and/or compressive strength and WAXS patterns. Sample to film distances are equivalent (74.1 mm) for all the Statton photos reproduced in this chapter, unless mentioned otherwise.

A photo reproduction of wide-angle X-ray scattering (WAXS) Statton films of PPTA fiber coagulated in water [PPTA/H₂O] and PPTA fiber coagulated in ethanol [PPTA/ETH] are shown in figure 3.2 and 3.3, respectively. Note that while the S/D ratio of the PPTA/ETH fibers is approximately one-quarter that of the PPTA/H₂O fibers, both patterns show a high degree of fiber symmetry, and are basically indistinguishable from each other. Unlike PPTA film coagulation studies conducted by Haraguchi [Haraguchi et al. 1979a, b], there is no apparent change in the crystal structure of the PPTA fibers coagulated in ethanol relative to the WAXS pattern for the fibers coagulated in water.

Figure 3.2 *Top:* Wide-angle X-ray scattering (WAXS) Statton film of PPTA fiber coagulated in water [PPTA/H₂O], S/D =12.2.
Bottom: Schematic of reflections.



Figure 3.3 WAXS Statton films of PPTA fiber coagulated in ethanol [PPTA/ETH], S/D=3.



The crystal structure for these fibers is the one which was discussed and analyzed in detail by Northolt [Northolt and van Aartsen, 1973; Northolt, 1974].

Scanning electron microscopy (SEM) micrographs of both tensile and compressive samples of PPTA/ETH and PPTA/H₂O help define the effect of coagulant on fiber smoothness and fibrillation. A PPTA/ETH fiber fractured in tension is shown in figure 3.4; a high degree of fibrillation was optically apparent even while performing the tensile tests. Figure 3.5, a PPTA/ETH fiber which has failed in compression during the recoil test, has a macroscopic hinge. Generally, no kink bands of the type seen in Kevlar 49[®] fibers were observed for these as-spun fibers. Figure 3.6 shows an SEM micrograph of a PPTA/H₂O tensile specimen. The fiber has split longitudinally, but with only one major split; also, a number of tiny horizontal cross-fibrils are seen bridging the split.

The wide-angle X-ray scattering Statton studies of the PPTA fiber coagulated in aqueous potassium iodide [PPTA/KI] (figure 3.7) show that there is a very low degree of orientation of the polymer chains along the fiber axis. The photograph shows a highly crystalline system with the standard d-spacings characteristic of the PPTA molecule [Northolt and van Aartsen, 1973; Northolt, 1974] but the expected fiber pattern is very nearly replaced by rings which are associated with a crystalline but unoriented system. As expected, when PPTA/ETH fibers are heat-treated, equatorial reflections become sharper and narrower, and the off-axis reflections are more apparent (figure 3.8). However, when PPTA/KI fibers are heat-treated (230-250°C, 65-80 MPa tension), the WAXS pattern does not change (figure 3.9).

Figure 3.4 Scanning electron micrograph of PPTA/ETH fiber fractured in tension.



Figure 3.5 A scanning electron micrograph of a PPTA/ETH fiber which has failed in compression during the recoil test.



Figure 3.6 Scanning electron micrograph of a PPTA/H₂O fiber fractured in tension.



Figure 3.7 *Top:* WAXS Statton film of PPTA fiber coagulated in aqueous potassium iodide [PPTA/KI], S/D=4.4. *Bottom:* Schematic of reflections.

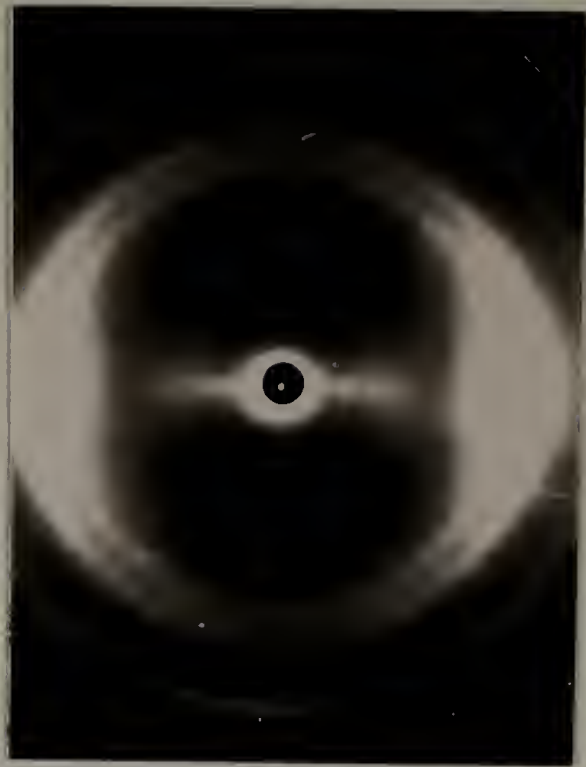


Figure 3.8 The WAXS pattern of heat-treated/tension-dried PPTA/ETH fibers.

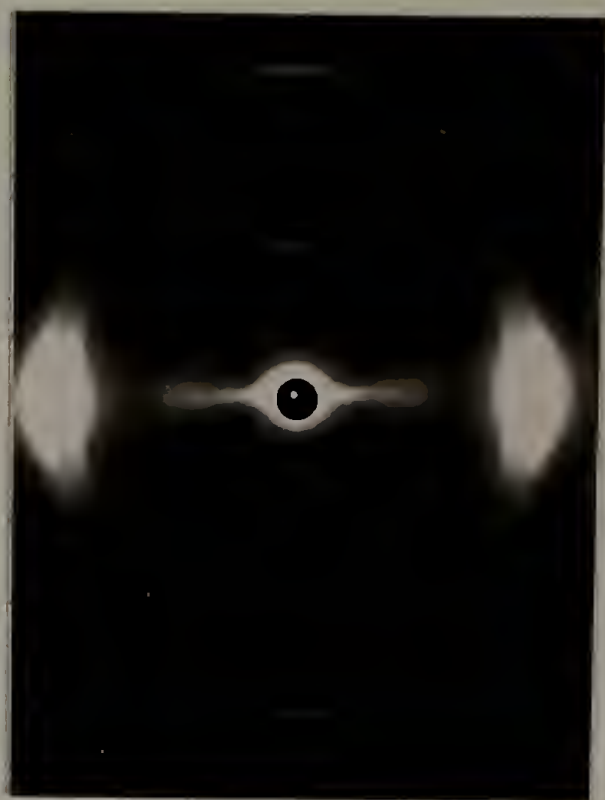
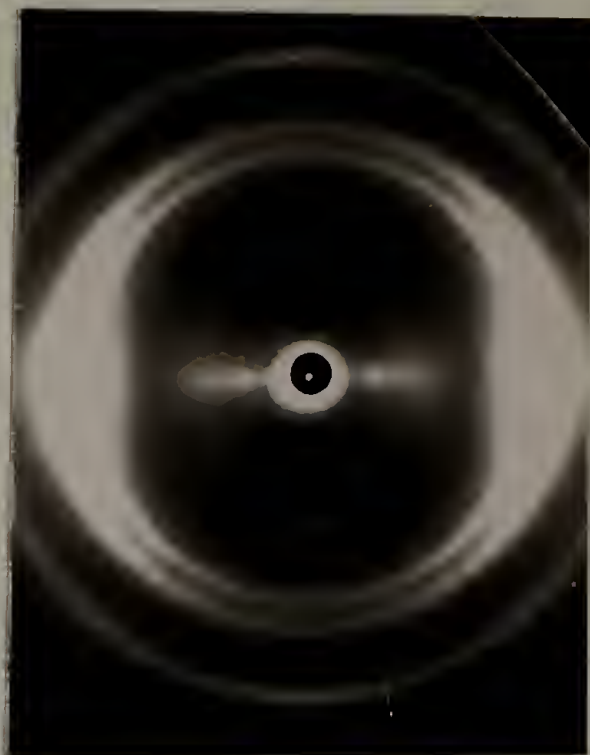


Figure 3.9 The WAXS pattern of heat-treated/tension dried (230-250°C, 65-80 MPa tension) PPTA/KI fibers.



SEM micrographs of PPTA/KI fibers (figures 3.10 and 3.11) show that the fiber surface is not as smooth as that of PPTA/H₂O fibers, but also that the fiber appears to contain "seams", or a thick outer skin. While the existence of a skin-core morphology has long been postulated for these fibers [Dobb et al. 1977; Morgan, 1983], it is postulated that this skin is only 0.1-1.0 μm thick [Morgan, 1983]. The specimen fractured in tension shows little fibrillation; that which has failed in compression seems to support the idea that this fiber has an thick outer skin.

To determine whether these changes were reversible, PPTA fibers were coagulated into the aqueous potassium iodide solution, and spun onto two bobbins at the same spin-draw (2.2). One of the bobbins was placed in a water bath immediately after spinning. The other was placed in a fresh solution of aqueous potassium iodide. Both were allowed to sit at room temperature in these baths for one week. After air-drying, it was found that mechanically and structurally, these two sets of fibers were identical, even sharing the seam-like fiber surface.

When PPTA fibers were coagulated in a room-temperature solution of 18% iodine in ethanol, fibers were soaked in either fresh iodine solution [PPTA/IET/IET] (figure 3.12) or in distilled water [PPTA/IET/H₂O]. In contrast with the PPTA/KI fibers, these fibers appeared as oriented as PPTA/ETH fibers, showing the expected layer lines which are indicative of ordering of the chains along the fiber axis. Soaking one set in water and one in fresh iodine solution had no apparent effect on fiber microstructure.

Figure 3.10 Scanning electron micrograph of a PPTA/KI fiber which has failed in tension.



Figure 3.11 Scanning electron micrograph of a PPTA/KI fiber which has failed in compression.

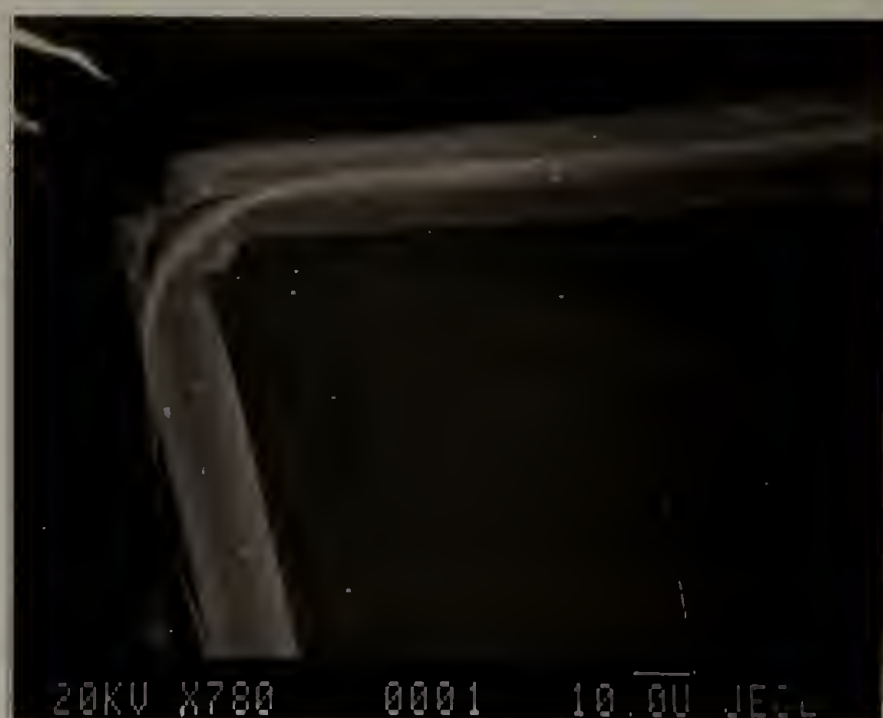


Figure 3.12 The WAXS pattern for PPTA fiber which was coagulated and soaked in fresh iodine/ethanol solution [PPTA/IET/IET], S/D=3.



There is no difference in d-spacings or degree of orientation for fibers coagulated in the 20% sulfuric acid solution [PPTA/AC], or for those having some degree of draw and coagulated in 50% (w/w) sodium silicate solution [PPTA/SS] or 20% NaOH [PPTA/BAS]. However, interesting results were obtained for PPTA/BAS fibers having no draw [FF/BAS], when compared to drawn PPTA/BAS fibers or to PPTA/H₂O fibers (drawn or with no draw). (Fiber classified as "no draw" or "free fall" was allowed to fall approximately one foot under its own weight, but was not drawn by use of the take-up device). Prints from Statton WAXS studies of free fall PPTA/H₂O fibers [FF/H₂O] are shown in figure 3.13, and FF/BAS fibers are shown in figure 3.14. The degree of orientation shown in the WAXS print of FF/BAS bears a much closer resemblance to that of figure 3.2, PPTA fiber spun at a spin-draw of 12.2 but coagulated into water; sharp layer lines as well as off-axis reflections are present in the FF/BAS fibers.

The SEM micrographs of PPTA/SS fibers shown in figures 3.15 and 3.16 have a rough, almost corrugated appearance, while PPTA/BAS fibers closely resemble PPTA/H₂O fibers. It should be stressed that these PPTA/SS fibers were not permitted to soak in the coagulant overnight, so the amount of time these fibers were exposed to the sodium silicate was relatively short, that is, five to ten minutes.

Figure 3.13 *Top:* WAXS pattern of free fall PPTA/H₂O fiber [FF/H₂O].
Bottom: Schematic of reflections.



Figure 3.14 *Top:* WAXS pattern of as-spun PPTA fiber coagulated in 20% NAOH solution (aq), no draw [FF/BAS]. *Bottom:* Schematic of reflections. Sample to film distance in the Statton film is 53.1 mm.

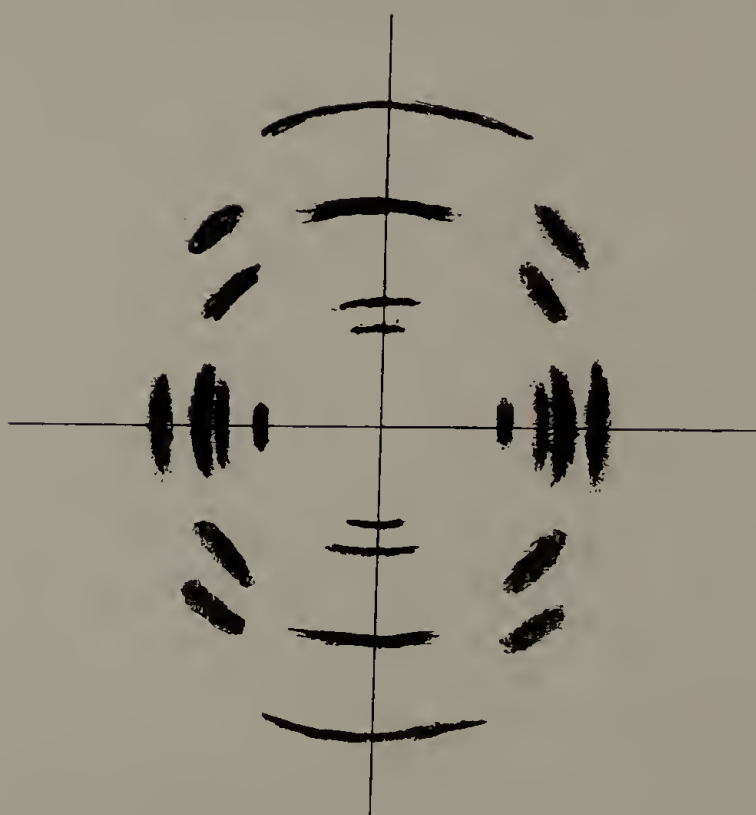


Figure 3.15 Scanning electron micrograph of a PPTA/SS fiber which has failed in tension.

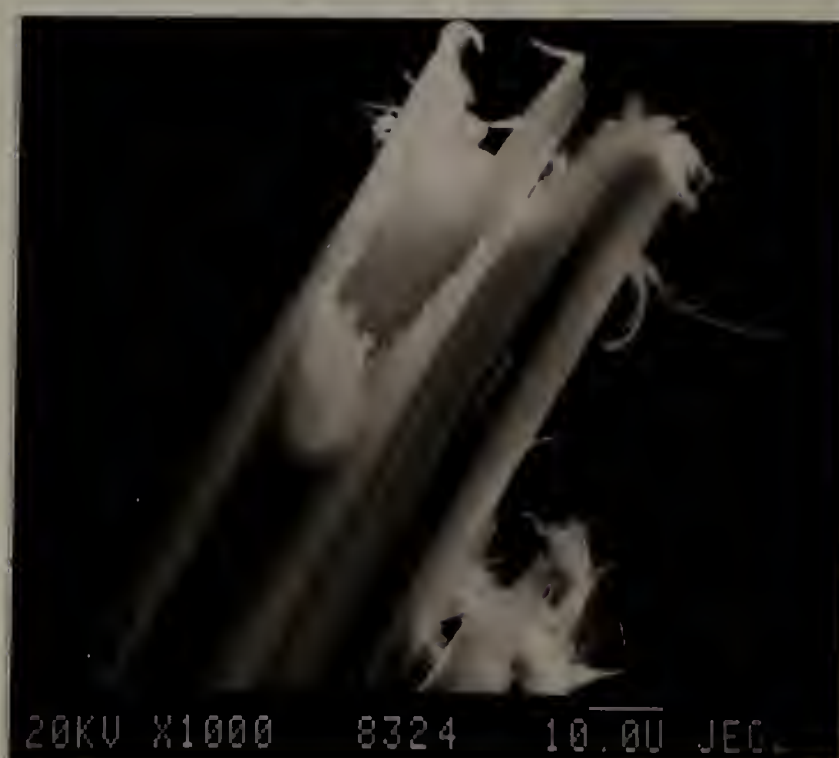


Figure 3.16 Scanning electron micrograph of a PPTA/SS fiber which has failed in compression.



3.3.2 Mechanical Properties

Table 3.1 lists the mechanical properties and spin/draw ratios for as-spun PPTA fibers coagulated into water, ethanol and hexane. The mechanical properties obtained for the PPTA/H₂O fibers agree well with accepted values for Du-Pont's Kevlar 29[®], a PPTA fiber which is not heat-treated or tension-dried. In tensile and torsion studies for Kevlar 29[®], an average tensile modulus of 58 GPa and an average tensile strength of 2.6 GPa were found, along with a torsion modulus of 1.41 GPa. The properties for the PPTA/H₂O fibers spun from the Du Pont solution are much better than those reported for PPTA fibers spun from redissolved Kevlar 29[®] fibers [Hancock et al. 1977; Aoki et al. 1978]. Those fibers were wet-spun; the tensile modulus was 3.8 GPa, with a tensile strength of 300 MPa. Also, WAXS patterns of the fibers spun from redissolved Kevlar[®] did not show the usual fiber pattern--reflections were not separated into equatorial and meridional orientations.

PPTA fibers coagulated into ethanol (designated as PPTA/ETH) were more difficult to spin than those coagulated into water. Attempts to produce fibers of spin/draw higher than about four were unsuccessful; the fiber line would repeatedly break. To make sure this difficulty was due solely to the coagulant, rather than chance, PPTA fibers were coagulated into ethanol on two different days, and the properties of both sets of fibers were tested. Both sets were unable to withstand high take-up velocities, and the mechanical properties were identical. The tensile modulus of PPTA/ETH fibers is lower than

Table 3.1 Mechanical properties of as-spun PPTA fibers coagulated in water, ethanol and hexane

Coagulant	Water	Ethanol	Hexane
Spinnability	Very good	Fair	Poor
S/D	12.2	3	Could not draw
Tensile Modulus (E), GPa	88 ± 5	54 ± 3	
Tensile Strength (σ_b , GPa)	2.3 ± 0.2	1.2 ± 0.1	
Elongation (ϵ),%	3.2	3.04	
Shear Modulus, GPa	1.36 ± 0.2	1.31 ± 0.1	
Compressive Strength (σ_c), MPa	375	230	

PPTA/H₂O fibers, but still within the expected range (60-80 GPa for as-spun PPTA/H₂O fibers). However, tensile strength is approximately one-third that of PPTA/H₂O fibers. Since only low take-up speeds could be used, the degree of orientation obtained in the air gap was much lower than that of PPTA/H₂O fibers; as a direct result, tensile strengths were lowered to 1.2 GPa, roughly half the value of the tensile strength of PPTA/H₂O fiber. Unexpectedly, however, compressive strength was lowered to 230 MPa, a decrease of 33%; the shear modulus was unchanged.

PPTA fibers which were "coagulated" into hexane were extremely brittle and generally broke when they were being guided under the dogbone. They fell apart when handled, so no mechanical properties could be obtained. Hexane only acted as a heat transfer agent, not a coagulant. This seems to indicate that coagulation from water present in the surrounding air either does not occur quickly enough to produce a fiber with mechanical integrity, or that the coagulated fiber has a microstructure which is very inferior to that of fiber coagulated directly by a falling stream of coagulant. Also, the fact that the coagulant cooled the fiber without coagulating it could also be a factor contributing to a lack of fiber integrity. In any case, there was no change in crystal structure of the PPTA/hexane fiber.

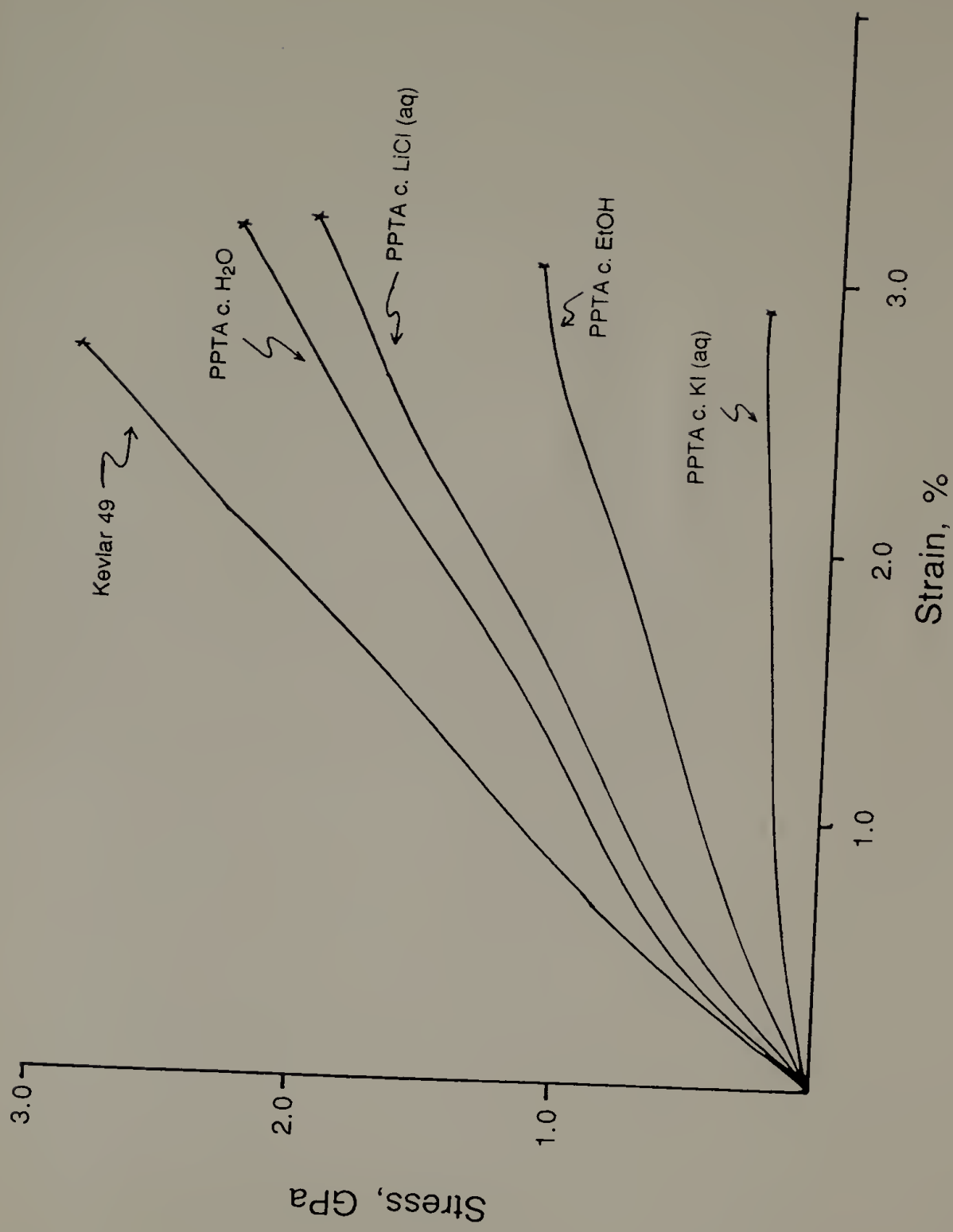
The mechanical properties of fibers coagulated into aqueous alkali salt solutions are given in table 3.2. Figure 3.17 compares the stress-strain curves for these fibers with PPTA/H₂O, PPTA/ETH and Kevlar 49[®] fibers.

Coagulating in 8% LiCl resulted in a fiber that was very easy to draw and had nearly identical mechanical properties as the PPTA/H₂O

Table 3.2 Mechanical properties of as-spun PPTA fibers coagulated in 8% aqueous LiCl solution and 0.5 M (8.3%) aqueous KI solution

Coagulant	<u>8.3% KI (aq)</u>	<u>8% LiCl(aq)</u>
Spinnability	Fair	Very good
S/D	4.4	11.5
Tensile Modulus (E), GPa	20 ± 2	84 ± 5
Tensile Strength (σ _b), GPa	0.28 ± 0.04	2.0 ± 0.1
Elongation (ε), %	2.90	3.00
Shear Modulus (G), GPa	0.46 ± 0.27	1.46 ± 0.14
Compressive Strength (σ _c), MPa	145	350

Figure 3.17 Typical stress-strain curves for Kevlar 49 and as-spun PPTA fibers coagulated in water, ethanol and aqueous alkali salt solutions.



fibers, with a tensile modulus of 84 GPa, a tensile strength of 2.0 GPa, and a compressive strength of 350 MPa. On the other hand, the PPTA/KI fibers were drastically different from any other fibers previously spun. First, spinnability was about as difficult as the PPTA/ETH fibers--but tensile properties were astonishingly low, with a tensile modulus of 20 GPa and a tensile strength of 0.28 GPa. The shear modulus was decreased to roughly one-third that of PPTA/H₂O fiber, from 1.36 GPa to 0.46 GPa, and compressive strength was lowered by about the same ratio, to 145 MPa.

Coagulation into an 18% solution of iodine in ethanol was performed to help determine the relationships between solvent and cation (K⁺ in the KI system; I⁺ in the iodine/ethanol system) on the effects of iodine species on the PPTA fiber. The properties of fiber soaked in iodine solution [PPTA/IET/IET] and water [PPTA/IET/H₂O] are given in table 3.3. The tensile moduli for PPTA/IET/H₂O fibers, 56 GPa, is about the same as for PPTA/ETH fibers; PPTA/IET/IET fibers have a tensile modulus that at 44 GPa is less than that of the PPTA/IET/H₂O fiber, and is about half that of the PPTA/H₂O fiber. There seem to be two major differences between the two fibers, breaking strength and compressive strength. The breaking strength of PPTA/IET/H₂O fiber is 0.86 GPa, and is about double that of PPTA/IET/IET (although both these values are lower than the breaking strength of PPTA/ETH fiber). The critical compressive strength for PPTA/IET/H₂O (the value above which all fibers failed in compression) is the highest obtained for any PPTA fibers produced in this laboratory, with a value of 464 MPa. Even the midpoint value for these fibers (the point at which 50% of the fibers fail), 443 MPa, is higher than has been observed for any

Table 3.3 Mechanical properties of as-spun PPTA fiber coagulated and soaked in iodine solution [PPTA/IET/IET] and coagulated in iodine solution but soaked in water [PPTA/IET/H₂O]

Fiber	<u>PPTA/IET/IET</u>	<u>PPTA/IET/H₂O</u>
S/D	3	3
E (GPa)	44 ± 3	56 ± 2
σ _b (GPa)	0.40 ± 0.08	0.86 ± 0.2
ε (%)	1.30	3.00
G (GPa)	1.27 ± 0.14	1.49 ± 0.06
σ _c (MPa)	323	464
	(309 mid)	443 (mid)

UMass-produced PPTA fibers. It seems as though the compressive strength of these fibers have slightly increased, although σ_c values of 420-440 MPa have been reported (Allen, 1988). PPTA/IET/IET fibers exhibit a critical compressive strength of 323 MPa--a value which is slightly lower than that of PPTA/H₂O fibers, but higher than the critical compressive strength of 230 MPa recorded for PPTA/ETH fibers.

Figure 3.18 shows the stress-strain curves for the fibers studied to determine the effect of large deviations from neutral pH on mechanical properties. Table 3.4 shows that the mechanical properties of fiber which was coagulated in the 20% sulfuric acid solution [PPTA/AC] are basically no different than those of PPTA/H₂O fibers. Although the critical compressive strength (σ_c) of the PPTA/AC fibers at 313 MPa is approximately 15% lower than that of PPTA/H₂O fibers, this is a relatively small decrease when compared with decreases in σ_c of fibers coagulated in ethanol or potassium iodide solution.

The tensile strength and percent elongation at break of PPTA fiber coagulated in the highly basic 20% NaOH solution [PPTA/BAS] are 0.78 GPa and 1.62%, respectively. In comparison, the tensile strength of PPTA/AC fiber is 2.3 GPa and the percent elongation to break is 2.9%. Since tensile strength is related to spin-draw, the low tensile strength may be traced to the poor spinnability of the fiber line. It is not reasonable to assume that the sodium hydroxide solution chemically-degraded the fiber; commercially-produced Kevlar[®] is routinely washed with an aqueous sodium hydroxide solution in order to neutralize any acid which remains after coagulation. As with PPTA/AC fibers, the compressive strength of these fibers is slightly lower than PPTA/H₂O fibers.

Figure 3.18 Typical stress-strain curves for as-spun PPTA fibers coagulated in water, 20% sulfuric acid, 20% sodium hydroxide and sodium silicate.

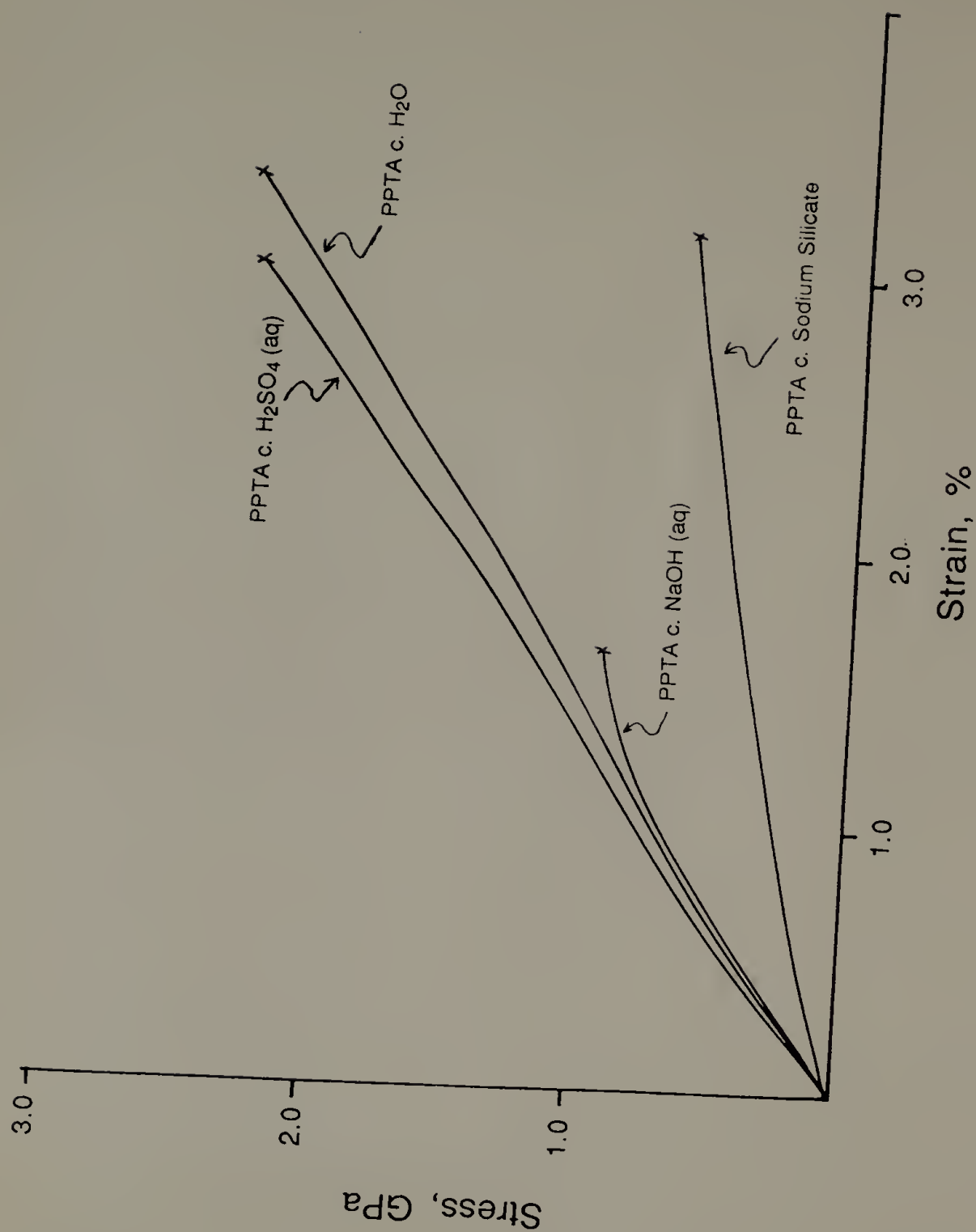


Table 3.4 Mechanical properties of as-spun PPTA fiber coagulated in strongly acidic and strongly basic aqueous solutions

Coagulant	20% H ₂ SO ₄ (aq)	20% NaOH(aq)
pH	2	12
Spinnability	Very good	Very poor
S/D	7.8	1.5
Tensile Modulus (E), GPa	94 ± 8	72 ± 10
Tensile Strength (σ _b), GPa	2.3 ± 0.2	0.78 ± 0.2
Elongation (ε), %	2.9	1.62
Shear Modulus (G), GPa	1.32 ± 0.1	1.28 ± 0.1
Compressive Strength, (σ _c) MPa	313	326

Fiber coagulated into a 50% aqueous solution of sodium silicate [PPTA/SS] had remarkably different properties and surface appearance than the PPTA/BAS fibers, although the pH of this solution was also about 10. The tensile modulus was lowered by a factor of 2, to 34 GPa; tensile strength was 0.65 GPa. The torsion modulus was decreased to 0.90 GPa. The critical compressive strength for the PPTA/SS fibers was nearly that of the PPTA/BAS fibers, with a value of 326 MPa.

3.4 PPTA Fiber Blends and PPTA Fiber Impregnation

3.4.1 Experimental

Materials used in the PPTA impregnation studies included sodium silicate, the silicate-based sol-gel glass preparation used for PBZT, an epoxy system which is generally used for microscopy embedding, and a commercial sol-gel glass based on a titanate chelate (Tyzor LA[®], manufactured by Du Pont). Impregnation with the epoxy system required that the fiber first be in an ethanol environment; the Tyzor LA[®] was itself an aqueous solution (50 wt%), and was added directly to the fiber/water mixture. After the solution exchanges were completed, fibers were allowed to soak in the impregnator material for 10 days. This increased time was decided upon after the 48-96 hours used for PBZT fibers produced disappointing results in PPTA fibers. Fibers were heat treated under no tension. PPTA fibers impregnated with sodium silicate

or the first sol-gel mixture were heated at the same temperature as the PBZT fibers; PPTA fibers impregnated with Tyzor LA[®] were heated to 150°C to complete the crosslinking reaction.

It was also attempted to spin PPTA fibers from spinning dopes of reduced concentration, in order to increase the pore size and degree of "openness" in the fiber. These spinning dopes were mixed in the Atlantic mixer as detailed in section 3.2. A solution of 12% dope was chosen, because the solution would still be anisotropic at that point [Aoki et al. 1978; Jaffe and Jones, 1985], and thus fibers spun from it would still retain a high degree of their tensile properties and spinnability. The first time this was attempted, spinning temperature was set at 85°C, and even though pressure was raised to 600 psi, it was not possible to get any output from the spinning cell. The chart recorder allowed the indirect observation of the piston, and it was seen that the piston was not moving. The usual remedies were tried--the spinneret die was replaced, the plate containing the Dynalloy filter was checked--but it could be seen that the dope had not even traveled that far in the spinning cell. The spinning cell was taken apart, and it was found that the dope, which appeared homogeneous during mixing and loading, had separated into a clear gel and an opaque fluid. These both coagulated upon exposure to air. A du Pont representative later suggested lowering the temperature--apparently some sort of phase transition was taking place in the spinning dope when under that pressure at 85°C. During the next attempt, the spinning dope was heated to 45°C; it was not possible to spin a fiber, however, because the dope either broke up in

the air gap or the fiber line snapped when it was being taken up. This was not due to dissolved gas in the dope, as it had been mixed under vacuum, but rather to poor spinnability.

Preparation of a PPTA/poly(vinyl chloride) "molecular composite" film was undertaken in order to raise the tensile moduli of the PVC component by including a small amount of PPTA in the film [Yamada et al. 1986]. Their theory was to use a small amount of PPTA (5-10 wt%) as a reinforcing agent, and it was indeed found that the tensile moduli of these films was increased from approximately 4 GPa [Rodriguez, 1982] to 16-20 GPa. This idea of using a small weight percent of one component in order to improve the properties of the major component was applied to a reverse situation in this laboratory. Namely, a small amount of a thermoplastic material, poly(amic acid) [PAA], would be added to the PPTA spinning dope. PAA would act as a microfibrillar "glue" and thus improve lateral interactions between microfibrils, resulting in higher compressive strength and torsion moduli. To keep tensile properties high, the system of 5% PAA/95% PPTA was tried.

In practice, however, this three-component system proved to be an immiscible system, although poly(amic acid) was soluble in sulfuric acid alone. A Du Pont associate suggested adding more 100% sulfuric acid to the mixture. This was done in PAA/H₂SO₄ ratios of 1:1, 1:2 and 1:3 (this last mixture actually lowered the amount of PAA to below three weight percent). None of these mixtures were miscible; the spinning dope was greenish-yellow, with large dark particles throughout, resulting in a two-phase system that could not be spun, due to the clogging of the die and filters by large undissolved particles.

3.4.2 Mechanical Properties

Figure 3.19 compares the tensile moduli for as-spun PPTA fibers and those impregnated with epoxy, sodium silicate and the silicate-based sol-gel glass. Figure 3.20 compares the torsion moduli of the same fibers. There is basically no enhancement of tensile or torsion moduli with "impregnation" of the fiber. This was believed to be due to difficulties in permeation of the fiber by the impregnator material, rather than a lack of reinforcement. When it was learned [Knoff, 1987] that treatment of the as-coagulated fiber with basic or alcoholic solution could lead to radial shrinkage of the fiber (with a resulting decrease in fiber pore size), a water-based impregnator material was thought to be a better impregnator material. Tyzor LA[®] was a water-soluble solution of a titanate chelate which would crosslink to form a sol-gel glass. The solution as-received is slightly acidic, and is very stable [Du Pont, 1988]. The stress-strain curves of the Tyzor[®]-impregnated fiber [PPTA/TY] and the as-spun PPTA fiber [AS-PPTA], are shown in figure 3.21; there seems to be little difference between the two fibers. Breaking strength remained the same, at 2.3 GPa. Figure 3.22 shows the average torsion moduli for as-spun and Tyzor[®]-impregnated PPTA, along with the standard deviation. There is some increase in torsion moduli for the impregnated fiber, but the larger standard deviation shows that impregnation is not uniform from one sample to another. The distribution range of torsion moduli for impregnated fibers extends from 1.54 GPa to 1.80 GPa. Although torsion modulus for impregnated fibers

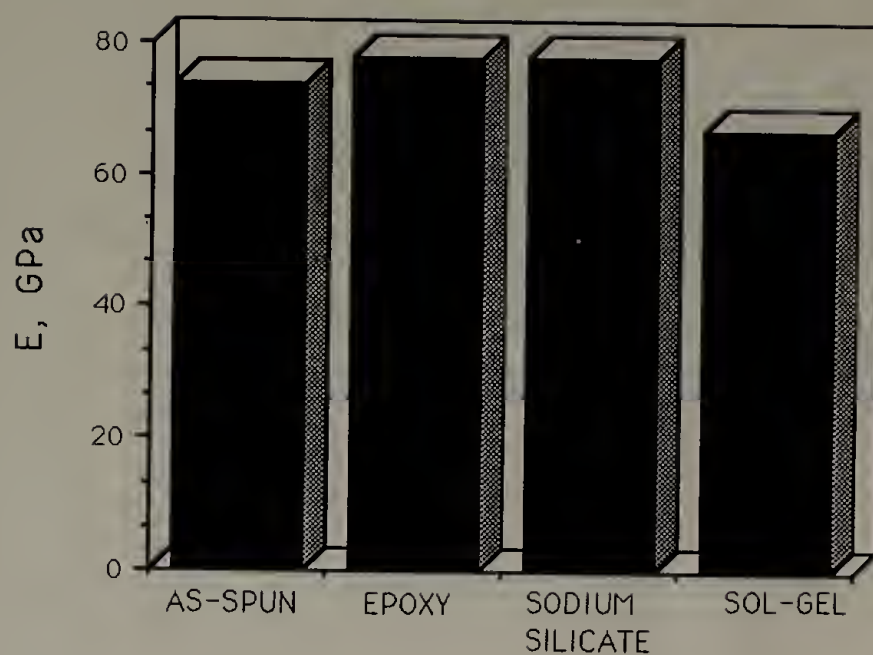


Figure 3.19 Tensile moduli of as-spun and impregnated PPTA fibers.

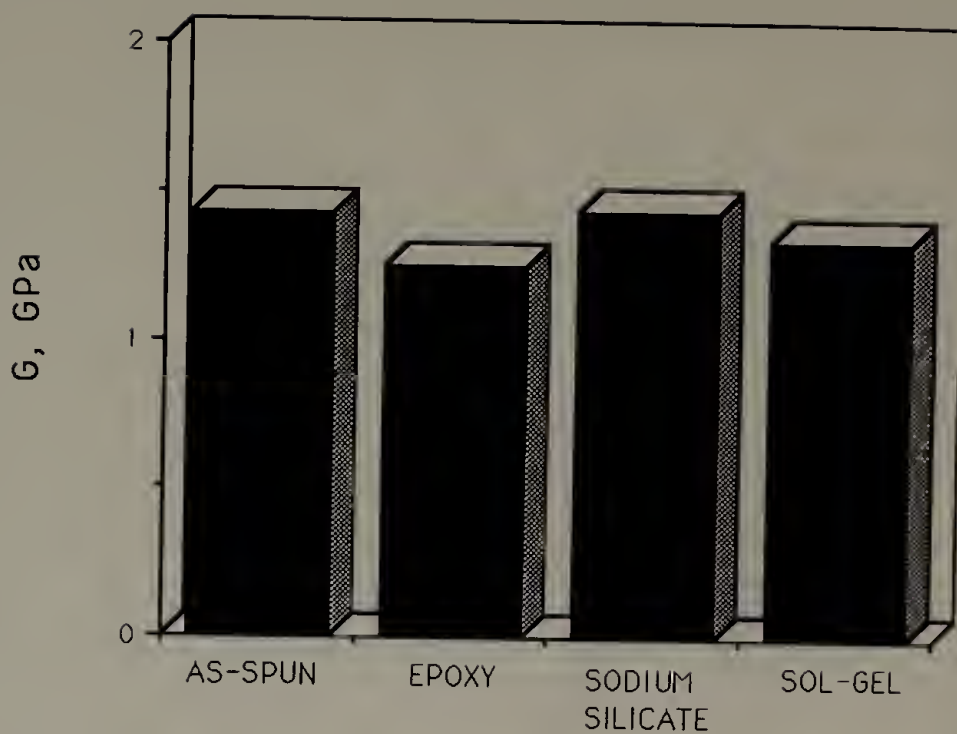
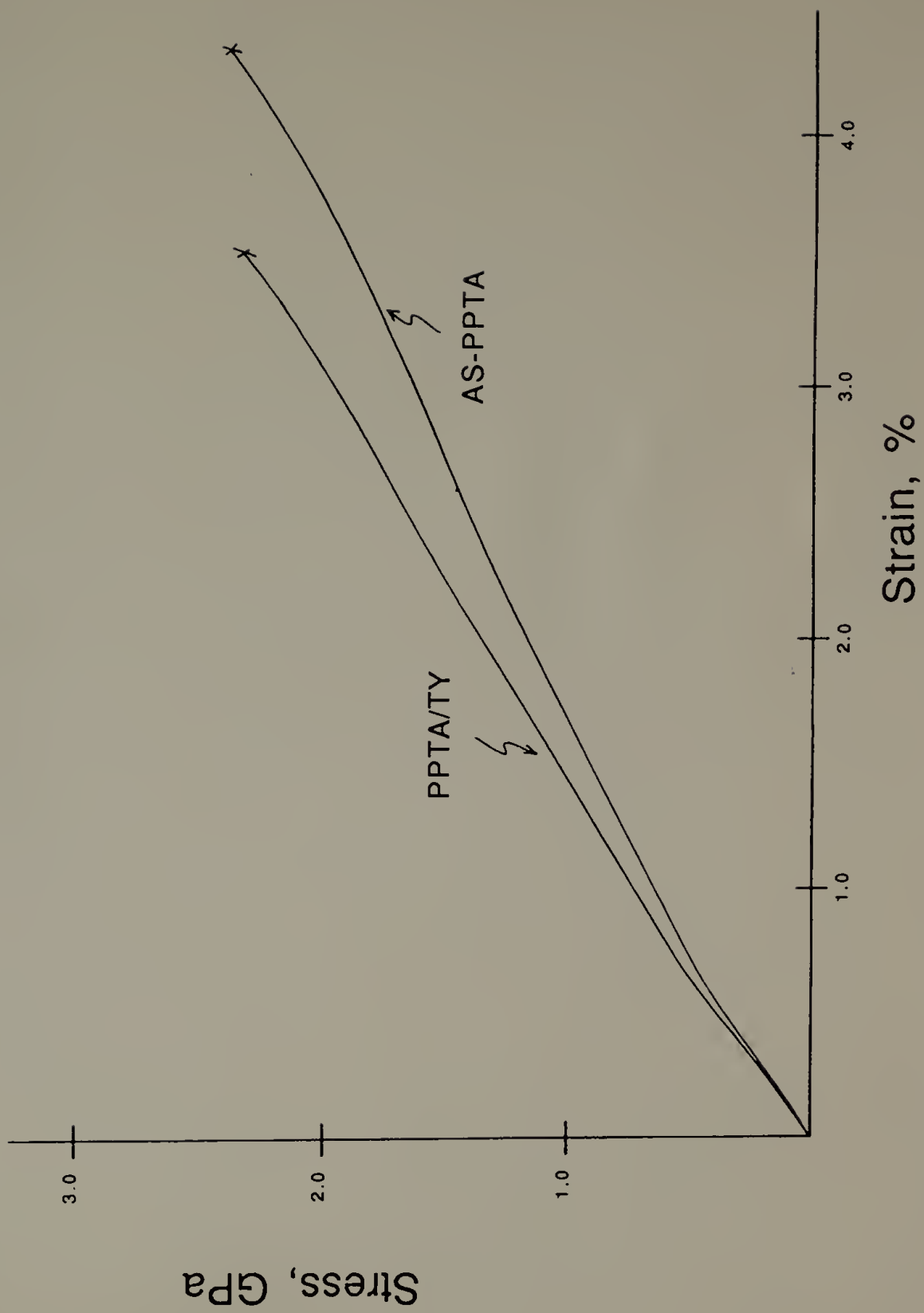


Figure 3.20 Torsion moduli of as-spun and impregnated PPTA fibers.

Figure 3.21 Typical stress-strain curves for as-spun PPTA [AS-PPTA] and PPTA impregnated with Tyzor LA [PPTA/TY].



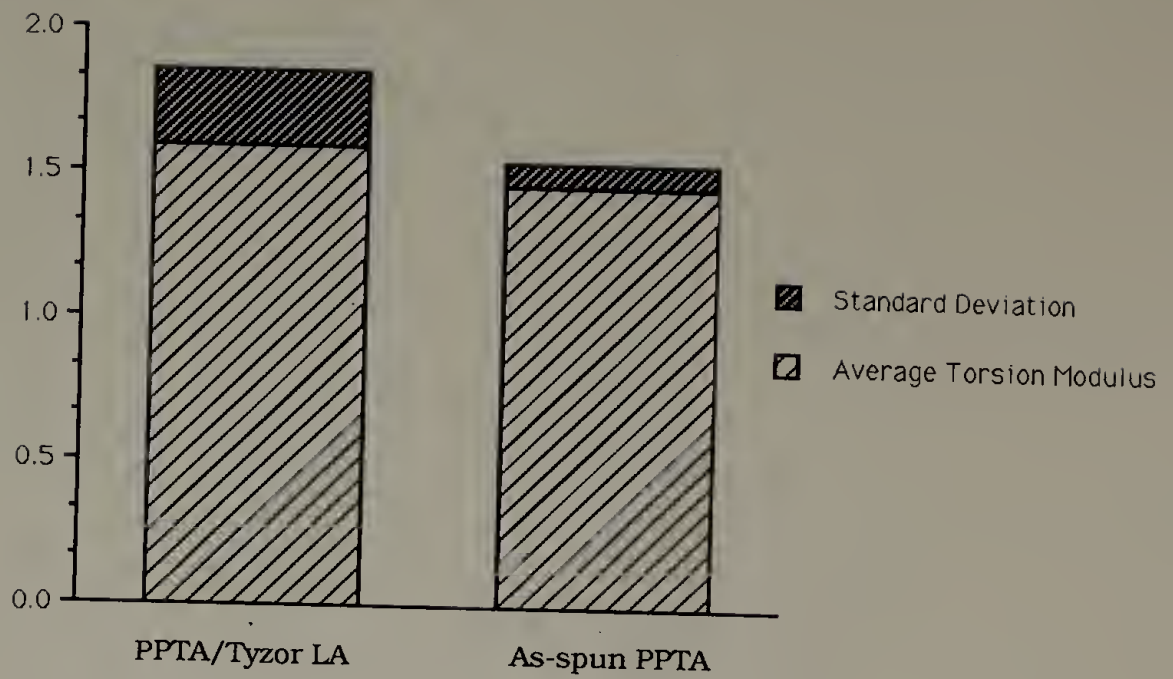


Figure 3.22 Torsion modulus distribution for PPTA fibers impregnated with Tyzor LA[®].

may increase to 1.80 GPa, this represents a few thoroughly impregnated samples. Further, there were no changes in compressive strength between impregnated and as-spun fibers-- σ_c was 350 MPa.

3.5 Conclusions

This work has shown that the choice of coagulant used in the production of PPTA fibers can have significant effects on mechanical properties. Further, some fibers exhibit no changes in tensile and torsion moduli while tensile and compressive strengths show large changes (PPTA/ETOH and PPTA/IET/H₂O fibers. These seem to be exceptions to the correlation which DeTeresa found for so many other types of fibers, and may indicate significant changes in fiber morphology.

It is significant to note that both LiCl and KI are alkali salts, yet only potassium iodide has a detrimental effect on PPTA fibers. Further, since both potassium iodide and iodine/ethanol solutions would generate I_3^- and I_5^- anions, the cation present in the system seems to be highly important in terms of fiber microstructure and properties. The potassium iodide molecule is able to interact strongly with some element of the PPTA chain (probably the amide linkages), thus producing a strong amount of interference of orderly chain packing. The result is that the degree of orientation of the chains in the fiber is low, even though the amount of iodine species left behind in the fiber is only 0.12% (weight percent by chemical microanalysis). There have been some studies done on orientation suppression in fibers spun from

polymer melt blends; in those systems, macro-rheological properties strongly suggest that the mechanism is based on nonuniform extensional flow, rather than on molecular interactions [Brody, 1986]. The PPTA/KI work, however, seems to suggest that molecular interactions are the cause of orientation suppression in these fibers. This seems to be consistent since the PPTA/IET/IET fiber contained 21% by weight iodine species, yet torsion modulus and compressive strength were basically unaffected. The interaction and the importance of the cation species merits some investigation.

Although coagulation of PPTA fiber into ethanol did not result in a change in crystal structure, both tensile and compressive strength were significantly decreased. The decrease in both the ability to highly draw the fiber and the compressive strength is not the result of any chemical reaction of the ethanol with the PPTA molecule [McCarthy, 1988]; rather, kinetic effects of the coagulant on the crystallization of the PPTA molecules are, for the moment, assumed to be responsible.

A coagulant of low pH has minimal effect on fiber properties; however, coagulation into a solution of high pH severely affects tensile strength and elongation to break. Studies conducted on Kevlar[®] fibers which were sprayed with a 1% solution of NaOH after coagulation in water found that NaOH molecules could penetrate the fiber and react with trapped sulfuric acid. This generated Na₂SO₄ salts which initiated microvoids 10 nm in diameter; these salts comprised 50% of the fiber impurities. While it was found that Na and SO₄²⁻ impurities could be leached out of fibers upon immersion in water, mobility of Na₂SO₄ salts within PPTA fibrillar crystals is sterically prohibited [Morgan and Pruneda, 1987]. Therefore, coagulation in a 20% NaOH solution would

probably result in the formation of a substantially greater amount of permanently trapped Na_2SO_4 salts, even though the fiber was soaked in distilled water for several days. This would result in a larger number of microvoids within the fiber, and could certainly be the cause of a decrease in tensile strength such as that observed.

It was also found that the PPTA/BAS fiber spun with no draw was highly oriented. Since it has been shown that in dry-jet wet spinning fiber orientation occurs during extensional flow in the air gap [Ziabicki, 1976], how coagulant can influence or alter the degree of orientation in the fiber is presently unexplainable. As with the PPTA/ETH case, these results point to a need to investigate the kinetics of coagulation and crystallization in this system.

Since coagulant temperature was a factor in only one of these experiments, some questions are raised about the coagulation process for PPTA fibers. Instead of coagulation being induced primarily by a temperature change, with the action of the non-solvent being secondary [Morgan et al. 1983], it is proposed that the role of the non-solvent is at least as significant as that of the temperature change. Coagulation sets the fiber structure; the coagulant can profoundly and permanently influence fiber properties. This view is supported by the fact that, after spinning, whether fibers were soaked in fresh aliquots of potassium iodide solution or in water, structural and mechanical properties remained the same.

The results of the WAXS investigations show that large changes in the shear modulus and/or compressive strength can occur without any accompanying change in the basic crystal structure of the PPTA molecule. It is reasonable to assume, then, that these properties in the

PPTA fiber are primarily dependent on an element of fiber microstructure that is above the molecular level, and that predictions of these properties from molecular studies will not be adequate for anticipating the compression and shear properties of real materials. These observations agree with the findings and conclusions presented by Cohen (1987) about the microstructure and properties of PBZT. He cited the microfibril as the structural element responsible for the fiber's compressive properties, postulating that the length:width ratio controls the compressive properties. This is set during coagulation; post-processing merely changes the packing within crystals. The ideal coagulant might be one which encouraged slow growth of only a few nuclei, rather than quick growth of many.

Finally, the impregnation technique which was successful for PBZT fiber is much less successful in PPTA fibers. The differences in morphology and pore size between the two fibers is at least partially responsible for this. Attempts were made to spin fibers with more open structures, via reduced-concentration solutions, but these solutions were found to have low integrity and could not be successfully spun into fibers.

CHAPTER 4

POLY(P-PHENYLENE BENZOBISOXAZOLE) [PBO]

4.1 Introduction

Poly(p-phenylene benzobisoxazole) [PBO], like PBZT, is a rigid-rod polymer that was synthesized at the Stanford Research Institute for the Air Force Ordered Polymers Program. This fiber is headed toward commercial production, with the rights to development having been purchased by the Dow Chemical Company. PBO has been found to have high thermal stability in air, degrading at 635°C, while exhibiting high tensile modulus and strength (370 GPa and 4.1 GPa, respectively, for heat treated/tension-dried fiber) [Adams et al., 1986]. Its compressive strength is an order of magnitude less than its tensile strength, an Achilles heel in terms of use in composite materials.

Coagulation and impregnation studies were performed on PBO fibers in order to compare the effects of these perturbations with changes caused in PBZT and PPTA fibers. Again, the emphasis was on raising shear and compressive properties through the increase of lateral interactions between microfibrils, either through specific interactions or by the physical presence of a stiff impregnator "glue". PBO has similarities with both PBZT and PPTA; with PPTA, it shares the commonality of a repeat unit containing both two nitrogen and two

oxygen atoms, as well as its lyotropic nature. It is much more closely related to PBZT, with the only difference being two oxygen atoms substituted for the two sulfur atoms in each repeat unit. PBO is also spun from poly(phosphoric acid), and its crystal structure is also very similar to that of PBZT. The unit cell is monoclinic, with dimensions of $\underline{a} = 5.64 \text{ \AA}$, $\underline{b} = 3.58 \text{ \AA}$ and $\underline{c} = 12.07 \text{ \AA}$.

4.2 The Effect of Coagulant on the Structure and Mechanical Properties

4.2.1 Experimental

Fibers were coagulated into a falling stream; the coagulant was at room temperature. Coagulants used were distilled water, 95% ethanol, an 18% solution of iodine in ethanol, and an 8.3% (0.5M) solution of potassium iodide in water. For each sample not coagulated in water, two bobbins of material were spun at the same take-up speed; after fiber was collected, one bobbin was soaked in water, while the other was soaked in a fresh aliquot of the coagulating liquid. Thus, fiber referred to as PBO/IEt/H₂O was coagulated in iodine/ethanol and then soaked in water; PBO/IEt/IEt was coagulated and soaked in the iodine/ethanol solution.

Tensile and torsion properties were determined as outlined in section 2.2; wide-angle X-ray scattering patterns were obtained using a

Statton camera, with a sample-to-film distance of 49.15 mm. As with as-spun PBZT fibers, reliable compressive strength measurements could not be obtained on as-spun fibers.

4.2.2 Fiber Microstructure

The wide-angle X-ray scattering studies of as-spun PBO fiber coagulated and soaked in water (PBO/H₂O) and in ethanol (PBO/ETH/ETH) are shown in figures 4.1 and 4.2, respectively; there appear to be no substantial differences between the two patterns. Fiber coagulated and soaked in iodine/ethanol (PBO/IET/IET, figure 4.3) also shows no apparent changes in crystal structure, although chemical microanalysis determined that the fiber contained 19% iodine species by weight.

The WAXS pattern for PBO fiber coagulated and soaked in potassium iodide (PBO/KI/KI, figure 4.4), however, is markedly different due to the presence of new reflections. These new reflections are not seen when fiber is coagulated in potassium iodide but then soaked in water (PBO/KI/H₂O, figure 4.5).

To determine whether exposure to potassium iodide in the coagulation step was crucial, fiber that was coagulated and soaked in water was impregnated with an 8.3% potassium iodide solution (PBO/H₂O/KI). This fiber was allowed to soak in the full-strength KI solution for 96 hours before removal for WAXS analysis; this was the

Figure 4.1 *Top:* The WAXS pattern of as-spun PBO fiber which was coagulated and soaked in water [PBO/H₂O/H₂O]. *Bottom:* Schematic of reflections.



Figure 4.2 The WAXS pattern of as-spun PBO fiber which was coagulated and soaked in ethanol [PBO/ETH/ETH].

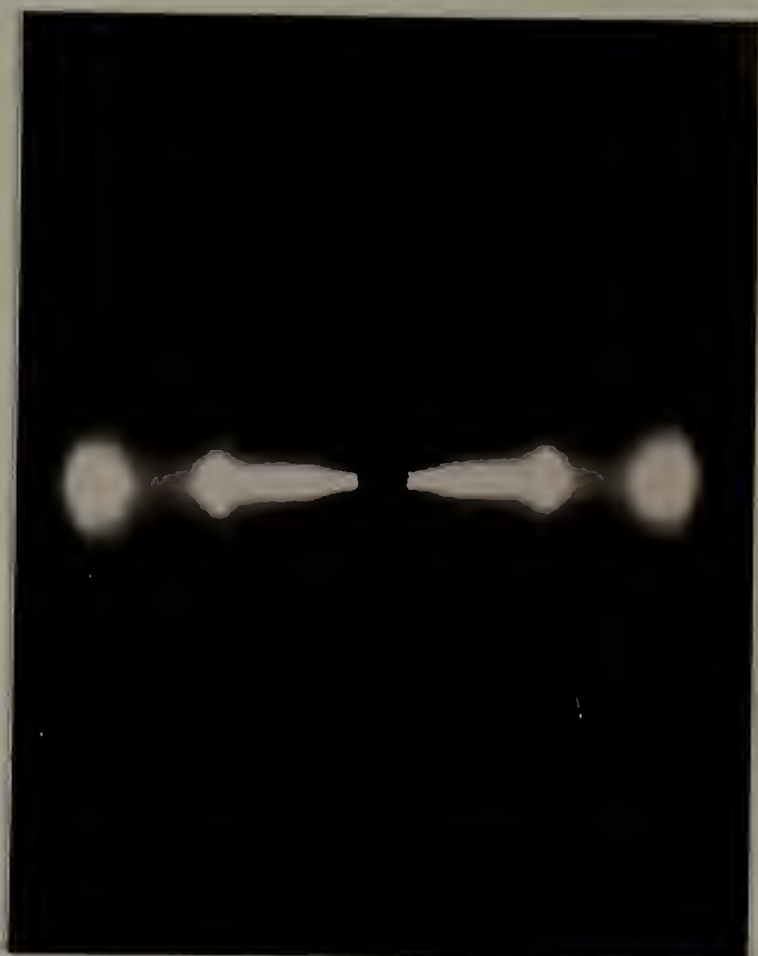


Figure 4.3 The WAXS pattern of as-spun PBO fiber which was coagulated and soaked in iodine/ethanol solution [PBO/IET/IET].

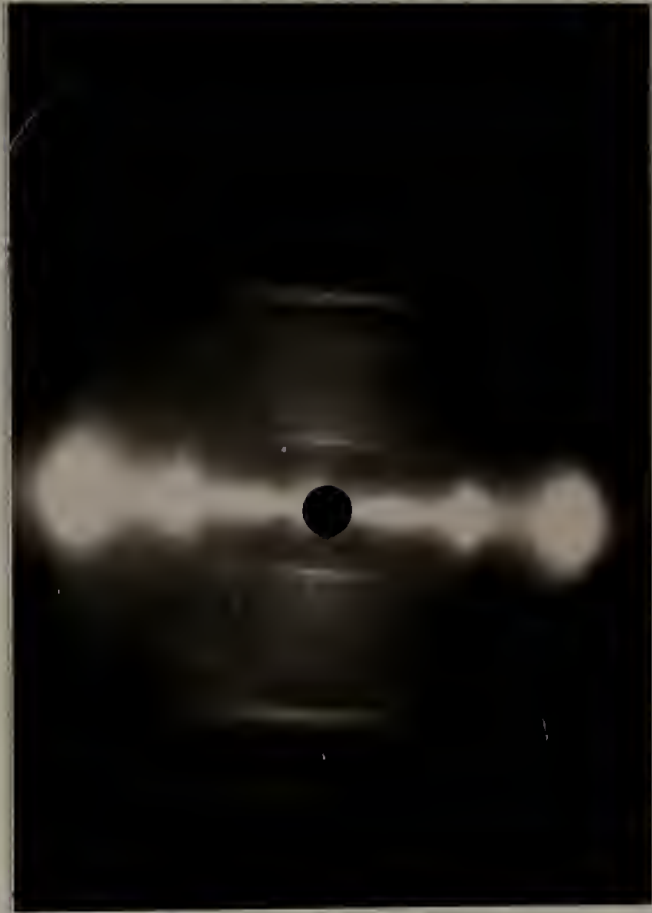


Figure 4.4 Top: The WAXS pattern of as-spun PBO fiber which was coagulated and soaked in 0.5 M potassium iodide solution [PBO/KI/KI]. Bottom: Schematic of reflections.



Figure 4.5 The WAXS pattern of as-spun PBO fiber which was coagulated in potassium iodide but then soaked in water [PBO/KI/H₂O].



amount of time the PBO/KI/KI fiber had soaked in aqueous KI solution before being removed for WAXS analysis. The WAXS results are shown in figure 4.6; the new reflections observed in the PBO/KI/KI fiber are not present in the PBO/H₂O/KI fiber.

The values of the d-spacings for PBO/H₂O and PBO/KI/KI fibers are given in tables 4.1 and 4.2, respectively. From these values, it can be seen that the new reflections, including off-axis reflections, in the PBO/KI/KI sample are superimposed on the standard PBO reflections. The fact that maxima on the Debye-Scherrer rings exist indicates that orientation of some species has occurred and suggests that epitaxy may be responsible for the ordered character of the reflections.

Use of the ASTM powder diffraction index indicated that the three most intense d-spacings for potassium iodide were at 4.08 Å, 3.53 Å and 2.498 Å and correspond to the 111, 200 and 220 reflections, respectively. These values are in good agreement with the observed reflections at 4.11 Å (and 4.01 Å), 3.48 Å and 2.46 Å in the PBO/KI/KI fiber. It is thus assumed that potassium iodide is the species undergoing some sort of orientation within the PBO fiber.

Microanalysis showed that 10.4 weight percent of the fiber was iodine species and that 2.3 weight percent was due to potassium. In terms of stoichiometry, potassium iodide contains 23.6 weight percent potassium, for a 1:3.2 weight ratio of K:I, or an atomic ratio of 1:1. The PBO/KI/KI fiber has a K:I weight ratio of 1:4.5, which indicates that there is some free iodine species also trapped within the fiber. Since there are no reflections at 15.4-15.5 Å or 9.4-9.8 Å, the "fingerprint" regions for I₅⁻ and I₃⁻, it is not likely these iodide anions are present. The ASTM powder diffraction table lists the three strongest reflections for

Figure 4.6 The WAXS pattern of as-spun PBO fiber coagulated and soaked in water, then impregnated for 96 hours with a 0.5 **M** (8.3%) potassium iodide solution (PBO/H₂O/KI).



Table 4.1 d-spacings of PBO fiber coagulated in water [PBO/H₂O]

<u>Reflection</u>	<u>d(Å)</u>
M ₁	11.75
M ₂	3.80
E ₁	11.73
E ₂	5.39
E ₃	3.39
E ₄	3.17

Table 4.2 d-spacings of PBO fiber coagulated and soaked in aqueous potassium iodide (PBO/KI/KI)

<u>Reflection</u>	<u>d(Å)</u>
M ₁	11.73
M ₂	3.88
M ₃	3.48
M ₄	2.89
E ₁	11.73
E ₂	5.48
E ₃	4.11
E ₄	3.48
E ₅	3.17
OA ₁	4.01
OA ₂	3.48
OA ₃	2.46

iodine (I_2) at d-spacings of 3.708 Å, 3.635 Å, and 3.10 Å. The PBO reflection at 3.17 Å might mask or include the appearance of the 3.10 Å reflection.

The PBO reflection that is found in the PBO/H₂O fiber at 3.39 Å is missing from the PBO/KI/KI fiber; the reason for this is presently unknown. The fact that one of the major equatorial reflections is missing could signal a change, possibly large, in the symmetry of the PBO unit cell. Because all the other expected PBO reflections are present, however, it will be assumed at this time that the crystal structure of the PBO molecule has been perturbed rather than totally altered.

Epitaxial crystallization, or epitaxy, is the oriented nucleation and growth of a crystalline substance on a single crystal substrate. Polymer epitaxy was first observed for polymers crystallized from solutions deposited onto alkali halide surfaces [Willems, 1957]. By studying a variety of polymers--polyethylene, polystyrene, polypropylene--it soon became apparent that whenever these were epitaxially crystallized onto a cleaved alkali halide (001) face, the polymer's chains would be aligned in the $\langle 110 \rangle$ direction of the crystal face [Koutsky et al. 1966].

This has been explained through a series of energy calculations which found that the low energy orientation of the chain on a (100) face is parallel to the substrate and aligned in the $\langle 110 \rangle$ direction [Mauritz, 1973]. In other words, the energetically favorable polymer chain positioning is along rows of positive ions, while alignment along rows of negative charge is energetically unfavorable.

Mr. John Reffner's help in attempting to determine the orientation of potassium iodide in relation to the PBO molecule is acknowledged and

appreciated. It was first attempted to fit the locations of the observed potassium iodide reflections with the predicted reflections if rotation was about the $\langle 110 \rangle$ axis of potassium iodide. This choice was made due to the overwhelming experimental evidence that was outlined above. However, attempting to index the reflections along this axis was impossible; the model predicted that the (111), (200) and (202) reflections would fall on the meridian, as layer lines. In reality, only the (200) reflection appears along the meridian. It did predict the equatorial (111) reflection (at 4.11 Å), but it also predicted two reflections which did not occur along the equator. This model was discarded due to too many discrepancies between predicted and observed reflections.

It was then attempted to index by rotation around potassium iodide's $\langle 100 \rangle$ axis, as this was reasonably straightforward. This model did predict the (200) reflection along the meridian, and correctly predicted no other meridional reflections. It also correctly predicted the (111) and (220) off-axis reflections (those at 4.01 Å and 2.46 Å), but did not predict the (200) reflection (at 3.48 Å). Along the equatorial axis, it predicted the only the appearance of reflections at 3.48 Å (200) and 2.46 Å (220). It did not predict the observed (111) reflection at 4.01 Å, and the predicted (220) reflection is not observed, although the absence of this last reflection in the Statton film could be due to the sample-to-film distance. So, while this model, based on rotation around the $\langle 100 \rangle$ axis, does predict many of the observed reflections, it still falls short and cannot alone be used to explain the orientation of the potassium iodide molecules within the PBO fiber. One possibility is that the $\langle 110 \rangle$ and the $\langle 100 \rangle$ orientations coexist. Since the equatorial (220) reflection is predicted in both, a test of this would be to use a shorter

sample-to-film distance, and see if the reflection did indeed appear. If so, the coupling of both orientations does do an adequate job of predicting the observed reflections.

Follow-up work to examine this hypothesis was performed by obtaining WAXS patterns at a sample-to-film distance of 18.1 mm for both PBO/H₂O/H₂O (figure 4.7) and PBO/KI/KI (figure 4.8). As shown in table 4.3, the equatorial (220) reflection is indeed present. This data seems to strengthen the case for the proposed model which contains both orientations of the potassium iodide crystals within the oriented PBO fiber. Although this model does not explain why 2 orientations would be present, the fact that PBO does not conform to the previous examples of 110-oriented epitaxy could be due to the fact that the PBO fiber consists of oriented rigid rods while the other studies involved flexible chain polyolefins. In the only other similar reference we could find in the literature, it was suggested that blow-molded specimens of nylon and polyethylene loaded with 20-60 parts per hundred of talc experienced epitaxy. This resulted in orientation of the nylon film and increased orientation of the PE film, although nylon films had the (002), not (110), planes parallel to the talc's (001) planes [Murthy et al. 1986].

Figure 4.7 WAXS pattern of PBO/H₂O/H₂O at a sample-to-film distance of 18.1 mm.



Figure 4.8 WAXS pattern of PBO/KI/KI at a sample-to-film distance of 18.1 mm.

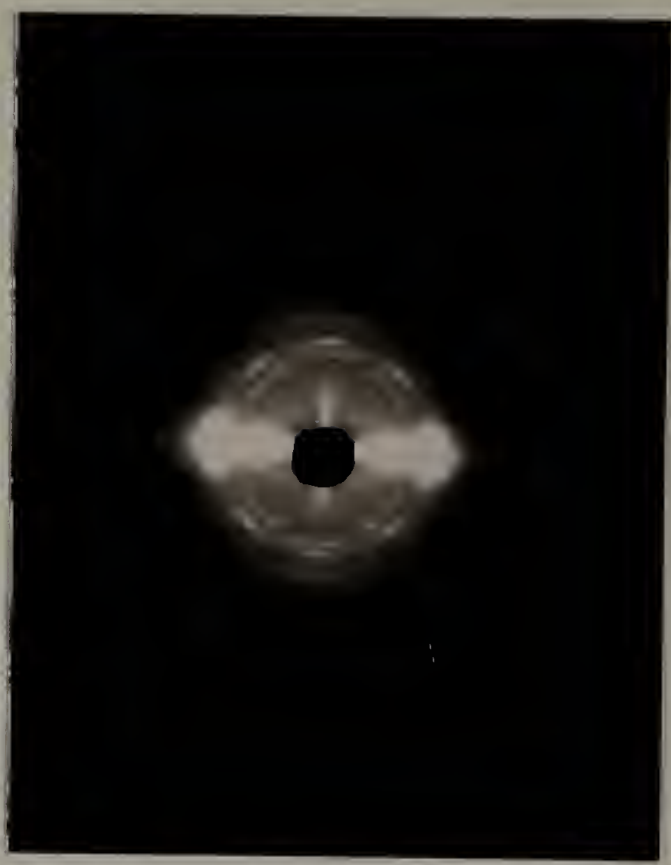


Table 4.3 d-spacings and assignment of reflections found in the PBO/KI/KI fiber

<u>Reflection</u>	<u>d(Å)</u>	<u>Assignment</u>
M ₁	11.73	PBO
M ₂	3.88	PBO
M ₃	3.48	200 (KI)
M ₄	2.89	PBO
E ₁	11.73	PBO
E ₂	5.48	PBO
E ₃	4.11	111 (KI)
E ₄	3.48	200 (KI)
E ₅	3.17	PBO
E ₆	2.49	220 (KI)
OA ₁	4.01	111 (KI)
OA ₂	3.48	200 (KI)
OA ₃	2.46	220 (KI)

4.2.3 Mechanical Properties

Tensile and torsion properties of the fiber/coagulant systems studied are summarized in table 4.4. Taking into account minor differences caused by the small variances in spin/draw ratios and the standard deviations, there are no significant changes in either tensile or torsion properties as a function of coagulant for any of the fibers.

While tensile and torsion properties are similar for the PBO/KI/KI, PBO/KI/H₂O, and PBO/H₂O fibers, there was a difference in the type of tensile failure shown by the PBO/KI/KI fiber. The PBO/KI/KI fiber was observed to fail longitudinally and stepwise, so that there were several sharp reductions in load before total failure. This occurred at rates which permitted the observer to watch the fiber fail, as well as listen for the cracking sounds which accompanied the longitudinal delamination. These events were simultaneously recorded as partial load reductions by the chart recorder; a reproduction of the chart recording is shown in figure 4.9. SEM photographs of typical PBO/KI/KI tensile fracture specimens are shown in figures 4.10 and 4.11. This type of failure was observed for roughly half of the PBO/KI/H₂O samples. PBO/H₂O fibers, however, failed with an immediate and total reduction of load. Typical SEM micrographs for PBO/H₂O tensile fracture specimens are shown in figure 4.12 and 4.13, respectively.

Table 4.4 The effect of coagulant on the mechanical properties of PBO fibers

Coagulant	S/D	G, GPa	E, GPa	σ_b , GPa
H ₂ O	17	0.53 ± 0.06	84 ± 11	3.2 ± 0.7
IET/H ₂ O	14	0.48 ± 0.04	115 ± 10	2.5 ± 0.3
IET/IET	14	0.54 ± 0.07	93 ± 10	1.8 ± 0.4
KI/KI	10	0.60 ± 0.06	90 ± 14	3.0 ± 0.5
KI/H ₂ O	10	0.56 ± 0.07	97 ± 10	3.0 ± 0.5
ETH/ETH	16	0.46 ± 0.09	94 ± 10	2.7 ± 0.4

Figure 4.9 A reproduction of a typical chart recording of a tensile test for PBO/KI/KI fibers, showing the partial load reduction before catastrophic failure.

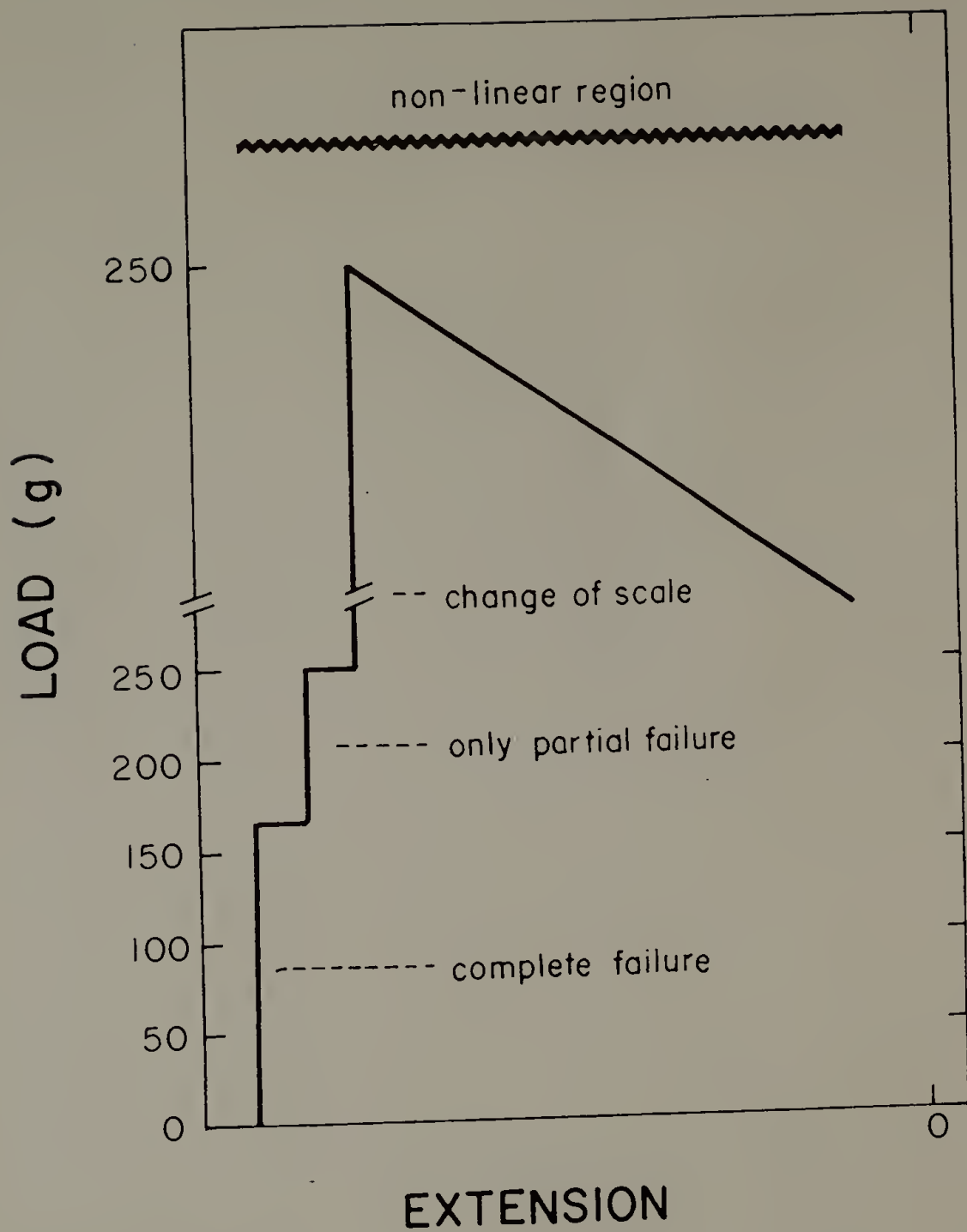


Figure 4.10 Scanning electron micrograph of a typical tensile specimen of PBO/KI/KI. This location is not near the actual fracture end of the fiber.

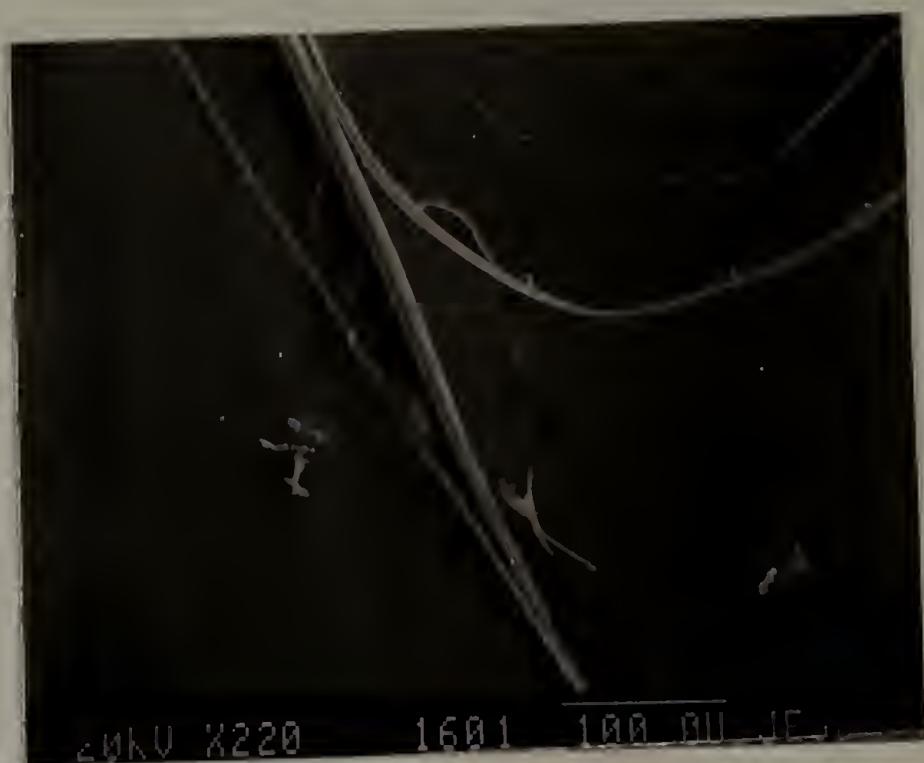


Figure 4.11 Two scanning electron micrographs of higher magnification of selected areas of the same sample shown in figure 4.10.

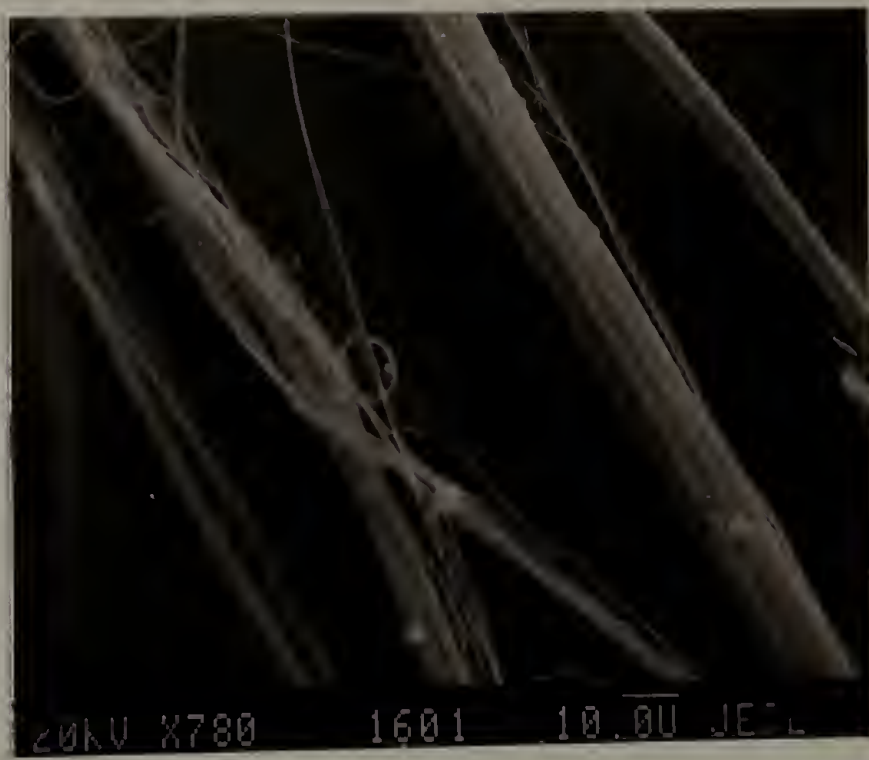


Figure 4.12 Scanning electron micrograph of a typical tensile specimen of PBO/H₂O/H₂O. This photo has the broken end of the fiber located at the top of the photograph.

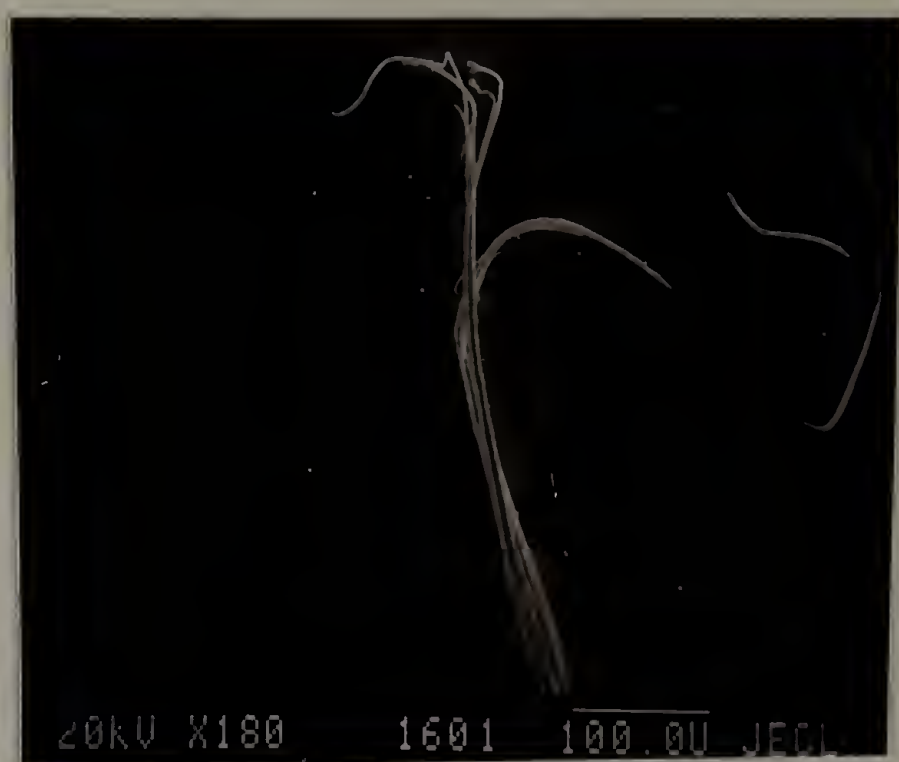
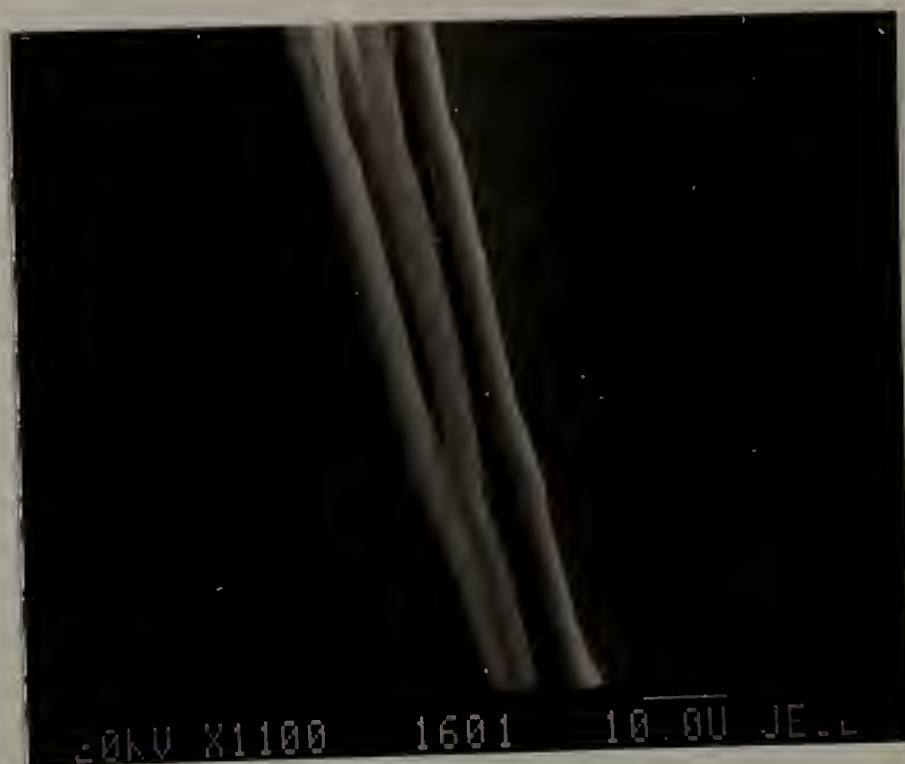
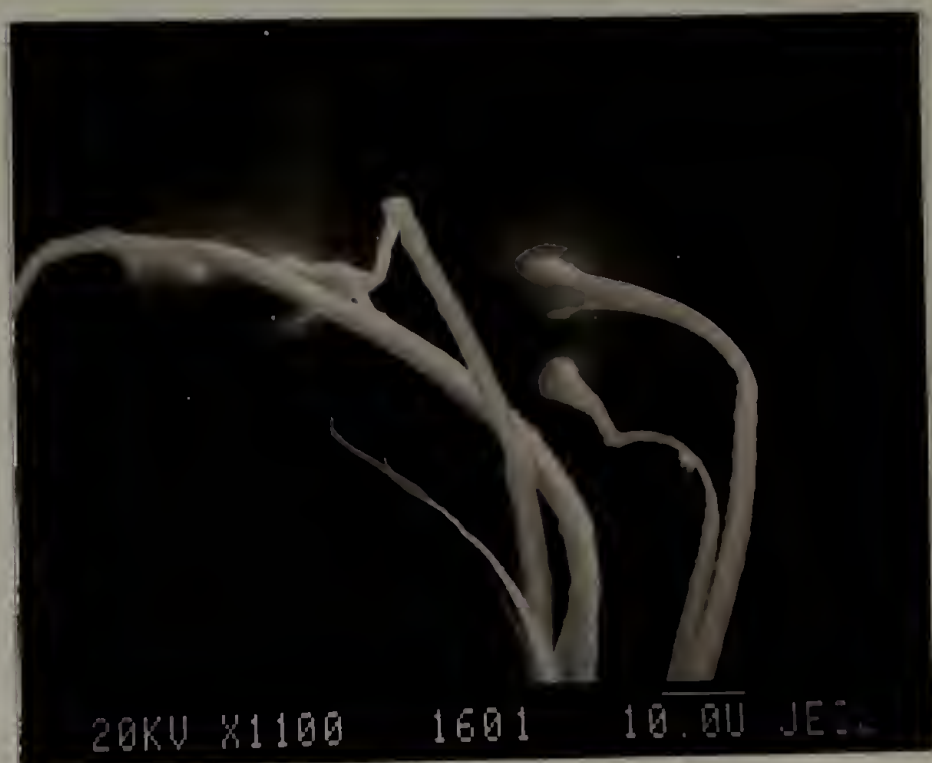


Figure 4.13 Two micrographs of higher magnification of selected areas from the same sample shown in figure 4.12. Top: Part of the fracture surface (with probable sample charging). Bottom: Further away from the fiber end.



4.3 Fiber Impregnation

4.3.1 Experimental

An impregnator material used in the PPTA impregnation studies, Tyzor LA[®], was the sole material used in the PBO impregnation studies. This material was chosen because it produced the best results seen so far in PPTA impregnation. The solution exchange procedure detailed in figure 2.1 was again followed, and the fiber was allowed to soak in the impregnator solution at room temperature for 108 hours.

It was initially desired to heat treat/tension dry the impregnated and control fibers while keeping them wet until the actual moment of tensioning/heat treatment. This method was outlined by Pottick (1985) and refers to the wet fiber as "as-coagulated". A temperature high enough to vitrify the impregnator material, 430°C [DuPont, 1988], and an initial tension corresponding to 860 MPa was chosen, along with a nitrogen atmosphere. Although the temperature was well below the degradation temperature, and the tension was approximately 30% of the tensile strength of the as-spun fiber, PBO coagulated in water could not be post-processed this way. Even when no tension was applied to the fiber, the fiber line consistently broke during its passage through the oven. After a number of failed attempts to post-process the wet fiber, it was allowed to dry on the wheel, and then was heat treated/tension

dried. It was possible to post process the as-spun PBO/H₂O fiber at 430°C, but a lower tension of 610 MPa had to be used. Residence time was 195 seconds.

The Tyzor LA[®]-impregnated fiber also could not be heat treated/tension dried while wet, even when no tension was applied. It was allowed to air dry, and then was post-processed at a temperature of 430°C for 195 seconds, but the maximum applied tension was 430 MPa. There was no difference in fiber appearance before and after heat treatment.

All fiber diameters were measured using the laser diffraction technique outlined in Chapter 2. Tensile, torsion and compressive properties were measured as outlined in Chapters 2 and 3. Due to constraints on both time and facilities, no microanalysis measurements to determine the amount of Tyzor LA[®] in the fiber were attempted.

4.3.2 Mechanical Properties

Although Tyzor LA[®] provided the best results so far for PPTA impregnation, it appears to have little or no effect on any of the mechanical properties of PBO fibers. Table 4.5 compares tensile, shear and compressive data for the control (PBO/H₂O) and the impregnated (PBO/TY) fibers. Tensile properties are somewhat lower for the PBO/TY fiber, but this fiber was of necessity post-processed at an applied tension approximately one-third less than that applied to the PBO/H₂O fiber (430 MPa versus 610 MPa). Compressive strength and torsion moduli

Table 4.5 The effect of impregnation with Tyzor LA[®] on the mechanical properties of PBO fibers

Property	PBO/H ₂ O	PBO/Tyzor LA [®]
Post-Processing Tension Applied, (MPa)	610	430
Tensile Modulus, (GPa)	220 ± 30	180 ± 20
Tensile Strength, (GPa)	3.8 ± 0.6	2.9 ± 0.6
Torsion Modulus, (MPa)	610 ± 120	640 ± 80
Compressive Strength, MPa: Above which all fibers failed	335	348
50% failure region	320-335	333-348

appear to be unaffected by impregnation as well, with all PBO/TY fibers failing above 348 MPa and all PBO/H₂O fibers failing above 335 MPa.

Possible reasons for the ineffectual impregnation with Tyzor LA[®] could be insufficient diffusion of the material into the fiber, perhaps due to size constraints or unfavorable molecular interactions. Also, once inside the fiber the titanate chelates may have been too isolated to effectively reinforce the microfibrils.

4.4 Conclusions

Coagulation studies showed that while mechanical properties were not affected by any of the coagulants used, coagulation in an aqueous potassium iodide solution resulted in a fiber containing both oriented PBO and oriented potassium iodide molecules. PBO fiber which was coagulated and further soaked in an iodine/ethanol solution was found to contain 19% iodine species by weight; however, no changes in the WAXS pattern were observed. This indicates that neither the nitrogen/iodide anion complexation observed in PBZT fiber nor the epitaxy observed for the PBO/KI/KI fiber occurs when PBO is coagulated in iodine/ethanol. The orientation of the potassium iodide molecules within the PBO fiber is unknown at this point, although it appears that the KI molecules are aligned along both the 100 and the 110 orientations. However, unlike many other examples of polymer epitaxy on alkali halide surfaces, it has been shown that in the PBO/KI/KI fiber, potassium iodide does not exhibit epitaxy along the $\langle 110 \rangle$ axis.

Actually, little or no interaction was expected between the PBO molecule and iodide anions. Hammond (1965) describes a class of compounds $C_wN_xO_y$ ($w \gg x, y$) which are good electron acceptors. Iodine and iodide anions are themselves acceptor molecules, and can only form complexes with donor molecules. In effect, the presence of the oxygen in the ring acts to withdraw electrons from the nitrogen, preventing complexation of nitrogen and iodine/iodide. Oxygen-iodine/iodide complexation, while it does occur, is a very much weaker interaction than nitrogen-iodine/iodide [Rose, 1967]. On the other hand, nitrogen-iodine/iodide complexation can occur in the PBZT molecule because the sulfur atom is much less electronegative than oxygen; valence electrons are well-shielded and size effects keep nitrogen's lone pair electrons concentrated around the nitrogen atom and available for complexation [Jackson, 1989].

It appears that for orientation of potassium iodide within a PBO fiber to occur, it is necessary to both coagulate and soak the fiber in the KI solution. Potassium iodide is water soluble, of course, and most likely was leached out of the PBO/KI/H₂O fiber, since chemical analysis found less than 0.2 weight percent iodine species in that fiber. While the attempt to produce ordered potassium iodide crystals within water-coagulated fiber was unsuccessful and supports the hypothesis that coagulation is the crucial event, more conclusive proof would be to coagulate PBO into water and then immediately soak it in the aqueous KI solution.

The mechanical properties of PBO impregnated with Tyzor LA[®] were not increased; within standard deviation, there was no difference between the heat treated/tension dried fiber and the

heat treated/tension dried impregnated fiber. The reason for the lack of reinforcement at this time is unknown. Due to problems experienced in post-processing PBZT impregnated with sodium silicate, impregnation with this material would not seem to be a good alternative to the Tyzor LA[®].

CHAPTER 5

SUMMARY AND FUTURE WORK

5.1 Summary

This research has found that when coagulants are used which can form strong associations with these lyotropic polymer molecules, it is indeed possible to influence the mechanical and/or structural properties of the fibers produced. For PBO and PPTA in particular, the presence of cations may be very important in terms of ability of the ionic species to successfully complex with the polymer. These conclusions were reached by reviewing the results of the coagulation studies and comparing them with the chemical structure of each polymer, as outlined below:

---Coagulation of PBO or PBZT fibers in ethanol does not affect mechanical or structural properties

---Coagulation of PPTA fibers in ethanol causes no change in crystal structure; the only affected mechanical property is compressive strength, which is decreased from 370 MPa to 230 MPa

---Coagulation of PBZT fiber in aqueous potassium iodide solution has no effect on structural or mechanical properties

---Coagulation of PPTA and PBO into potassium iodide results in changes in fiber which are reflected in the diffraction pattern of each. PPTA molecules become much less oriented along the fiber axis; in the PBO fiber, orientation of the potassium iodide crystals within the fiber, as well as orientation of the PBO chains, occurs

---Coagulation of PPTA into potassium iodide results in massive decreases in all mechanical properties, while PBO fiber coagulated in the same solution shows no change in tensile or torsion properties

---Coagulation of PBZT into an 18% iodine/ethanol solution results in changes in the crystal structure of PBZT, and in some cases, significantly increases the fiber's tensile and torsion properties

---Coagulation of PPTA and PBO into the same iodine/ethanol solution produces no changes in diffraction patterns or mechanical properties, even though chemical microanalysis shows that those fibers have 19-21 weight percent iodine species in them

Basically, coagulation in potassium iodide affects structural and/or mechanical properties of PBO and PPTA; it has no discernible

effect on PBZT. In contrast, coagulation in iodine/ethanol affects mechanical and/or structural properties of PBZT, but has no discernible effect on PBO or PPTA. Since both solutions produce iodide anions (I^- , I_3^- , I_5^- , generalized as I_x^-), why do PBO and PPTA fibers react differently to these coagulants than PBZT?

Since both aqueous potassium iodide and iodine/ethanol solutions produce the same anions, a literature study was undertaken to try to determine if there was any precedent for cations, particularly cations of alkali salts, to affect the behavior of other polymers. And also, because of the very different results seen in coagulating PPTA in LiCl vs. KI, were there any similar incidents with other alkali salt series? After completing this literature search, it was found that the effects of various alkali salts on a number of polymers have been the object of several studies, which are summarized below.

It has been found that when lithium salts such as lithium chloride and lithium bromide are mixed with nylon-6 and then extruded into single filaments, the elastic modulus of the polymer increases from 5 GPa to 14 GPa; on the other hand, potassium chloride has absolutely no effect on the tensile properties [Acierno et al. 1979]. No change in crystal structure accompanies the increase in tensile modulus, however.

The addition of lithium salts, either lithium bromide or lithium chloride, to polyacrylonitrile films cast from DMF results in complexation of the lithium salt with the nitrile group. This complexation does not occur when potassium bromide or sodium chloride are added to the solution, and strongly points to the lithium cation as being responsible for the ability of alkali halide salts to complex with polyacrylonitrile [Padhye and Karandikar, 1985].

Finally, the effect of sodium iodide and potassium iodide on solutions of poly(methacrylic acid) in methanol showed that at small concentrations of KI and NaI, the reduced viscosity of the solutions steeply decreased. This effect was more pronounced in the solution containing sodium iodide. The control solution, PMA in methanol, showed the opposite behavior. By comparing different salts, it was found that their effect on the reduced viscosity of the PMA solution was mainly dependent on the cation [Horsky et al. 1986].

What these polymers have in common with PPTA and PBO is their sensitivity to alkali salts, and in particular, sensitivity to the presence of the cations of those salts. In terms of similarities in molecular structures, all contain chemical groups having one or more heteroatoms containing a lone pair of electrons, or an electron-withdrawing structure, such as a carbonyl; PPTA, PBO, PMA and nylon-6 all contain 2 oxygen atoms per repeat unit. The accumulated evidence seems to suggest that alkali halide salts can have a very strong effect on some polymers, particularly those containing oxygen, and that the cation may determine whether changes in mechanical or structural properties occur. This seems to be the best "first order" answer to the question of why aqueous potassium iodide, not iodine/ethanol, affected PBO and PPTA fibers; however, the reason for cation-sensitivity of these oxygen-containing polymers has not been satisfactorily answered by anyone yet.

With this information, it is thus not so surprising that one alkali halide salt, lithium chloride, is listed in the Du Pont patent literature as an additive to the spinning dope [Blades, 1973b], while another alkali halide salt, potassium iodide, is remarkable for its ability to reduce torsion modulus of PPTA fiber from 1.36 GPa to 0.46 GPa, and tensile

modulus from 88 GPa to 20 GPa. While neither cation nor anion have been kept constant, the above discussion underscores the need to consider both the possible action of the cation as well as the anion on the polymer.

It is highly interesting that this association can occur in the time scale ongoing in the coagulation process, and does not seem to be able to occur if the fiber is coagulated in water and then soaked in the ion-containing solution. Two examples of this "irreversibility" are the PBZT fiber coagulated in water and then soaked in iodine/ethanol solution, and the PBO/H₂O fiber that was soaked in aqueous KI solution. From WAXS studies, it was seen that neither complexation of iodine species nor orientation of potassium iodide was able to occur in these water-coagulated fibers.

We have found that coagulation in water renders subsequent impregnation with the complexing molecules ineffective. This leads to the hypothesis that rather than a quasi-two-phase system (polymer and coagulant), the acid-coagulant interactions as well as the acid-coagulant-polymer interactions and chemical reactions together determine the fiber microstructure. While this thesis work did serve to expose the importance of these two factors during the actual fiber spinning process, they were not explored. Certainly, further research is needed to clarify the importance of the acid/solvent to the final structural and mechanical properties of the fiber. However, this will not be an easy task, due to the fact that these lyotropic polymers are soluble in very few substances. For example, while PBZT is soluble in either PPA or MSA (methane sulfonic acid), it can only be dry-jet wet spun from PPA solution--and so there will be some uncertainties in determining whether

some effects are due to molecular or chemical interactions between the three components, or to the different spinning processes used. PBZT has also been found to be soluble in some aprotic organic solvents via reversible complex formation with Lewis acids [Jenekhe et al. 1989]; again, studies involving the effect of coagulants and possible interactions between the three component system will yield a great deal of information, but direct comparisons to the PPA system will be difficult.

The results of this work raise more questions than can be answered. Why are the structural and/or mechanical properties of PBO and PBZT fibers more readily influenced by coagulant? Why is water the "best" coagulant for PPTA fibers? One possible reason to explain why structural and mechanical properties of PBO and PBZT are more easily influenced by coagulant is that their fiber microstructure is more amenable to interaction and interference by chemical species. PBZT is a network of interconnected microfibrils; each microfibril is composed of a number of PBZT molecules. This allows coagulants with specific interactions, and small molecules for impregnation, access within and/or between the microfibrillar regions. PPTA, however, has a very different structure--radially oriented, pleated sheets which have hydrogen-bond linkages between the sheets. There is not as much room for maneuverability here--the hydrogen bonds appear to prevent most materials from having any substantial effect on the fiber, and if these bonds are destroyed, it has not been possible so far to replace them with anything better.

While the "best" coagulant for PBZT and PBO fibers is still a matter for further experimentation and refinement, it seems fairly certain that water is the best coagulant for the PPTA dopes spun in this

research. At best, properties were slightly raised; at worst, in the case of potassium iodide coagulation, all mechanical properties were seriously diminished. A plot of compressive strength versus shear modulus is shown in figure 5.1. A slope of 0.25 is obtained from linear regression, with a correlation of 0.93. This is in relatively good agreement with DeTeresa's findings of a slope of 0.3 for the same type of plot. Differences could be attributed to the way in which the compressive strength was obtained. DeTeresa used a technique which directly measured compressive strain [1984] and then calculated compressive strength, whereas in this research Allen's recoil technique [1987] was exclusively used to measure compressive strength directly. This seems to imply that the compressive failure mechanism, microbuckling, is generally not coagulant-dependent. Of the eight samples plotted, only the fibers coagulated in ethanol (PPTA/ETH) and in iodine/ethanol with further soaking in water (PPTA/IET/H₂O) fell far from the fitted line.

Water's strength as a coagulant could be due to its hydrogen bonding character. The hydrogen bonding ongoing in water might somehow facilitate the formation of the hydrogen-bonded PPTA microstructure. Coagulation in non-aqueous liquids could result in a fiber with a different microstructure, and possibly one which, for unknown reasons, did not share the same relationship between shear modulus and compressive strength.

For a given fiber, changes in crystal structure and/or mechanical properties have been observed, and can be attributed to the action of a particular coagulant. The PBO/KI/KI fiber is an example of some very interesting "transcrystallization"; however, its tensile properties and torsion modulus fall within the range of all the other PBO fibers tested.

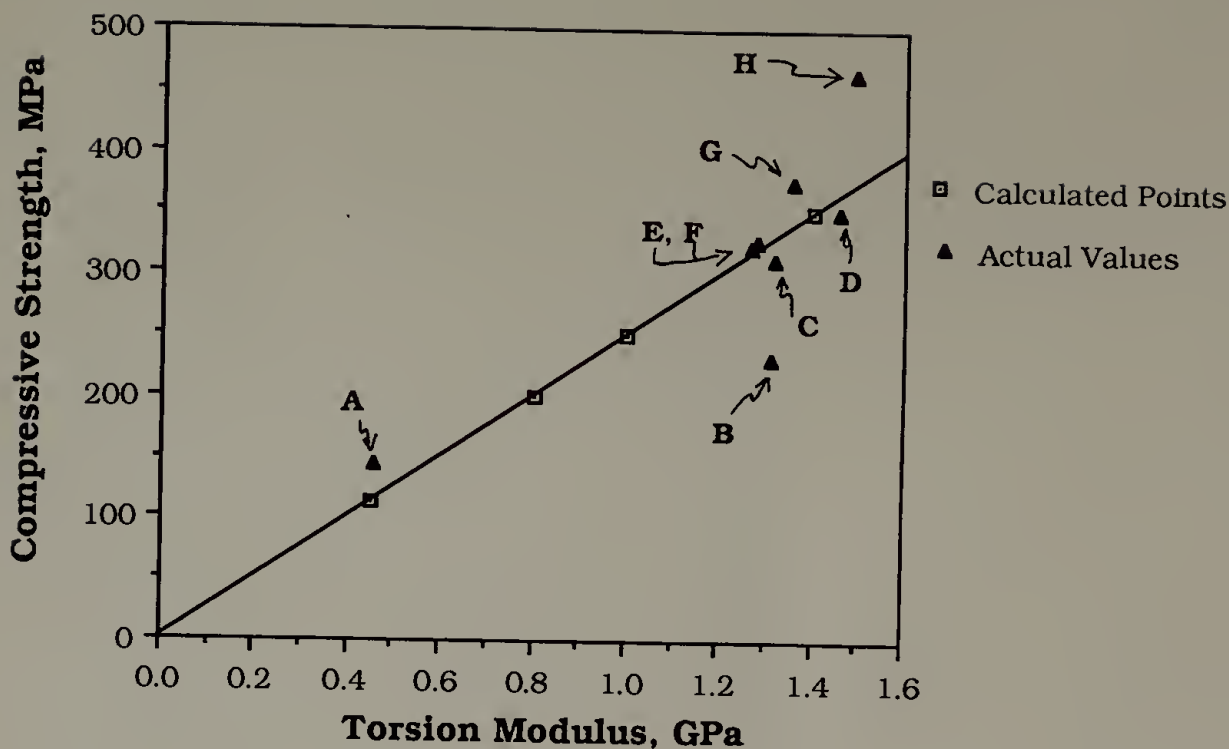


Figure 5.1 A plot of the experimental values of compressive strength versus torsion modulus for the PPTA fibers spun during the course of this thesis work, as well as calculated values. The identity of the individual experimental points are as follows: A) PPTA/KI; B) PPTA/ETH; C) PPTA/H₂SO₄; D) PPTA/LiCl; E) PPTA/NaOH; F) PPTA/IET/IET ; G) PPTA/H₂O; H) PPTA/IET/H₂O

The PPTA/KI fiber had substantial changes in all its mechanical properties; although there was very little orientation of the polymer chains along the fiber axis, the crystal structure of the fiber remained unchanged. With the exception of the PBZT fiber coagulated in iodine/ethanol, it has not been possible to correlate changes in torsion modulus or compressive strength with changes in the fiber's crystal structure as monitored by WAXS. This implies that the factors responsible for torsion modulus and compressive strength are primarily dependent on an element of fiber microstructure that is above the molecular level.

5.2 Future Work

This dissertation has shown that the mechanical and structural properties of fiber-forming lyotropic liquid crystal polymers can be strongly influenced by choosing a coagulant which has a strong chemical interaction with some portion of the polymer. Further, changes in structure and properties can occur in the coagulation step which cannot occur if the fiber is merely soaked in the same solution after coagulation in water. And it has been found that the cation present in the coagulant can play a very important role in the ability of the coagulant to interact with the polymer, particularly in the case of oxygen-containing polymers.

No detailed studies of the microstructure of the PPTA, PBO or PBZT fibers produced from the coagulation studies were performed, due to time and instrument constraints. It would be highly interesting and

informative to determine if and how coagulants changed fiber microstructure. This would presumably involve small-angle X-ray scattering and transmission electron microscopy, using the investigative method outlined by Cohen (1987). It is suggested that the first fibers investigated be the PPTA/ETH and the PPTA/IET/IET fibers, due to their deviation from the torsion modulus/compressive strength relationship which seems to hold for all the other fibers produced. This could be indicative of differences in microstructure which lead to a different type of failure mechanism. Also, this type of research might result in a clearer understanding of how the iodine species in the PBZT fiber can influence torsion properties, and how this seems to be dependent on the amount of iodine species present.

An extension of this work would be to study a series of aqueous alkali halide solutions as coagulants with both PPTA and PBO fibers, first by holding the cation constant and varying the anion, and then holding the anion constant and varying the cation. Heavily-concentrated salt solutions should also be investigated. Only one non-polar coagulant was investigated--the PPTA/hexane system--and the coagulation of PBZT or PBO into a non-polar coagulant might be considered. Further, only iodide anions have been considered. Iodine forms the I_3^+ cation in sulfuric acid [Huheey, 1978]; in non-polar solvents such as toluene or chloroform, only molecular iodine is present. The effect of these species on PBZT, PBO and PPTA should be investigated. Lastly, the PBZT/PPA crystal solvate that was formed by slow coagulation of PBZT film into an 85%PPA/15% H_2O solution [Cohen and Thomas, 1987] should be investigated for its application to PBZT fibers.

Approaching the problems of balancing the high tensile properties of these fibers with the shear and compressive properties from another angle could be a very exciting, though challenging, project. What seems to be required in order to produce major advances in this area is to approach the problem from the middle, rather than from either end. It is altogether one thing to look at a polymer's structure and deduce that it would be a rigid-rod, and another to engineer a process whereby it would be highly and irreversibly oriented during processing--but neither of these things guarantee anything about the fiber's microstructure, and it seems that compressive properties are most dependent on microstructure. The "ideal" fiber should be designed first with microstructure in mind. One place to start would be to design a polymer, and the appropriate processing, that would mimic the microstructure--and compressive properties--found in graphitic fibers.

Another promising aspect is underway in Dr. Farris's laboratory, with experiments whose goal is to graft onto the rigid-rod polymer. While physical reinforcement could be gained in this way, it should also be possible to graft a small molecule onto the rigid-rod backbone which would have a very strong specific interaction with a chosen coagulant. This could lead to a tailor-made polymer and coagulant system; perhaps properties could be balanced by the amount of complexing molecule grafted onto the chain.

REFERENCES

- Acierno, D., La Mantia, F.P., Polizzotti, G., and Ciferri, A. "Bulk Properties of Synthetic Polymer-Inorganic Salt Systems. V. Mechanical Properties of Oriented Poly(Caproamide)", *J.Polym.Sci.Polym.Phys.Ed.*, **17**, 1903-1912 (1979).
- Adams, W.W., et al., "Processing, Structure and Morphology of PBO and ABPBO Fibers", AFWAL-TR-86-4011, August 1986.
- Ahmed, I., Pritchard, J.G. and Blakely, C.F., "Studies on the Characterization of Partly Hydrolysed Derivatives of poly(vinyl acetate) and Their Red Iodine Complex", *Polymer*, **25**, 543-550 (1984).
- Allen, Stephen A., "Tensile Recoil Measurement of Compressive Strength for Polymeric High Performance Fibers", *J.Mat.Sci.*, **22**(3), 853-859 (1987).
- Allen, Stephen A., private communication, October 1988.
- Andrews, E.C., Equilibrium Statistical Mechanics, Wiley, New York, 1975.
- Aoki, H., Coffin, D.R., Hancock, T.A., Harwood, D., Lenk, R.S., Fellers, J.F. and White, J.L., "Synthesis, Characterization, Rheological, and Fiber Formation Studies of p-Linked Aromatic Polyamides", *J.Polym.Sci.: Polym.Symp.*, **65**, 29-40 (1978).
- Arimoto, H., Ishihashi, M. and Hirai, M., "Crystal Structure of the γ -form of Nylon 6", *J.Polym.Sci., Part A.*, **3**, 317-325 (1965).
- Bair, T.I. and Morgan, P.W., U.S. Patent 3,817,941, (1974).
- Bair, T.I., Morgan, P.W. and Killian, F.L., "Poly(1,4-phenylene terephthalamides). Polymerization and Novel Liquid-Crystalline Solutions", *Macromolecules*, **10**(6), 1396-1400 (1977).
- Balik, C.M., Tripathy, S.K. and Hopfinger, A.J., "Epitaxial Morphologies of Polyoxymethylene. I. Electron Microscopy", *J.Polym.Sci.: Polym.Phys.Ed.*, **20**, 2003-2016 (1982).
- Bashir, Z., and Keller, A., "Melt Drawing as a Route to High Performance Polyethylene", *Colloid and Poly.Sci.*, **267**, 116-124 (1989).

- Baughman, R.H., Murthy, N.S., Miller, G.G. and Shacklette, L.W., "Staging in Polyacetylene-Iodine Conductors", *J.Chem.Phys.*, **79**(2), 1065-1074 (1983).
- Bhaumik, D., Welsh, W.J., Jaffe, H.H. and Mark, J.E., "Interchain Interactions in Some Benzobisoxazole and Benzobisthiazole Rigid-Rod Polymers", *Macromolecules*, **14**, 951-953 (1981).
- Blades, Herbert, U.S. Patent 3,767,756, assigned to E.I. du Pont de Nemours and Company (1973).
- Blades, H., U.S. Patent 3,869,429 assigned to E.I. du Pont de Nemours and Company (1975a).
- Blades, H., U.S. Patent 3,869,430 assigned to E.I. du Pont de Nemours and Company (1975b).
- Boehm, H.P., Ko, Y.-Sh., Ruisinger, B. and Schlogl, R. in Chemical Reactions in Organic and Inorganic Constrained Systems, R. Setton, Ed, pp. 429-220, D. Reidel Publishing Company, Boston, 1986.
- Brinker, C.J., Keefer, K.D., Schaefer, D.W. and Ashley, C.S., "Sol-Gel Transition in Simple Silicates", *J.Non-Cryst.Sol.*, **48**, 47-64 (1982).
- Brody, H., "Orientation Suppression in Fibers Spun From Polymer Melt Blends", *J.Appl.Polym.Sci.*, **31**, 2753-2768 (1986).
- Burzynski, Ryszard, Prasad, Paras N. and Murthy, N.S., "Structure of the Iodine Columns in Iodinated Nylon-6", *J.Polym.Sci: Polym.Phys.Ed.*, **24**, 133-141 (1986).
- Cheng, H.N., Smith, T.E. and Vitus, D.M., "Studies of Solution Dynamics of Poly(N-Vinyl Pyrrolidone) and Its Iodine Adduct", *J.Polym.Sci: Polym.Phys.Ed.*, **23**, 461-470 (1985).
- Choe, E. Won and Kim, Sang Nim, "Synthesis, Spinning and Fiber Mechanical Properties of Poly(p-phenylene benzobisoxazole)", *Macromolecules*, **14**, 920-924 (1981).
- Chuah, Hoe H., "Structure-Property Studies in the Deformation of Semi-Crystalline Polymers", Ph.D Thesis, University of Massachusetts, Amherst, 1985.
- Chuah, Hoe H. and Porter, Roger J., "A New Drawing Technique for Nylon-6 by Reversible Plasticization with Iodine", *Polymer*, **27**(2), 241-246 (1986).

- Cohen, Yachin, "Structure Formation in Solutions of Rigid Polymers Undergoing a Phase Transition", Ph.D thesis, University of Massachusetts, Amherst (1987).
- Cohen, Yachin and Thomas, Edwin L., "Structure Formation During Spinning of Poly(p-phenylene benzobisthiazole) Fiber", *Polym.Eng.Sci.*, **25**(17), 1093-1096 (1985).
- Cohen, Yachin, Frost, Herbert H., and Thomas, Edwin L., "Structure Formation and Phase Transformations in Solutions of a Rigid Polymer", in P.S. Russo ed., Reversible Gelation in Polymers, ACS Symposium Series (1987).
- Cohen, Yachin and Thomas, Edwin L., *Mol.Cryst.Liq.Cryst.*, **153**(Part A), 375 (1987).
- Coppens, Phillip in Extended Linear Chain Compounds, J.S. Miller, Ed., Plenum, New York, 1982, Vol.1, pp.333-356.
- Danno, Tetsuya, Miyasaka, Keizo and Ishikawa, Kinzo, "Dynamics and Mechanism of Iodine Sorption by Polyacetylene", *J.Polym.Sci., Polym.Phys.Ed.*, **21**, 1527-1537 (1983).
- DeTeresa, Steven J., doctoral research proposal, Department of Polymer Science and Engineering, University of Massachusetts, Amherst, 1984.
- DeTeresa, Steven J., Allen, Steven R., Farris, Richard J. and Porter, Roger S. , "Compressive and Torsional Behavior of Kevlar 49 Fiber", *J.Mat.Sci.*, **19**, 57 (1984a).
- DeTeresa, Steven J., "The Axial Compressive Strength of High Performance Polymer Fibers", Ph.D thesis, University of Massachusetts, Amherst, (1984b).
- DeTeresa, Steven J., Farris, Richard J. and Porter, Roger S., "A Model for the Compressive Buckling of Extended-Chain Polymers", *J.Mat.Sci* **20**, 1645 (1985).
- DeTeresa, Steven J. and Rakas, Margaret A., unpublished results, May 1986.
- DeTeresa, Steven J., Porter, Roger J. and Farris, Richard J., "Experimental Verification of a Microbuckling Model for the Axial Compressive Failure of High-Performance Polymer Fibers", *J.Mat.Sci.*, **23**(5), 1886-1894 (1988).
- Diefendorf, R.J. and Tokarsky, E., "High Performance Carbon Fibers", *Polym.Eng.Sci.*, **15**(3), 150-159 (1975).

- Dobb, M.G., Johnson, D.J. and Saville, B.P., a) "Supramolecular Structure of a High-Modulus Polyaromatic Fiber (Kevlar 49)", *J. Polym. Sci.: Polym. Phys. Ed.*, **15**, 2201-2211 (1977); b) "Direct Observation of Structure in High-Modulus Aromatic Fibers", *J. Polym. Sci.: Polym. Sym.*, **58**, 237-251 (1977).
- Dobb, M.G., Johnson, D.J. and Saville, B.P., "Compressional Behaviour of Kevlar Fibres", *Polymer*, **22**(7), 960-965 (1981).
- Downs, A.J. and Adams, C.J. in Comprehensive Inorganic Chemistry, Vol.2, J.C. Bailar. H.J. Emeleus, R. Nyholm and A.F. Trotman-Dickenson, Eds., Pergamon Press, Oxford, pp.1107-1594.
- Du Pont technical bulletin, "Du Pont Performance Products/Tyzor Titanates", 1988.
- Farris, Richard J., Cohen, Yachin and DeTeresa, Steven J., British patent application number 8,717,424, filed July 23, 1987, published April 13, 1988.
- Greenwood, J.M. and Rose, P.G., "Compressive Behavior of Kevlar 49 Fibres and Composites", *J.Mat.Sci.*, **9**(11), 1809 (1974).
- Hancock, T.A., Spruiell, J.E. and White, J.L., "Wet Spinning of Aliphatic and Aromatic Polyamides", *J.Appl.Polym.Sci.*, **21**, 1227-1247 (1977).
- Haraguchi, K., Kajiya, T. and Takayanagi, M., a) "Uniplanar Orientation of Poly(p-phenylene terephthalamide) Crystal in Thin Film and Its Effect on Mechanical Properties", *J.Appl.Polym.Sci.*, **23**, 903-914; b) "Effect of Coagulation Conditions on Crystal Modification of Poly(p-phenylene terephthalamide)", *J.Appl.Polym.Sci.*, **23**, 915-926 (1979).
- Hassel, O. and Romming, C., "Direct Structural Evidence for Weak Charge-Transfer Bonds in Solids Containing Chemically Saturated Molecules", *J.Chem.Soc., Quarterly Reviews*, **16**, 1-18 (1962).
- Holliday, L., in "Structure and Properties of Oriented Polymers", I.M. Ward ed, Applied Science Publishers, London, 1975.
- Horsky, J., Petrus, V. and Bohdanecky, M., "A Specific Effect of Alkali-Metal Iodides and Thiocyanates on the Viscosity of Solutions of Poly(methacrylic acid) in Methanol", *Polymer*, **27**, 1948-1950 (1986).
- Huheey, James E., Inorganic Chemistry, pp.240-241, second edition, Harper & Row, New York, 1978.
- Iovleva, M.M. and Papkov, S.P., "Polymer Crystallosolvates. Review", *Polymer Science U.S.S.R.*, **24**(2), 236-257 (1982).

- Jackson, B.E., private communication, May 1989.
- Jaffe, Michael and Jones, R. Sidney, "High Performance Aramid Fibers", pp. 349-92, in The Handbook of Fiber Science and Technology: Vol.3, High Technology Fibers, Part A, M. Lewin and S. Preston, eds., Marcel Dekker, NY (1985).
- Jenekhe, Samson A., Johnson, Paul O., and Agrawal, Ashwini K., "Solubilization, Solutions and Processing of Aromatic Heterocyclic Rigid Rod Polymers in Aprotic Organic Solvents: Poly(p-phenylene-2,6-benzobisthiazole) [PBT]", *Macromolecules*, **22**(8), 3216-3622 (1989).
- Joshi, D.P. and Pritchard, J.G., "Partly Alcoholized Poly(vinyl alcohol) Polymers: Kinetics of Formation and Reaction with Iodine", *Polymer*, **19**, 427-430 (1978).
- Kanomoto, T, Tsuruta, A., Tanaka, K., Takeda, M., and Porter, R.S., "On Ultra High Modulus by Drawing Single Crystal Mats of High Molecular Weight Polyethylene", *Polymer J.*, **15**, 327 (1983).
- Kavesh, S. and Prevorsek, D.C., "Gel Spinning of Extended Chain Flexible Macromolecules-Process, Structure and Properties", *Polymeric Materials: Science and Engineering*, **58**, 668 (1988).
- Kavesh, S., and Prevorsek, D.C., U.S. Patent 4,413,110 (1984).
- Kavesh, S., at the Division of Polymeric Materials: Science and Engineering, Third Chemical Congress of North America, Toronto, June 1988.
- Keifer, W., "Laser-excited Resonance Raman Spectra of Small Molecules and Ions--A Review", *Applied Spectroscopy*, **28**(2), 115-123 (1974).
- Knoff, W.F., private communication, June 1987.
- Knudsen, J.P., "The Influence of Coagulation Variables on the Structure and Physical Properties of an Acrylic Fiber", *Textile Res.J.*, January, 13-20 (1963).
- Kojima, Y., Furuhashi, K. and Miyasaka, K., "Sorption and Permeation of Iodine in Water-Swollen Poly(Vinyl Alcohol) Membranes and Iodine Complex Formation", *J.Appl.Polym.Sci.*, **30**, 1617-1628 (1985).
- Koutsky, J.A., Walton, A.G. and Baer, Eric, "Epitaxial Crystallization of Homopolymers on Single Crystals of Alkali Halides", *J.Polym.Sci.: Part A-2*, **4**, 611-629 (1966).

- Ma, T.S. and Rittner, Robert C., Modern Organic Elemental Analysis, Marcel Dekker, Inc., New York, 1979.
- Marks, Tobin J. and Kalina, Davida W. in Extended Linear Chain Compounds, Vol.1, pp.197-331, J.S. Miller, Ed., Plenum, New York, 1982.
- Martin, D.C. private communication, March 1989.
- Mauritz, K.A., Baer, Eric and Hopfinger, A.J., "Molecular Energetics of the Epitaxial Crystallization of Polyethylene on Alkali Halide Substrates", *J.Polym.Sci.: Polym.Phys.Ed.*, **11**, 2185-2197 (1973).
- McCarthy, T.J., private communication, July 1988.
- Morgan, P.W., *Macromolecules*, **10**(6), 1381-1390 (1977).
- Morgan, R.J., Pruneda, C.O. and Steele, W.J., "The Relationship between the Physical Structure and the Microscopic Deformation and Failure Processes of Poly(p-phenylene Terephthalamide) Fibers", *J.Polym.Sci.: Polym.Phys.Ed.*, **21**, 1757-1783 (1983).
- Morgan, Roger J. and Pruneda, Cesar O., "The Characterization of the Chemical Impurities in Kevlar 49 Fibres", *Polymer*, **28**, 340-346 (1987).
- Mulliken, R.S. and Person, W.B., Molecular Complexes, Pergamon Press, Oxford, 1967.
- Murthy, N.S., Szollosi, A.B. and Sibilis, J.P., "Structure of Iodide Ion Arrays in Iodinated Nylon 6 and the Chain Orientation Induced by Iodine in Nylon 6 Films", *J.Polym. Sci., Polym. Phys. Ed.*, **23**, 2369 (1985).
- Murthy, N.S., Kotliar, A.M., Sibilis, J.P. and Sacks, W., "Structure and Properties of Talc-Filled Polyethylene and Nylon 6 Films", *J.Appl.Polym.Sci.*, **31**, 2569-2582 (1986).
- Northolt, M.G. and van Aartsen, J.J., "On the Crystal and Molecular Structure of Poly(p-phenylene terephthalamide)", *J.Polym.Sci., Polym.Let.Ed.*, **11**, 333 (1973).
- Northolt, M.G., "X-ray Diffraction Study of Poly(p-phenylene terephthalamide) Fibers", *Euro.Polym.J.*, **10**, 799 (1974).
- Padhye, M.R. and Karandikar, A.V., "The Effect of Alkali Salt on Solvent-Polyacrylonitrile Interaction", *J.Appl.Polym.Sci.*, **30**, 667-673 (1985).
- Panar, M., Avakian, P., Blume, R.C., Gardner, T.D., Gierke, D. and Yang, H.H., "Morphology of Poly(p-phenylene terephthalamide) Fibers", *J.Polym.Sci.: Polym.Phys.Ed.*, **21**, 1955-1969 (1983).

- Pennings, A.J., *J.Polym.Sci., Polym Symp.*, **59** (1977), 55.
- Perry, A.J., Ineichen, B. and Eliasson, B., "Fibre Diameter Measurement by Laser Diffraction", *J.Mat.Sci.Lett.*, **9(8)**, 1376-1378 (1974).
- Point, J.J. and Coutelier, C., "Linear High Polymers as Host in Intercalates. Introduction and Example", *J.Polym. Sci., Polym. Phys. Ed.*, **23**, 231-239 (1985).
- Pottick, Lorelle A., "The Influence of Drying on the Structure and Mechanics of Poly(p-phenylene benzobisthiazole) Fibers", Ph.D thesis, University of Massachusetts, 1986.
- Pottick, Lorelle A. and Farris, Richard J., "Alterations in the Structure and Mechanics of Poly(p-phenylene benzobisthiazole) Fibers due to the Collapse Process During Drying", *TAPPI Proceeding: 1985 Non-Wovens Symposium*, **85**, 65 (1985).
- Reddy, J.M., Knox, K. and Robin, M.B., "Crystal Structure of $\text{HI}_3 \cdot 2\text{C}_6\text{H}_6\text{CONH}_2$: A Model of the Starch-Iodine Complex", *J.Chem.Phys.*, **40(4)**, 1082-1089 (1964).
- Rickert, S.E. and Baer, E., "Epitaxial Crystallization of Polyesters on Inorganic and Organic Substrates", *J.Polym.Sci.: Polym.Phys.Ed.*, **16**, 895-906 (1978).
- Rodriguez, Ferdinand, Principles of Polymer Systems, MacGraw-Hill, New York, (1982).
- Rose, J., Molecular Complexes, Pergamon Press, London, 1967.
- Sakka, S. and Kamiya, K., "The Sol-Gel Transition in the Jydrolisis of Metal Alkoxides in Relation to the Formation of Glass Fibers and Films", *J.Non-Cryst.Sol.*, **48**, 31-46 (1982)
- Smith, Paul and Lemstra, Piet J., "Ultra-High-Strength Polyethylene Filaments by Solution Spinning/Drawing", *J. Mat.Sci.*, **15**, 505 (1980).
- Takahashi, Toshisada, and Okazaki, Hideo, "Epitaxial Crystallization of Polyoxymethylene during Cationic Polymerization of Trioxane", *J.Polym.Sci.: Polym.Phys.Ed.*, **16**, 2049-2056 (1978).
- Tam, T.Y., Boone, M.B., and Weedon, G.C., "New Horizons in Advanced Oriented Fiber", *Polym.Eng.Sci.*, **28(13)**, 871-874 (1988).
- Teitelbaum, R.C., Ruby, S.L. and Marks, T.J., "On the Structure of Starch-Iodine", *J.Am.Chem.Soc.*, **100:10**, 3215-3217 (1978).
- Wallace, S. and Hench, L.L., "Metal Organic-Derived 20L Gel Monoliths", *Ceramic Eng.Sci.Proc.*, **5(7-8)**, 568-573, (1984).

Ward, I.M., "The Structure and Properties of Ultra High Modulus Films and Fibres", pp. 265-273, from Macromolecules, H. Benoit and P. Rempp, eds., Pergamon Press, 1982

Wilfong, R.E., and Zimmerman, J., "Strength and Durability Characteristics of Kevlar Aramid Fiber", *J.Appl.Polym.Sci., Appl. Polym.Symp.* **31**, 1-21 (1977).

Willems, J., "Oriented Growth in the Field of Organic High Polymers", *Discussions Faraday Soc.*, **25**, 111 (1957).

Wolfe, James F. and Arnold, F.E., "Rigid-Rod Polymers. 1. Synthesis and Thermal Properties of Para-Aromatic Polymers with 2,6-Benzobisoxazole Units in the Main Chain", *Macromolecules*, **14**, 909-915 (1981a).

Wolfe, James F., Loo, Bock H. and Arnold, F.E., "Rigid-Rod Polymers. 2. Synthesis and Thermal Properties of Para-Aromatic Polymers with 2,6-Benzobisthiazole Units in the Main Chain", *Macromolecules*, **14**, 915-920 (1981b).

Yamada, Kenji, Uchida, Masafumi and Takayanagi, Motowo, "Preparation of Poly(p-Phenylene Terephthalamide)/Poly(vinyl chloride) Molecular Composite and Its Thermal and Mechanical Properties", *J.Appl.Polym.Sci.*, **32**, 5231-5244 (1986).

Ziabicki, A., Fundamentals of Fibre Formation, Wiley-Interscience, New York, (1976).

Zwijnenburg, A., and Pennings, A.J., "Longitudinal Growth of Polymer Crystals from Flowing Solutions III. Polyethylene Crystals in Couette Flow", *Colloid and Polymer Science*, **254**, 868-81 (1976).

